Investigation of ER retention machinery in CHO cells for understanding its biology and probable IgG production bottlenecks

Doctoral thesis

Andrew Samy AbdelMalak Robair
August 2021
Department of Biotechnology
Division of Advanced Science and Biotechnology
Graduate School of Engineering
Osaka University

Table of Contents

Table of Figures

Table of Tables

Abbreviations

BFA: Brefeldin A, **BHK**: Baby hamster kidney, **BiP**: Binding immunoglobulin protein, **bp**: Base pair, **Calr**: Calreticulin, **CBB**: Coomassie brilliant blue, **CDS**: Coding DNA sequence, **cDNA**: Complementary deoxyribonucleic acid, **CHO**: Chinese hamster ovary, **CHOP**: C/EBP homologous protein, **CTD**: C-terminal domain, **DAPI**: 4' ,6-diamidino-2-phenylindole, **DMSO**: Dimethyl sulfoxide, **DNA**: Deoxyribonucleic acid, **ELISA**: Enzyme-linked immunosorbent assay, **ER**: Endoplasmic reticulum, **ERGIC**: ER-Golgi intermediate compartment, **FBS**: Fetal bovine serum, **GRP94**: Glucose-regulated protein 94, **IgG**: Immunoglobulin G, **IP**: Immunoprecipitation, **Kb**: Kilo bases, **kDa**: Kilo Dalton, **KDEL**: Lysine, Aspartic acid, Glutamic acid and Leucine, **KDELR1**: KDEL receptor 1, **KDELR2**: KDEL receptor 2, **KDELR3**: KDEL receptor 3, **LAF**: Laminar airflow, **mAb**: Monoclonal antibody, **MD**: Middle Domain, **mRNA**: Messenger ribonucleic acid, **mTOp2**: Modified TOp2 medium, **NTD**: N-terminal domain, **PBS**: Phosphate buffered saline, **PBST**: Phosphate-buffered saline with Triton (PBS-Triton), **PCR**: Polymerase Chain Reaction, **PDI**: Protein disulfide isomerase, **rCHO**: Recombinant CHO cells, **RNA**: Ribonucleic acid, **ROI**: Region of interest, **RT-PCR**: Reverse transcriptase polymerase chain reaction, **RT-qPCR**: Reverse transcriptase quantitative polymerase chain reaction, **SDS-PAGE**: Sodium dodecyl (lauryl) sulfate-polyacrylamide gel electrophoresis, **TG**: Thapsigargin, **TM**: Tunicamycin, **VCD**: Viable cell density, **WB**: Western blot

Chapter 1:

Introduction

1.1 Chinese Hamster Ovary cells

Chinese Hamster Ovary (CHO) cells are an immortal cell line that was first isolated in 1957 by Prof. Dr. Theodore T. Puck at the University of Denver, Colorado (Puck et al., 1958). CHO cells were generated by a biopsy of hamster ovary. When first isolated, it was observed that these cell lines were able to divide rapidly while maintaining good culture performance and consistent cell morphology for up to ten months. Later, CHO cells were used as a platform to produce recombinant proteins for different downstream processes in both research and biopharmaceutical industry. CHO cells are epithelial cells with a fibroblast-like morphology (Gamper et al., 2005) as shown in **Figure 1.**

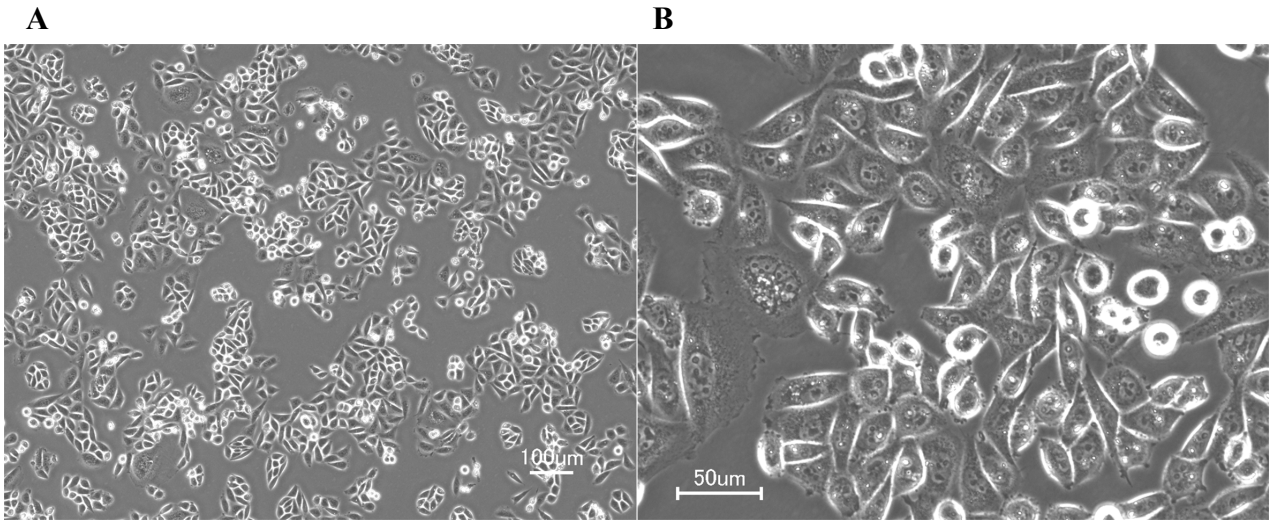

Figure 1: Morphology of CHO-K1 cells.
Showing fibroblast-like shape. Image was taken by the phase contrast mode of Keyence All-in-One Fluorescence Microscope using (**A**) 10x lens and (**B**) 40x lens

1.2 CHO cells as the workhorse for recombinant protein production

Chinese Hamster Ovary (CHO) cells are considered the workhorse in the manufacturing of biopharmaceutical proteins (Jayapal et al., 2007) owing to their ability to accommodate post-translational modification and maintain high product titers. More than half of the FDA approved biopharmaceuticals in 2016 (Lalonde & Durocher, 2017; Tripathi & Shrivastava, 2019) as well as half the of approved monoclonal antibodies use CHO cells as host cells (Omasa et al., 2010).

Compared to other mammalian cell lines derived from murine, hamster driven cells such as: Chinese Hamster Ovary (CHO) cells and Baby Hamster Kidney (BHK) cells lacks the immunogenic epitopes: galactose-alpha1,3-Gal (alpha-gal), and N-glycolylneuraminic acid (Neu5Gc) (Kunert & Reinhart, 2016). This led to its great utilization in pharmaceutical proteins manufacturing.

Monoclonal antibodies (mAbs) are a class of molecules characterized by their capability to bind specifically to a target epitope, this allowed their utilization in bio-therapeutics especially targeting cancerous cells, as well as in analytical technologies and other biochemical applications (Weiner, 2015).

During 2014 to 2018, 68 out of 132 approved biopharmaceutical drugs belonged to the monoclonal antibody class (Walsh, 2018) as shown in **Figure 2**.

Out of these 68 mAbs, 57 products (84%) were manufactured using CHO cells as a host cell platform. The biopharmaceutical industry is a multibillion-dollar industry. In particular, the sales of monoclonal antibody therapeutics were $75 billion globally in 2013 (Ecker et al., 2015).

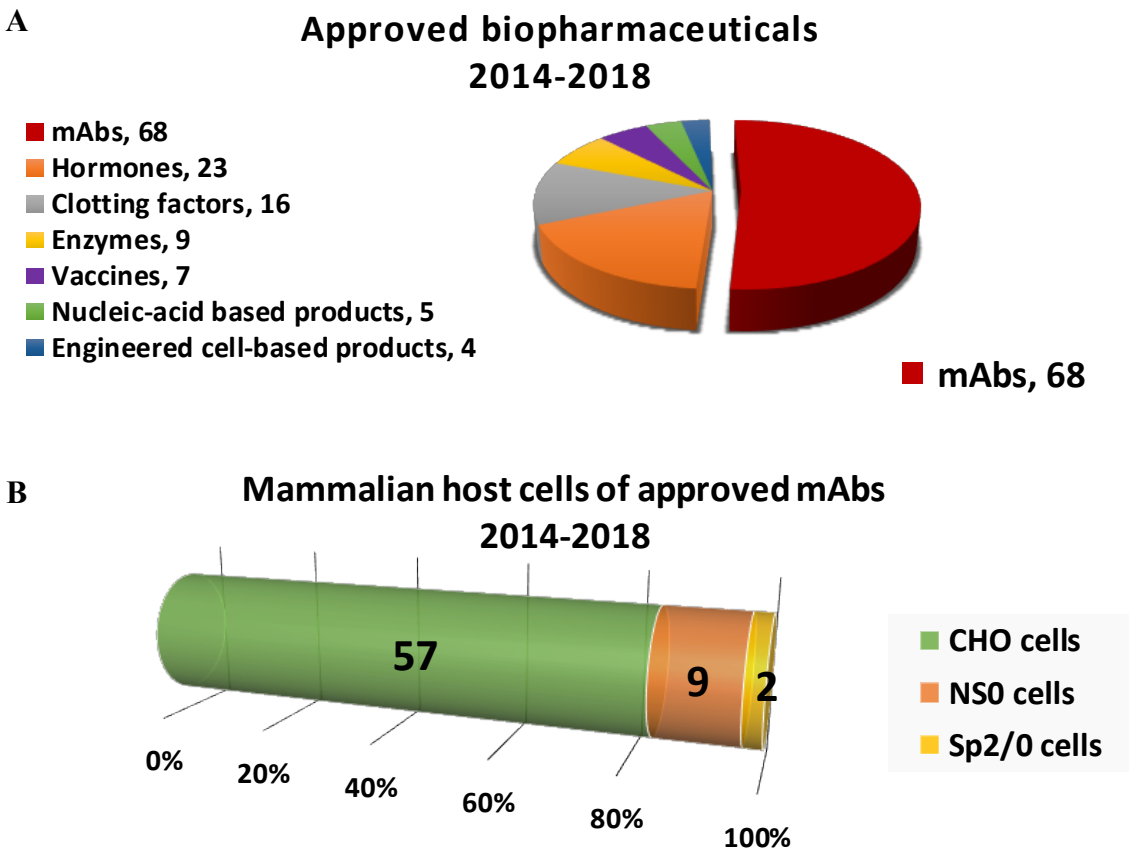

Figure 2: Biopharmaceutical benchmarks 2018.
(**A**) Products approved over the four and a half years showing 68 approved mAbs. (**B**) CHO cells are the host cells used for 57 mAbs out of 68 in total.

However, the production cost of biopharmaceuticals driven from mammalian cells are highly expensive. Cell engineering approaching were able to improve culture characteristics and performance by improving the specific productivity or boosting the lifespan of cells, leading to higher production titers (Kim et al., 2012).

1.3 Endoplasmic Reticulum and the retention mechanisms

1.3.1 KDEL tagged ER chaperones

In the endoplasmic reticulum (ER), several ER chaperones are responsible for protein folding and assembly. Once a nascent protein enters the ER, chaperones start acting on them to reach their native form. Examples of these chaperones are Binding Immunoglobulin Protein (BiP), Calreticulin, Endoplasmin (GRP94), Protein Di-sulfide Isomerases (PDI), Calnexin and others. After the protein reaches its native conformation, it leaves from the ER to Golgi to be prepared for further processing or secretion (Hebert & Molinari, 2007).

Some of these ER chaperones are retained inside the ER by their natural KDEL motif. KDEL stands for the amino acids Lysine, Aspartic acid, Glutamic acid and Leucine normally found at the C- terminal of ER resident proteins for the purpose of retaining them in the ER lumen (Munro &

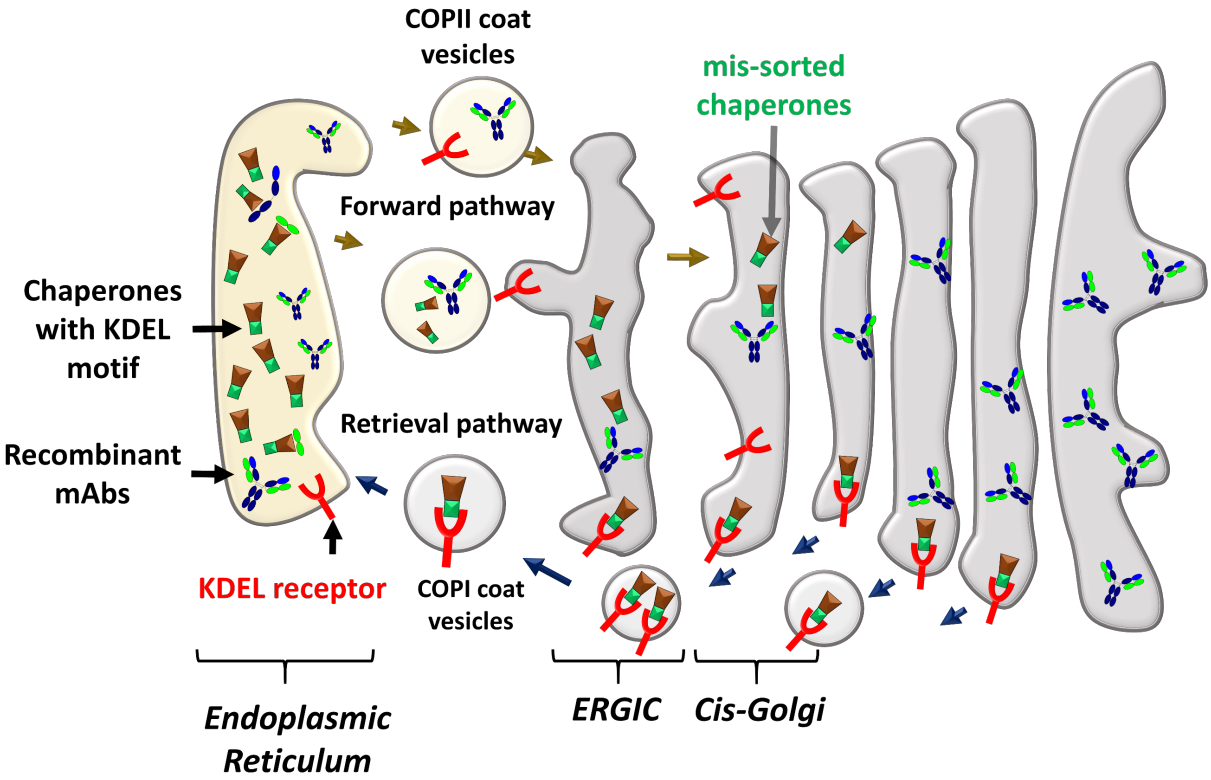

Figure 3: Mechanism of ER to Golgi transport and KDEL receptor retention mechanism
Redesigned from (Alberts et al., 2008)

Pelham, 1987). Once these chaperones leave the ER, KDEL receptor ensures their retrieval from post ER compartments like ER-Golgi Intermediate compartment (ERGIC) and *cis*-Golgi as shown in **Figure 3** (Alberts et al., 2008).

Examples of the chaperones having KDEL motif are shown in **Figure 4**.

Cell engineering approaches aim at increasing production of recombinant production from CHO cells. For instance, co-overexpression of calreticulin/Calnexin showed 1.9-fold increase in the productivity of thrombopoietin (Chung et al., 2004). Other PDI engineering approaches are discussed in the following section.

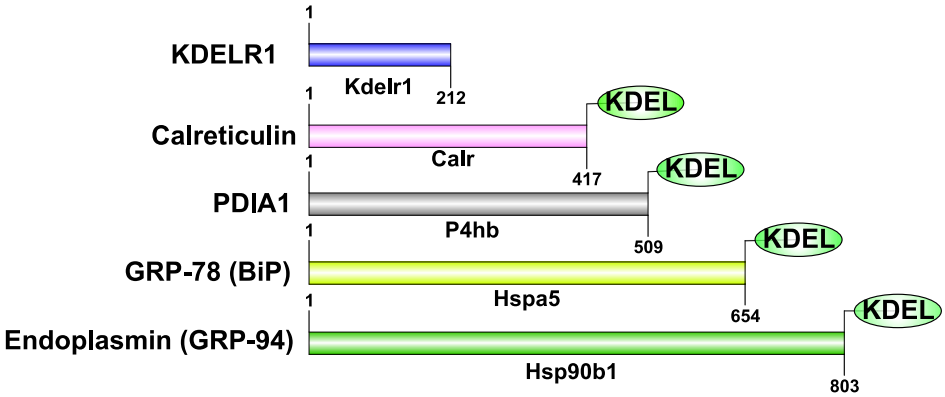

Figure 4: Common soluble ER chaperones with C-terminal KDEL motif in *C. griseus*
KDEL receptor 1 (KDELR1) and four of the most studied soluble KDEL ER chaperones: Calreticulin (Calr), Protein disulfide isomerase family A member 1 (PDIA1/P4hb), Binding immunoglobulin protein (BiP/GRP-78/Hspa5) and Endoplasmin (GRP-94/Hsp90b1).
The labels show: protein name (left label), gene name (bottom label) and protein size including the motif (right number).

1.3.2 Protein Di-sulfide Isomerase family

One major post-translational modification that occur inside the endoplasmic reticulum is the formation of disulfide bonds in multi-meric proteins. Protein Di-sulfide isomerases are a family of 21 members as reported by HUGO Gene Nomenclature Committee (HGNC) (Appenzeller-Herzog & Ellgaard, 2008). They are enzymes that catalyze the formation and breakdown of disulfide bonds between cysteine residues in multi-meric proteins as they fold (Feige & Hendershot, 2011).

Mohan *et al.* have investigated the effect of PDI family member A1 (PDIA1/P4hb: AF364317_1) overexpression on mAbs productivity. They were able to achieve an increase in productivity of 15-27% by doxycycline regulated PDI expression (Mohan et al., 2007).

Additionally, doxycycline regulated overexpression of PDI family member A3 (PDIA3/ERp57) showed 2.1-fold increase in the specific productivity of thrombopoietin without any observed inhibition of growth (Hwang et al., 2003).

The first 6 members of PDI family in Cricetulus griseus with their C-terminal motif are shown in **Table 1**. A summary of the previous cell engineering approaches involving ER chaperones is collected in **Table 2**.

Table 1: Gene Family: Members of protein disulfide isomerase (PDI) family and their C-terminus motif in *Cricetulus griseus*

Symbol	Name	NCBI Reference Sequence (Transcript/protein)	Protein size	C-terminus sequence
P4HB/ PDIA1	Prolyl 4-hydroxylase subunit beta	XM_007654094.1 XP_007652284.1 AF364317_1	509 aa	KDEL
PDIA2	Protein disulfide isomerase family A member 2	XM_003501477.3 XP_003501525.1	527 aa	KEEL
PDIA3/ ERp57	Protein disulfide isomerase family A member 3	NM_001246774.1 NP_001233703.1	505 aa	QEDL
PDIA4	Protein disulfide isomerase family A member 4	XM_003512972.3 XP_003513020.1	642 aa	KEEL
PDIA5	Protein disulfide isomerase family A member 5	XM_003495441.2 XP_003495489.1	523 aa	REEL
PDIA6	Protein disulfide isomerase family A member 6	XM_007641914.2 XP_007640104.1	445 a	KDEL

Table 2: Approaches in chaperones' engineering

Target chaperones	Target	Effect on productivity	Reference	C-terminal	Gene ID
ERp57 (PDI A3)	mAbs	↑ 2.1 folds	(Hwang et al., 2003)	QEDL	100689343
PDI A1	mAbs	↑ 15-27%	(Mohan et al., 2007)	KDEL	100689433
Calnexin/ Calreticulin	Thrombopoietin	↑ 1.9 folds	(Chung et al., 2004)	Calnexin: PRRE Calreticulin: KDEL	Calnexin: 100689345 Calreticulin: 100689096
BIP/PDI	mAbs	BiP: ↓ 34% PDI: ↑ 37% BiP + PDI: ↓ 35%	(Borth et al., 2005)	BiP: KDEL PDI A1: KDEL	BiP: 100689305 PDI: 100689433
Grp170 (Hyou1)	mAbs	Decrease	L Jossé and CMSmales, unpublished data, as cited by (Jossé et al., 2012)	NDEL	100689308

1.3.3 KDEL receptor family mechanism and function

KDEL stands for the amino acids Lysine, Aspartic acid, Glutamic acid and Leucine normally found at the C- terminus of ER resident proteins for the purpose of retaining them in the ER lumen (Munro & Pelham, 1987).

KDEL receptors are seven transmembrane domain proteins found in the *cis*-Golgi and ER-Golgi intermediate compartment (ERGIC) , known to be responsible for the recycling of ER chaperones that carry folded proteins from ER to Golgi, back to ER after the delivery of the cargo (Capitani & Sallese, 2009; Giannotta et al., 2012). Once these chaperones bind to KDEL receptor, the receptors can recapture them and return them back to the ER (Wiersma et al., 2015). Functions of KDEL receptors are: binding and recycling of KDEL-bearing ER chaperones that escape the ER and reach the Golgi during traffic back to the ER, and organizing intra-Golgi traffic in mammalian cells (Cancino et al., 2014). In addition to their affinity to KDEL motif, the three human KDEL receptors have been reported to bind to HDEL, KEEL, RDEL, REEL, QDEL motifs and others in human cell lines (Raykhel et al., 2007).

KDEL-bearing chaperones bind to KDEL receptors in a pH dependent manner according to the pH difference between endoplasmic reticulum and ERGIC. KDEL ligands bind to KDEL receptor in the acidic environment of *cis*-Golgi; contrarily, this binding becomes significantly weaker in neutral or basic pH of ER (Capitani & Sallese, 2009; Wilson et al., 1993).

Under ER stress, expression of KDEL receptor was upregulated by only 1.8 folds in HeLa cells upon tunicamycin or thapsigargin treatments (Wang et al., 2011). On the other hand, a different team reported the failure of HeLa cells to upregulate KDEL receptor 1 in response to ER stress induction. Additionally, they were able to detect calreticulin in the medium by

immunoprecipitation after 18 hours of exposure to tunicamycin. They suggested that to be due to the saturation of the retention machinery; or simply the failure of HeLa cells to significantly upregulate KDEL receptor expression (Llewellyn et al., 1997).

Also, as reported by Wiersma *et.al.*, during ER stress, ER chaperones are upregulated causing the saturation of KDEL receptors leading to the escaping of some ER chaperones to the cytoplasm, and even to the extracellular fluid which can cause immunogenic responses in some kinds of cancer (Wiersma et al., 2015).

Misfolded proteins have been shown to cycle between ER and Golgi through a mechanism that prevents their secretion and contributes to ER quality control system (Hammond & Helenius, 1994). This mechanism was also investigated by Yamamoto et al. (2001) using T-cell antigen receptor (TCR) α as a model of a misfolded protein. It was found that this retention from post ER compartments is due to the binding of misfolded proteins to soluble ER chaperones like BiP. This misfolded protein-BiP complex is then retrieved from post ER compartments through binding of BiP to KDEL receptor and recycling back to ER. Misfolded proteins then proceed to ER associated degradation (ERAD) pathway. This suggested that KDEL receptor contributes to the quality control in endoplasmic reticulum (Yamamoto et al., 2001).

KDEL receptor family in human consists of three members: KDELR1, KDELR2 and KDELR3 (Capitani & Sallese, 2009). This is conserved as well in Chinese hamster. Coding nucleotide sequences between transcripts as well as amino acid sequences show high identities between the three members as shown in **Table 3** and **Table 4**, respectively. Amino acid alignment of the three KDEL receptors in *Cricetulus griseus* is shown in **Figure 5**.

Amino acid sequence alignment of KDEL receptors between human and Chinese hamster shows high identity. All the three receptors show conserved protein size to the complementary protein. KDELR1 shows only one amino acid difference L77M as shown in **Figure 6**, KDELR2 shows three amino acid differences V65L, L68I and L80M as shown in **Figure 7** ,while KDELR3 shows 15 amino acid differences as shown in **Figure 8**.

Table 3: Coding nucleotide sequences identities of KDEL receptor family in *Cricetulus griseus.* (i.e. from predicted transcripts)

	Kdelr1 (XM_007652679.1)	***Kdelr2*** (XM_007648732.1)	***Kdelr3*** (XM_003514679.2)
Kdelr1		**76%**	**73%**
Kdelr2	**76%**		**72%**
Kdelr3	**73%**	**72%**	

Table 4: Amino acid sequence identities of KDEL receptor family in *Cricetulus griseus* (i.e. from predicted transcripts)

	Kdelr1 **(**XP_007650869.1**)**	***Kdelr2*** **(**XP_007646922.1**)**	***Kdelr3*** **(**XP_003514727.2**)**
Kdelr1		**83%**	**73%**
Kdelr2	**83%**		**76%**
Kdelr3	**73%**	**76%**	

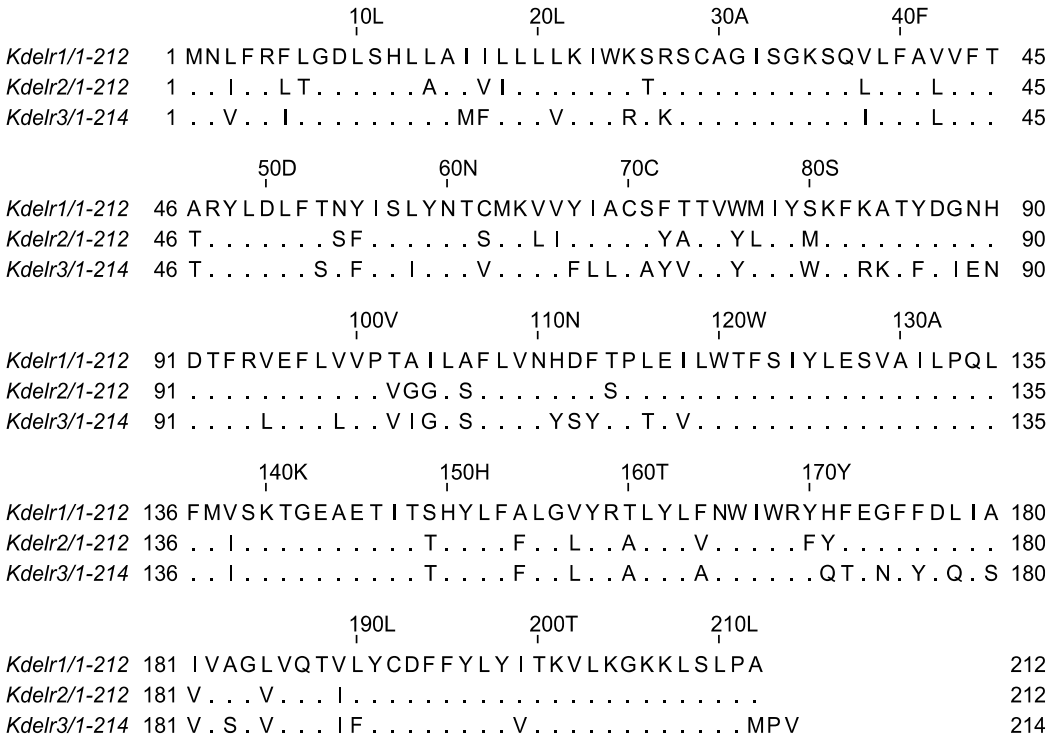

Figure 5: Amino acid sequence alignment of KDEL receptor family in *C. griseus*

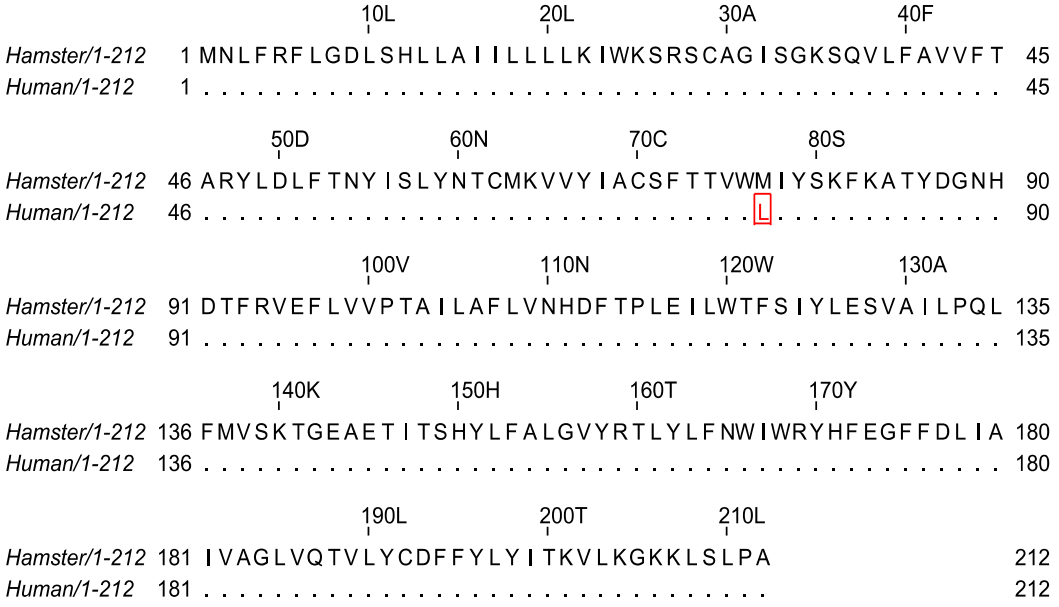

Figure 6: Amino acid sequence alignment of KDELR1 between hamster and human *Cricetulus griseus* (*XP_007650869.1*) and *Homo sapiens* (*NP_006792.1*) shows only one amino acid

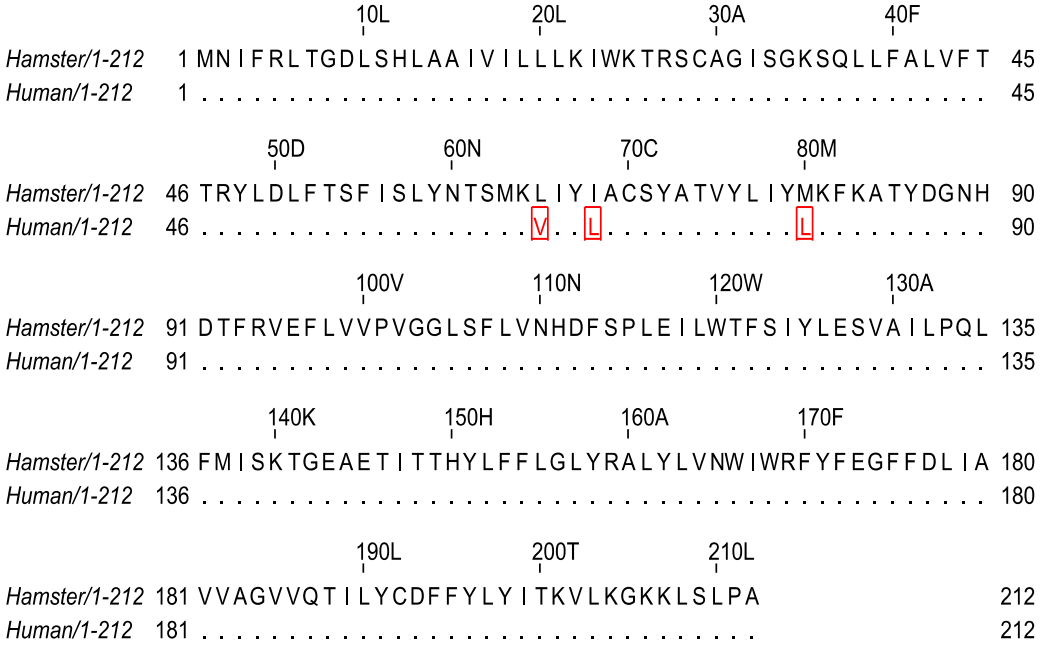

Figure 7: Amino acid sequence alignment of KDELR2 between hamster and human in Cricetulus griseus (XP_007646922.1) and Homo sapiens (NP_006845.1) shows three amino acid differences V65L, L68I and L80M

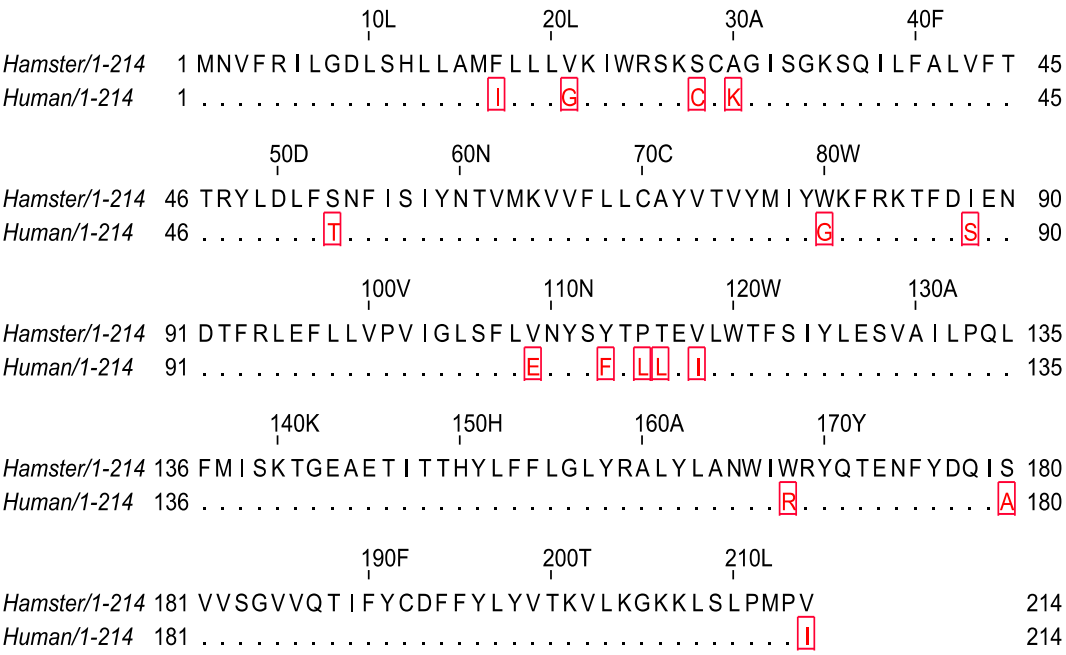

Figure 8: Amino acid sequence alignment of KDELR3 between hamster and human in *Cricetulus griseus* (*XP_003514727.2*) and *Homo sapiens* (*NP_006846*) shows 15 amino acid differences

1.4 The unfolded protein response (UPR)

There are a variety of responses in which cells respond to stresses in order to regain homeostasis or to clear the highly damaged cells. Examples of these cellular responses are: the heat shock response, the unfolded protein response (UPR), the DNA damage response and the response to oxidative stress (Fulda et al., 2010). In this report, only the unfolded protein response will be discussed for its importance in recombinant biopharmaceutical production owing to the high load put on the ER to achieve high production and maintain the quality of these proteins.

The unfolded protein response (UPR) is the cell defense mechanism against conditions of accumulated proteins in the ER owing to changes in intracellular pH, calcium ion concentrations, variations in culture temperature or chemical exposure. The UPR involves upregulation and/or activation of several transcription factors that mediate the upregulation of ER chaperones and other intermediate molecules that allow the cell to properly fold or degrade the accumulated proteins (Nishitoh, 2012; Torres et al., 2020). This cell response allow the restoration of cell homeostasis; accordingly, demonstrating the functional role of UPR and GRP proteins in keeping organ homeostasis (Liu et al., 2013; Zhu & Lee, 2015).

UPR consists of three major arms: the activating transcription factor 6 (ATF6), protein kinase RNA-like ER kinase (PERK) and inositol-requiring kinase 1 (IRE1a). The Glucose Regulated Protein 78 (GRP78/Hspa5) which is also called Binding Immunoglobulin protein (BiP) is the master regulator of the three arms of the UPR. In normal conditions, BiP binds to these three proteins independently. When ER stress is induced by the accumulation of unfolded proteins inside the ER lumen, BiP sets free these three proteins and binds the misfolded proteins to assist in their folding and/or degradation. The released ATF6 (ATF6p90) is then translocated from the ER to Golgi where it is cleaved by S1P and S2P proteases forming its active nuclear form (ATF6p50).

Likewise, IRE1α is phosphorylated and exhibits RNase activity when released to the cytosol; it then acts on the mRNA encoding the transcription factor X- box binding protein 1 (XBP1). This activity involves the production of a spliced form of XBP1 (XBP1s). Both XBP1s and ATF6p50 act to increase the transcription of the genes responsible for ER chaperones and those involved in protein folding, maturation, secretion and degradation of unfolded proteins. Similarly, when PERK is released from BiP, it activates eukaryotic translation initiation factor 2 subunit- α (eIF2α) by phosphorylation. Then eIF2αp functions by diminishing the protein synthesis to decrease the load of ER, and by selective translation of another transcription factor ATF4 which controls the genes responsible for amino acid metabolism, antioxidant response, autophagy and ER protein folding. This pathway is reviewed in detail in (Hetz et al., 2020; Luo & Lee, 2013). An illustration showing the three arms of UPR is simplified in **Figure 9**.

Different chemicals are used to induce the unfolded protein response in mammalian cells. Examples of these are tunicamycin and thapsigargin. Tunicamycin inhibits N-linked glycosylation in the ER and thus causes the proteins to misfold and accumulate in an improperly folded state in the ER. Thapsigargin is an inhibitor of sarco- endoplasmic reticulum Ca^{+2} ATPase (SERCA) which causes the depletion of calcium stores in the endoplasmic reticulum needed for proper folding of proteins in the ER. Thapsigargin also affects autophagy because of the imbalance it causes in the calcium stores and distribution across the cell.

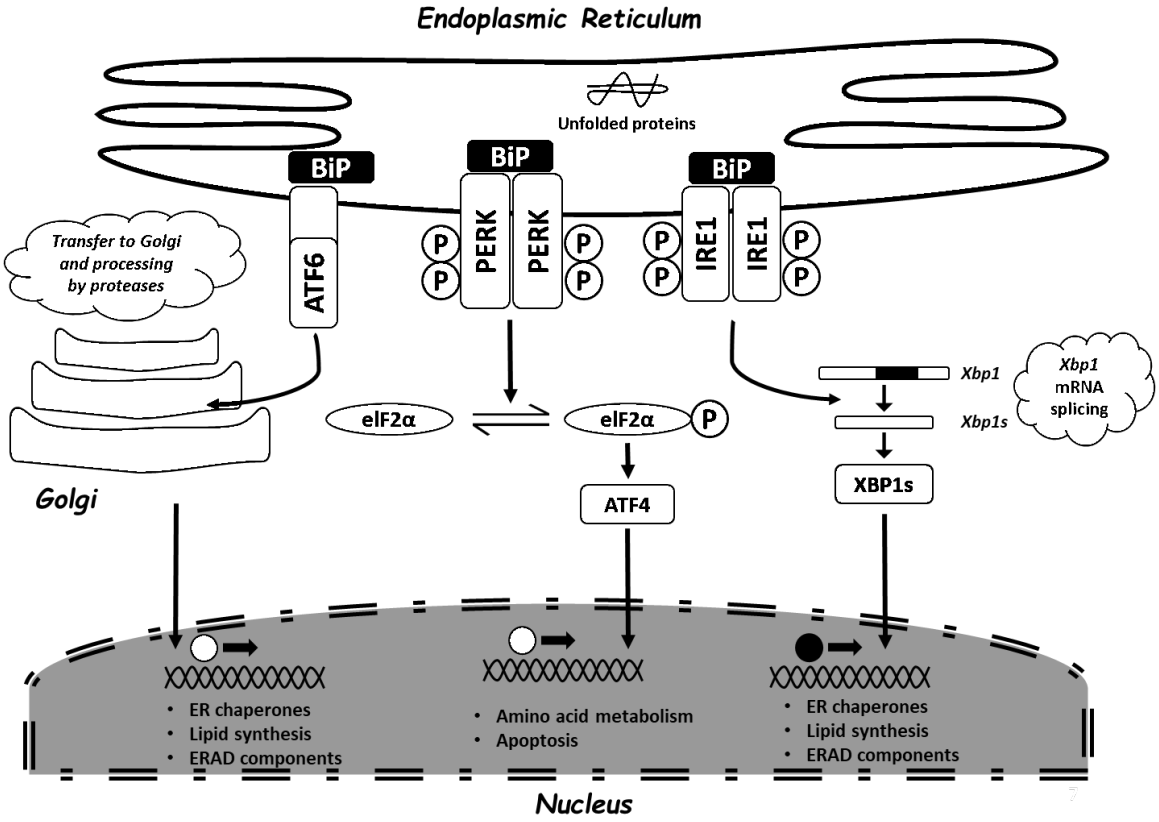

Figure 9: Mechanism of unfolded protein response (UPR)

An illustration showing the three arms of UPR and the outcome of their activation.

1.5 Hypothesis and objective

Engineering of CHO cells as a host cell for the production of recombinant proteins allowed high yield of production reaching up to 13 g/L of monoclonal antibodies and increasing (Huang et al., 2010). However, this increase in the synthesis demand sheds light on different bottlenecks in the posttranscriptional processes; for instance, the rate of synthesis, folding and maturation, posttranslational processing and secretion (Zhou et al., 2018).

Accordingly, this study investigates possible ways to improve the capacity of the endoplasmic reticulum in Chinese hamster ovary cells to perform additional folding beyond its natural folding capacity. This is investigated in several aspects. **In chapter two**, the ER retention machinery (KDEL receptors) is investigated in terms of their response to ER stress on the expression level (mRNA), and whether or not it is coordinated between the chaperones and the receptors. Then, the effect of the constitutive overexpression of KDELR1 on the specific productivity of recombinant IgG1 in recombinant CHO-K1 cells. **In chapter three,** the secretion of ER chaperones to the medium is investigated on the protein level during normal and ER stress conditions. Also, the effect of expression of the ER stress insensitive KDELR1 expression under and ER stress sensitive promoter (BiP promoter) is investigated, and whether this can improve the retention of ER chaperones and prevent their secretion. The aim was to engineer a CHO cell model capable of making the best use of chaperones and allowing it to reach its maximum folding capacity. **In chapter four**, GRP94; a KDEL-motif bearing chaperone and a unique chaperone for IgG heavy and light chains, is investigated. It was found to be secreted as a low molecular weight species specially during ER stress and secreted abundantly to the culture medium. This chaperone specifically is a strong candidate for engineering and was used in different disciplines. Accordingly, any further understanding of this chaperone will be of great value for engineering CHO cells.

Chapter 2:

ER retention machinery response and engineering

Samy Andrew

2.1 Overview

In this chapter, I detect whether or not CHO cells are capable of upregulating Kdelr1 gene expression during ER stress conditions; in addition, to compare the difference in cell response to ER stress between Kdelr1 and other KDEL-chaperones. As reported earlier, HeLa cells were unable to upregulate KDEL receptor 1 expression upon ER stress induction by one group (Llewellyn et al., 1997) or showed 1.8-fold increase by another group (P. Wang et al., 2011). However, a comprehensive study on the stress response of cells to both Kdelr1 and KDEL-chaperones has never been performed, particularly in CHO cells. Additionally, in this study the dynamics of gene expression was also investigated in batch culture of CHO cells.

The hypothesis of this study is to use a cell line that stably expresses IgG1 antibody and use it to overexpress KDEL receptor 1. It is hypothesized that it will increase the rate of retention of KDEL-chaperones from post ER-compartments and consequently, increase the abundance of ER chaperones inside ER -where they are functional- leading to increased rate of folding of IgG1 and increased specific productivity of the cells.

According to our knowledge, this approach has never been conducted in cell engineering research for the sake of improving recombinant protein production. Therefore, it is a novel cell engineering approach, which sheds light on the capacity of endoplasmic reticulum folding machinery and the possibility of improving the retention of mis-sorted chaperones.

2.2 Materials and Methods

Batch culture: CHO-K1 (RRID: CVCL_0214) and CHO-HcD6 suspension cells were grown in 125 ml Erlenmeyer flasks as a batch culture of total volume of 30 ml. The CHO-HcD6 cells will be denoted hereafter as CHO-K1-IgG1. The culture was continued for eight days as a suspension batch culture at 5% CO_2, 90 rpm, 80% humidity and 37°C in a Climo-shaker ISFI-X (Kühner, Birsfelden, Switzerland). Samples were taken daily from the cultures from day one to day six for cell counting and total RNA extraction. Vi-CELL™ Cell Viability Analyzer (Beckman Coulter, Brea, CA, USA) was used to measure viability and viable cell density using the trypan blue dye exclusion method. The samples were centrifuged at 17,000 × *g* for 2 minutes at 4°C to separate the supernatant and the cell pellet, cells were then lysed for toal RNA extraction using the FastGene RNA extraction Premium Kit (Nippon Genetics, Tokyo, Japan) according to the manufacturer's protocol. For storage, RNA samples were stored at -80°C until further processing.

RT-qPCR: The Prime script 1st strand cDNA synthesis Kit (Takara Bio, Kusatsu, Japan) was used for the synthesis of first cDNA strands. Quantitative real time PCR was conducted using the SYBR Green Master Mix (Thermo Fisher Scientific, Waltham, MA, USA). StepOnePlus Real-Time PCR System (Thermo Fisher Scientific) was used for amplification and analysis.

The mRNA transcript sequences of the target genes were downloaded from NCBI database in FASTA format. Then, *Genome Compiler* software (Genome Compiler Corporation, Los Altos, CA, USA) was used to manually design qPCR primers specific for these genes. The target genes are housekeeping gene beta-actin, *Kdelr1*, PDI (P4hb), Calreticulin, CHOP, Hspa5 (BiP) and Hsp90b1 (GRP94/endoplasmin). The designed primers are shown in **Table 8**.

Melt curve analysis was used to confirm the specificity of the primers using the StepOnePlus™ software, followed by running the RT-qPCR product on agarose gel electrophoresis.

ER stress induction: CHO-K1 were grown as suspension batch culture in 30 mL culture volume at a seeding viable cell density of of 0.4×10^6 cells/mL in 125 mL Erlenmeyer flasks as mentioned earlier. Tunicamycin (LKT Labs, St. Paul, MN, USA) was used at a concentration of 5 µg/mL (Ohya et al., 2008; Segar et al., 2013) to induce ER stress. Briefly, tunicamycin or equivalent amount of vehicle (DMSO) were added to the cells when they reached around 3×10^6 cells/ml. After 20 hours of exposure to tunicamycin or the vehicle, total RNA was extracted as previously mentioned. Similarly, the first strand cDNA was synthesized and RT-qPCR was performed as previously described. Expression levels of KDEL receptor 1 (*Kdelr1*), KDEL receptor 2 (*Kdelr2*), KDEL receptor 3 (*Kdelr3*), PDI (*P4hb*), BiP (*Hspa5*), GRP94/Endoplasmin (*Hsp90b1*) and Calreticulin (*Calr*) were measured.

Construction a plasmid expressing Kdelr1: The mRNA transcript of KDEL receptor 1 (Accession: XM_007652679) was downloaded from NCBI database. Then, it was used as template to clone the coding DNA sequence of *Kdelr1* gene. The primers incorporated the *Kdelr1* open reading frame with a length of 639 bp and encoded KDELR1 protein with 8 glycine residues to be inserted in frame with myc and His tag in pBudCE4.1 vector (Invitrogen, California, United States) under CMV promoter. Total RNA was extracted from suspension CHO-K1 using the previously mentioned kits; similarly, first cDNA synthesis was synthesized. The primers used for cloning are shown in **Table 5**.

Table 5: Cloning primers for *Kdelr1* in pBudCE4.1 backbone

Forward primer	CAGAAGCTT**ATG**AACCTCTTCCGATTCCTGG	BamHI restriction site
Reverse primer	CAGGGATCCACCACCACCACCACCAC CACCACCGCTTGCCGGTAAGCTCAGCTTC	8 glycine residues and HindIII restriction site

The gene was PCR amplified using Q5 High-Fidelity 2X Master Mix (New England Biolabs, Massachusetts, US) using the conditions mentioned in **Table 6**.

Table 6: PCR amplification conditions of *Kdelr1*

Step	Temp	Duration	
Pre-denaturation	98 °C	30 sec	
Denaturation	98 °C	10 sec	8x
Annealing	68 °C	30 sec	
Extension	72 °C	30 sec	
Denaturation	98 °C	10 sec	30 x
Annealing	72 °C	30 sec	
Extension	72 °C	30 sec	
	72 °C	2 minutes	
	4 °C	∞	

The PCR amplified gene was digested using BamHI and HindIII and inserted in the corresponding sites in pBudCE4.1 vector. The vector was amplified in *E.coli* and was endotoxin purified using MiraCLEAN Endotoxin Removal Kit (Takara Bio) and then linearized using SpeI enzyme. A sketch of the constructed plasmid is shown in **Figure 10**.

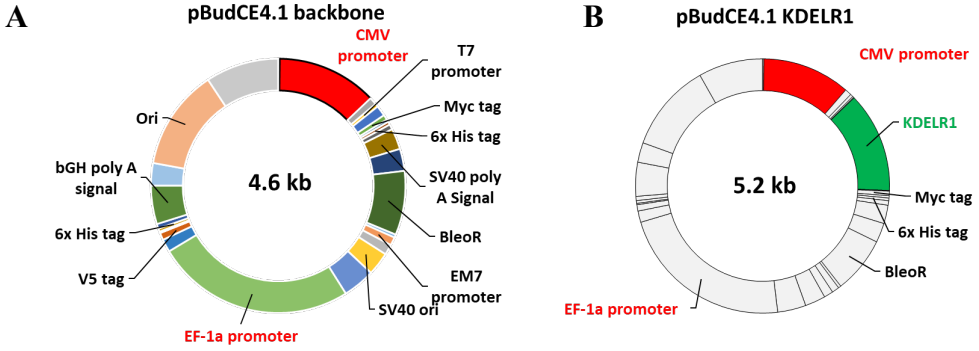

Figure 10: Illustration of the constructed plasmid expressing KDELR1

Transfection and stable cell line generation: The CHO-HcD6 (RRID: CVCL_9Y69) cell line was developed in Tokushima university from CHO-K1 parental cells. This cell line expressed IgG1 stably under puromycin selection (Onitsuka & Omasa, 2015). CHO-HcD6 will be referred to as CHO-K1-IgG1 hereafter. CHO-K1-IgG1 cells growing in the exponential phase in

suspension batch culture were transfected once using Neon Transfection System (Thermo Fisher Scientific) as per the manufacturer protocol. Briefly, 4 x 10^5 cells were transfected by two micrograms linearized empty vector or *Kdelr1*-encoding plasmid. The transfected cells were then seeded in 6 well plates. Two days after the transfection, cells were selected by 100 µg/mL Zeocin (Invitrogen) for two weeks while exchanging medium every three days. Cells were expanded and then grown in 125 mL shake flask as appropriate. The generated cell pool was called CHO-K1-IgG1-KDELR1. Cells were adapted for two passages in a shaker incubator at 90 rpm, 80% humidity, 37 °C and 5% CO_2. For reservation, Cell Reservoir One (with DMSO) (Nacalai Tesque, Kyoto, Japan) was used to resuspend cells and store directly in -80°C or at the vapor phase of liquid nitrogen.

Growing the engineered cell pool in batch culture: The mock cell pool CHO-K1-IgG1 and the engineered cell pool CHO-K1-IgG1-KDELR1 suspension cell lines were seeded in 30 mL mTOp2 medium supplemented with 6 mM L-glutamine and 15 µg/mL puromycin and 50 µg/mL Zeocin. Samples were taken daily for viable cell density and viability checking using Vi-CELL™ Cell Viability Analyzer. Total RNA was extracted at day 4 of the batch culture and RT-qPCR was run against *Kdelr1*, IgG1 heavy chain, IgG1 light chain, *Kdelr2*, *Kdelr3* and the four KDEL chaperones: Calreticulin (*Calr)*, PDI (*P4hb)*, GRP94 (*Hsp90b1*) and BiP (*Hspa5*) as previously mentioned. The batch culture was run four independent times using the same engineered cell pool.

Enzyme linked immunosorbent assay: Standard protocol for sandwich enzyme linked immunosorbent assay (ELISA) was performed for the quantification of IgG1 as previously described (Onitsuka et al., 2012). The reagents used for this ELISA assay are summarized in **Table 7**. Protein A purified IgG1 was used as a reference for the standard curve.

Table 7: ELISA reagents

Primary antibody goat anti-human IgG-Fc fragment antibody	A80-104A	BETHYL laboratories, Montgomery, TX, USA
Secondary antibody goat anti-human IgG-Fc fragment antibody horseradish peroxidase (HRP) conjugated	A80-104P	BETHYL laboratories
KPL ABTS Peroxidase Substrate	5120-0034	SeraCare
KPL ABTS Peroxidase Stop Solution	5150-0018	SeraCare

Specific growth rate and productivity: Specific growth rate and specific productivity were calculated as previously mentioned (Ohya et al., 2008; Omasa et al., 1992). The integral viable cell density was calculated as shown in the below equation. The exponential growth curve was constructed. The points that showed high linearity (based on the fitting of best-fit curve and R^2 value) were considered the exponential stage of the batch culture. It was found to be during the first four points of batch culture from the first day to the fourth day. The period from the fourth day to the seventh day showed reduced growth and was considered as the deceleration phase.

The equations are briefly described below:

$$IVCD_2 = \frac{(V_1 + V_2)}{2} \times \frac{(t_2 - t_1)}{24} + IVCD_1$$

$$q_p = \frac{IgG1\ titer}{IVCD}$$

Where IVCD is integral viable cell density, V_1 is viable cell density at t_1, t_1 is time in hours, q_p is specific production rate as calculated in (Aghdam et al., 2019; Ohya et al., 2008; Omasa et al., 1992).

Chase assay of CHO-K1-IgG1-KDELR1 pool: A chase assay of intracellular IgG1 was performed as previously described (Kaneyoshi et al., 2019). The purpose of this experiment was

to check whether the KDELR1 overexpression has any effect on the secretion process of IgG1. Briefly, cells growing in suspension batch culture were treated by 50 µg/mL cycloheximide when they reached 2×10^6 cells/mL. Sampling was performed for 8 hours. The rest of the chase assay experiment was performed as previously mentioned (Kaneyoshi et al., 2019).

The *Kdelr1* gene in the constructed plasmid backbone was sequenced and submitted to DDJB under accession number LC342268. The open reading frame showed full identity to the predicted transcript.

Statistical analysis: In this chapter, error bars represent the standard deviation. Unpaired two tailed student t-test was used to calculate significance as previously mentioned (Ohya et al., 2008).

Table 8: List of RT-PCR primers used for gene expression analysis

Gene	Protein name	Gene ID (NCBI database)	RT-PCR forward primer	RT-PCR reverse primer	Product size
Kdelr1	KDEL receptor 1	100750912	CTGTGGTGTTTACTGCCCGG	CCACACCGTAGTAAAGGAACAAGC	107 bp
Kdelr2	KDEL receptor 2	100765889	GAATTTCTGGTGGTTCCCGTGG	GGTCTCAGCCTCGCCAGTC	153 bp
Kdelr3	KDEL receptor 3	100750636	ACCAACGGAGGTACTCTGGAC	AGTGAGTGGTGATGGTCTCAGC	110 bp
P4hb	Protein disulfide isomerase (PDI)	100689433	TCTGACTACGATGGCAAGTTGG	GGCCAAAGAACTCCAGGATACG	115 bp
Hspa5	Binding immunoglobulin protein (GRP78/BiP)	100689305	TCGGTGGGTCTACTCGGATTC	CCGTATGCTACAGCCTCATCTG	106 bp
Hsp90b1	Endoplasmin (GRP94)	100773331	GGAATCTCCTTGTGCTCTTGTGG	TAGAGATGTCCTTGCCCGTTTGG	101 bp
Calr	Calreticulin	100689096	ACCTGCCGTCTATTTCAAAGAGC	TCCCCGTAGAATTTGCCAGAACT	123 bp
Ddit3	CCAAT-enhancer-binding protein homologous protein (CHOP)	100763514	GGAAACAGAGTGGTCAGTGC	AGCTGTGCTACTTTCCTCTC	88 bp
Actb	Beta-actin	100689477	ACTCCTACGTGGGTGACGAG	AGGTGTGGTGCCAGATCTC	117 bp

2.3 Gene expression analysis of KDEL receptor and KDEL chaperones

2.3.1 During Batch culture

RT-qPCR was used to detect the relative gene expression level during batch culture of IgG1 producing cell line and its parental CHO-K1 cells. The checked gene showed gradual increase in their expression level along the batch culture. This gradual increase was very minimal in some genes while very noticeable in others. The results are shown in **Figure 11**. At the beginning of the culture, *Kdelr1* expression was mildly upregulated, as well as in other chaperones. Compared to CHO-K1, CHO-K1-IgG1 showed tendency to reach ER stress faster. This is indicated by the upregulation of BiP to 3.82 ± 0.99-fold increase in CHO-K1-IgG1 cells at day 6 of culture. Similarly, endoplasmin (GRP94) also showed a gradual increase in expression reaching 2.23 ± 0.56-fold increase in CHO-K1-IgG1 on day 6 of batch culture. Additionally, PDI A1 (P4hb) showed less than 2-fold increase in both cell lines. A well-known indicator of the activation of apoptosis is CCAAT-enhancer-binding protein homologous protein (CHOP). It is a transcription factor that is induced during ER stress by the UPR and mediates apoptosis (Nishitoh, 2012). At day 6 of batch culture, CHOP showed a 7.07 ± 1.47-fold increase in CHO-K1 cell expression and an 8.85 ± 2.63-fold increase in the CHO-K1-IgG1 cells, indicating that the cells are entering the apoptotic phase. However, *Kdelr1* showed almost a linear expression level of no more than 2-fold increase during the batch culture. This result shows that Kdelr1 expression does not respond equally to the increase in expression level of other KDEL chaperones as well as the activation of apoptotic pathway by the upregulation of CHOP. This phenomenon is better illustrated by the ER stress induction in the following section.

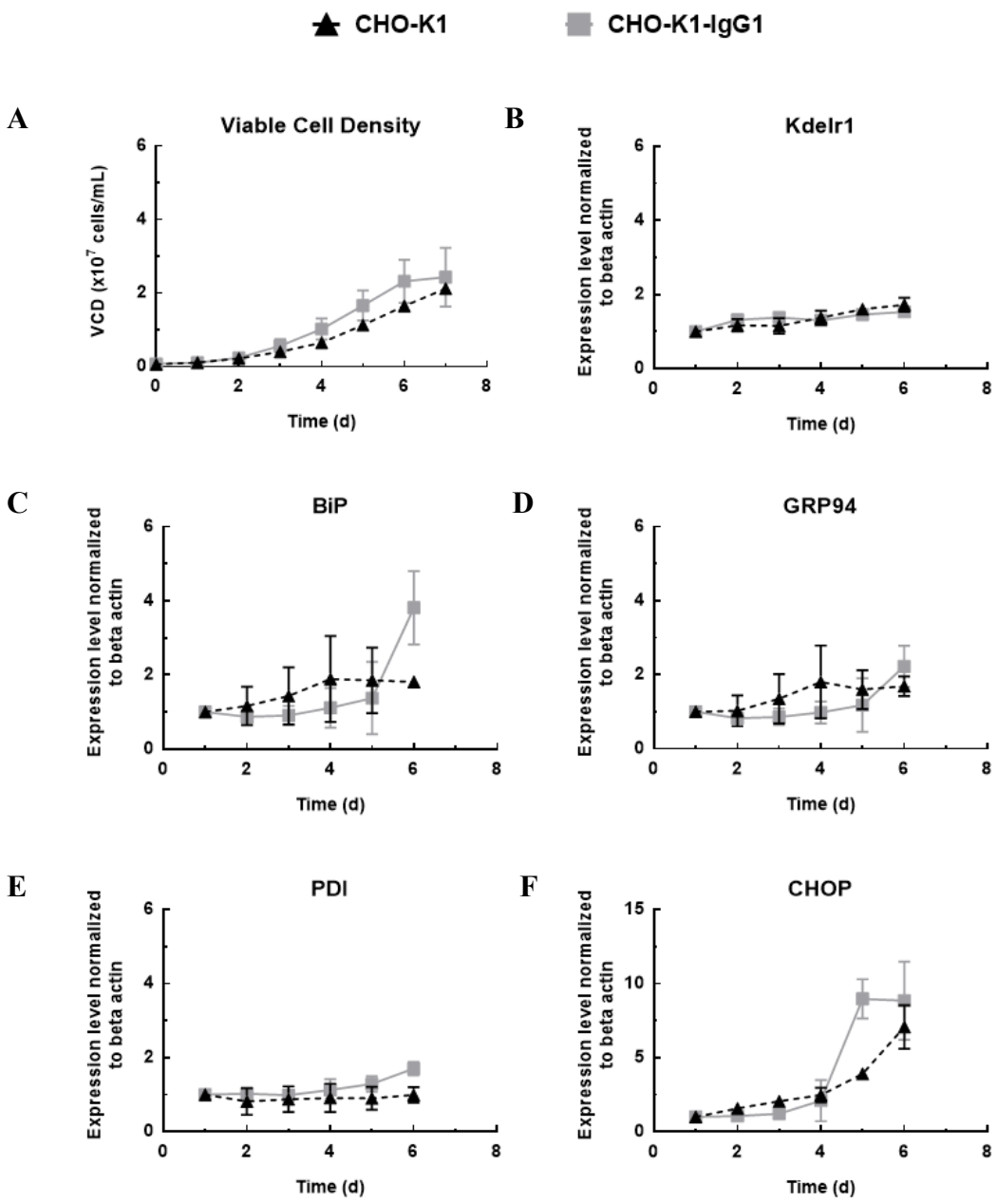

Figure 11: Dynamics of *Kdelr1* and KDEL chaperones gene expression during batch culture
CHO-K1 (n = 2) and CHO-K1-IgG1 (n = 3) normalized to Beta-actin and to day 1 of batch culture for each gene. **(A)** viable cell density (**B**) Kdelr1 (**C**) BiP (**D**) GRP94 (**E**) PDI (**F**) CHOP (Error bars indicate the mean ± SD). Gene expression analysis was performed using the ΔΔCT method by the StepOnePlus™ software.

2.3.2 During ER stress

In the previous section, the dynamics of gene expression of KDEL chaperones and KDELR1 were compared. However, in order to reach the maximum applicable gene expression level and compare between them more clearly, a chemical induction of ER stress is necessary. Therefore, tunicamycin was used to induce ER stress in suspension batch culture of CHO-K1 cells. Total RNA was then extracted after 20 hours of exposure, and cDNA was synthesized. RE-qPCR was run as previously mentioned. Each sample was normalized to its Beta-actin expression level, and then the treated samples (tunicamycin) were normalized to the vehicle samples (DMSO). The vehicle-treated samples were given a value of one. The upregulation of genes indicates the values of gene expression after 20 hours of exposure to tunicamycin.

The ER stress induction results are shown in **Figure 12**. The KDEL receptors showed less than 2-fold increase during ER stress. Contrarywise, the four KDEL motif-bearing chaperones were highly upregulated. GRP78 (BiP) and Endoplasmin (GRP94) showed the highest response to ER stress with more than 10-fold increase in gene expression. Calr showed 5-fold upregulation, while PDI showed 2-fold increase. The experiment was performed three independent times. All upregulation values were significant ($n = 3$, $p < 0.01$). It is obvious from these results that the response of KDEL receptors and chaperones to ER stress is not coordinated. The chaperones show several-fold upregulation in order to allow the cell to handle the accumulation of unfolded proteins that were induced by tunicamycin.

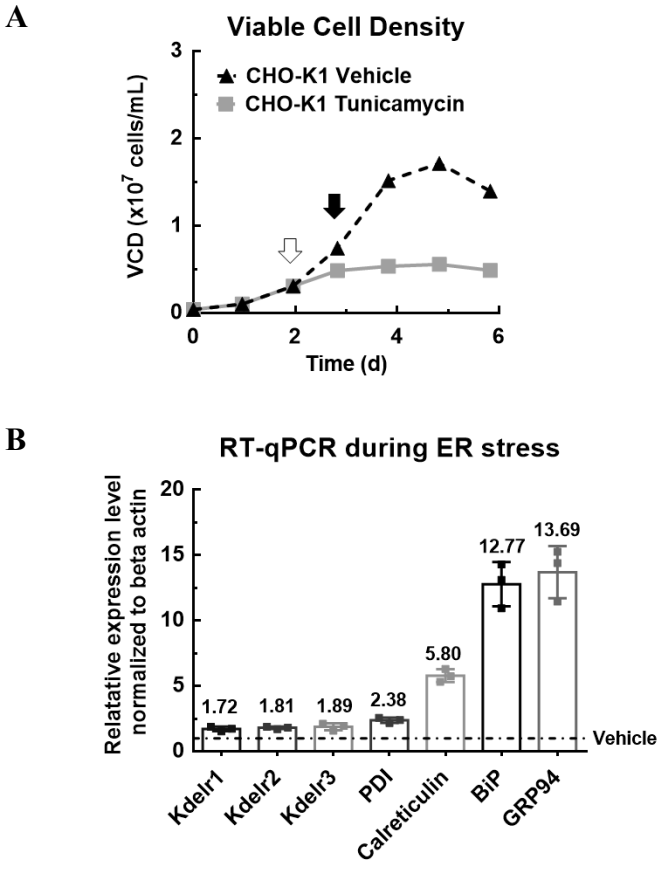

Figure 12: ER stress induction in CHO-K1 cells.

Effect of ER stress induction on the expression level of KDEL receptors and KDEL bearing chaperones in CHO cells by RT-qPCR after exposure to 5 µg/mL tunicamycin.

(A) A batch culture of the CHO-K1 cells was cultured. When the cells reached about 3×10^6 cell/mL at 48 hours (white arrow), the culture was treated with tunicamycin at 5 µg/mL or 30 µL volume of DMSO vehicle as control. The growth of the CHO cells almost stopped after treatment with tunicamycin, while the vehicle treated sample showed normal growth. The culture was sampled 20 hours after treatment for total RNA extraction at 68 hours (black arrow). **(B)** RT-qPCR data showing the upregulation of the three KDEL receptors and the four KDEL bearing chaperones; PDI, Calr, BiP and GRP94. (Error bars indicate the mean ± SD, $p< 0.01$, n = 3).

2.4 Overexpression of KDELR1 in CHO-IgG1 cells

The generated cell pool overexpressing KDELR1 was called CHO-K1-IgG1-KDELR1. In this experiment one stable cell pool was generated and then batch culture was performed four independent times. Briefly, the stable cell pool and the mock transfected pool were seeded as batch culture in 30 ml culture volume. Samples were taken daily for the analysis viable cell density, viability, IgG1 concentration and gene expression level. The viable cell density, titer, and viability of the batch culture are shown in **Figure 13**.

Samples from day four (96 hours) were used for total RNA extraction, first strand cDNA analysis and RT-qPCR analysis. The engineered cell pool showed a significant 2.77-fold increase in *Kdelr1* gene expression when compared to CHO-K1-IgG1 ($n = 3$, $p < 0.05$). Nevertheless, IgG1 heavy chain and light chain expression did not show any significant change. These results are represented in **Figure 14A**. *Kdelr2*, *Kdelr3* expression levels remained the same in both cell pools. The relative gene expression levels of GRP94, BiP, PDI and Calr were unaffected by the overexpression of *Kdelr1*. These RT-qPCR were anticipated because KDELR1 is expected to be working on the protein level and not on the mRNA level of chaperones.

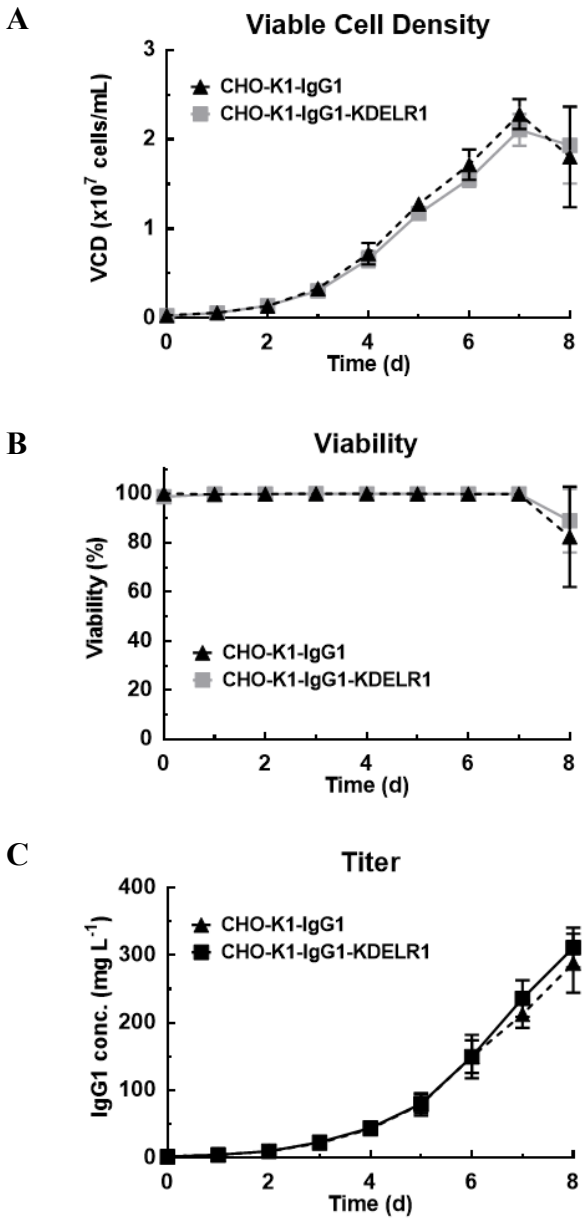

Figure 13: Batch culture of CHO-K1-IgG1-KDELR1 cell pool.

Stable overexpression of Kdelr1 in suspension batch culture. (**A**) Viable cell density, (**B**) viability, (**C**) IgG1 titer. The batch culture was performed four independent times of the same cell pool.

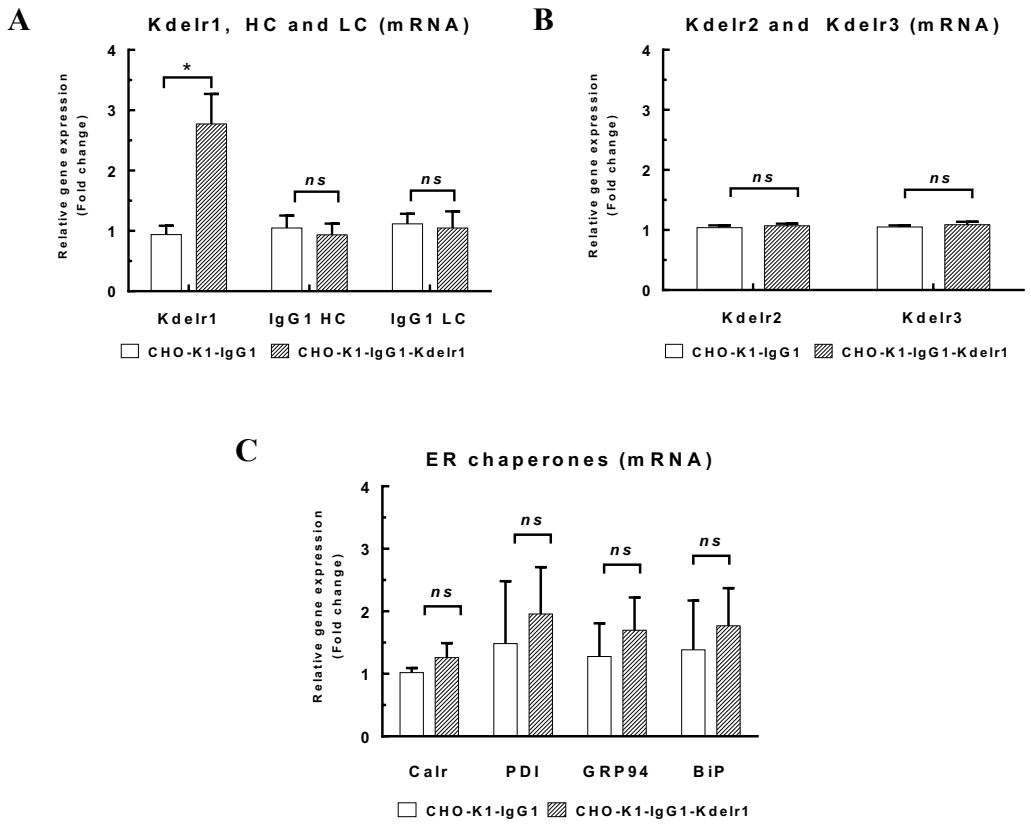

Figure 14: Relative gene expression levels during batch culture

Relative gene expression levels of different genes during day four of the batch culture of CHO-K1-IgG1 and CHO-K1-IgG1-KDELR1

(A) Kdelr1 and IgG1 heavy chain (HC) and light chain (LC), **(B)** Kdelr2 and Kdelr3 growth, **(C)** the four KDEL chaperones. Samples were taken at day four of the batch culture (Error bars indicate the mean ± SD, *$p < 0.05$, ns, non-significant).

Th exponential phase of batch culture was determined according to the linearity of the integral viable cell density of the culture. Day one to day four of the culture were linear and had a greater slope than those of the later points as shown by comparing **Figure 15C** and **Figure 15D**. accordingly; they were considered as the exponential phase of the culture. The following days of the culture from day 4 to day 7 showed reduced cell growth; therefore, they were considered as the deceleration phase of the culture. During the exponential phase of the culture (day 1 to 4), CHO- K1-IgG1-KDELR1 stable pool showed specific IgG1 productivity of 5.04 pg cell^{-1} day^{-1} compared with the parental CHO-K1-IgG1 which was 4.45 pg cell^{-1} day^{-1} revealing 13.2% improvement. Similarly, during the end-stage batch culture (deceleration phase), CHO-K1-IgG1-KDELR1 higher productivity of 4.74 pg cell^{-1} day^{-1} compared with the parental CHO-K1-IgG1 3.83 pg cell^{-1} day^{-1} revealing 23.8% improvement in specific production rate as shown in **Figure 15**. The batch culture was conducted four independent times of the same cell pool.

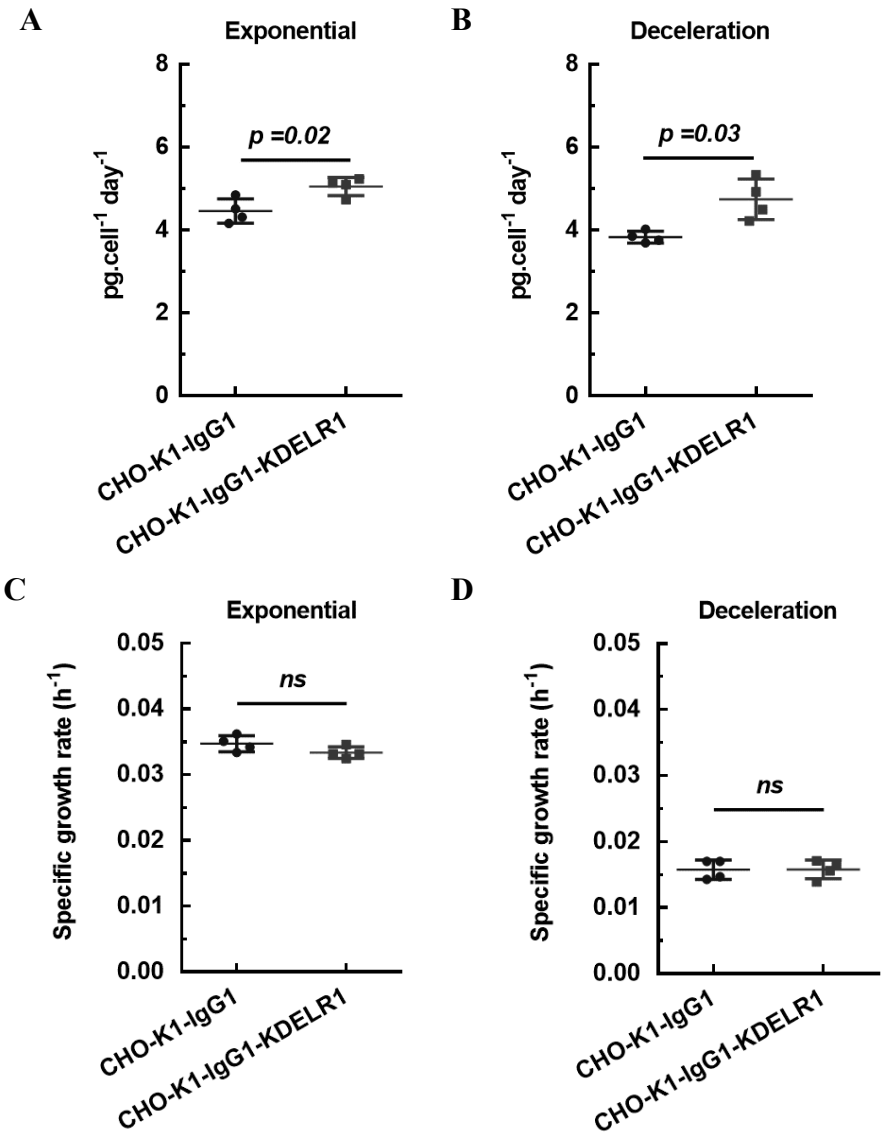

Figure 15: Specific production and growth rates

Specific production rates of the engineered CHO-K1-IgG1-KDELR1 in comparison to the mock transfected CHO-K1-IgG1 during (**A**) exponential phase (day 1-4) or (**B**) deceleration phase (day 4-7). Specific growth rates during (**C**) exponential and (**D**) deceleration phases. The calculation if from 4 different experiments of the same transfected cell pool. p values less than 0.05 are considered significant. Significance was calculated using unpaired student t-test.

2.5 Discussion

The KDEL receptors are seven-transmembrane-domain proteins that recycle between the endoplasmic reticulum and *cis*-Golgi and responsible for the retention of missorted ER chaperones from post-ER compartments (Capitani & Sallese, 2009; Wilson et al., 1993). The retention mechanism is based on the pH difference between the ER and *cis*-Golgi. Particularly, the pH of the ER is higher than that of the *cis*-Golgi, promoting KDEL receptor and KDEL motif binding in the low pH and release in the higher pH. Several engineering approaches overexpressed chaperones aiming at increasing the cell productivity. In this chapter the expression level of KDEL receptors and chaperones were investigated. Additionally, the effect of overexpression of KDELR1 on IgG1 production rate is reported.

In this chapter, the changes in of *Kdelr1* expression during parental CHO-K1 cells and rCHO cells are reported. During batch culture, *Kdelr1* showed no more than 2-fold upregulation in CHO-K1 by comparing day 1 to day 6 of the batch culture in both cell lines. BiP and GRP94 showed upregulation at the end stage of batch culture. This could be explained by the depletion of glucose from the culture at the end stage causing ER stress. Since BiP and GRP94 are glucose regulated proteins, this may be the reason for the increase in expression.

ER stress was induced in CHO-K1 cells using tunicamycin. Tunicamycin is a common ER stress inducer that blocks the initial glycosylation step of newly synthesized glycoproteins. This consequently induces ER stress and activates the UPR pathway as mentioned in **Section 1.4**.This leads to the upregulation of several transcription factors and ER chaperones to regain cell homeostasis. During ER stress induction in CHO-K1 cells, the three KDEL receptors were mildly changed by less than 2-fold increase after 20 hours of exposure to the ER stress compared with the control. Nevertheless, the expression level of BiP and GRP94 showed more than 12-fold increase.

Calr and PDI showed more than 2-fold upregulation. This outcome confirms with a described 1.8-fold upregulation of KDEL receptor 1 in HeLa cells using ER stress inducers (P. Wang et al., 2011). Noticeably, the expression levels of the three KDEL receptors were mildly affected by the activation of the UPR signaling pathway, although their target proteins were significantly upregulated. In this study, I show that the three KDEL receptors were upregulated similarly during ER stress induction by tunicamycin in CHO cells. Our data confirms with other studies where the expression levels of ER chaperones like BiP, PDI, and GRP94 were described to increase several folds during tunicamycin treatment in CHO cells (Maldonado-Agurto & Dickson, 2018; Segar et al., 2013).

Overexpression of chaperones in recombinant CHO cells showed different responses on their productivity from reduction in productivity to 2-fold increase in productivity as summarized in **Table 2**. Despite that most of these chaperones have a KDEL motif at their C-terminal, the effect of KDELR1 overexpression on recombinant protein productivity has never been reported. Accordingly, in this study I report the effect of this overexpression on IgG1 productivity in CHO cells. KDELR1 overexpression showed no significant effect on the overall titer, the specific growth rate or the viable cell density. Also, the mRNA level of heavy and light chains did not change. However, the specific production rate increased during the exponential and late-stage batch culture. It was a little increase but a significant one. This could be reported better in a fed-batch culture where the culture extends longer and the effect can appear better. However, this study focuses only on the molecular aspect of KDEL receptors and their functional role.

Chapter 3:

Secretion of ER chaperones to the medium

3.1 Overview

Owing to their substantial role in protein folding, maturation and trafficking, ER chaperones have been extensively studied in CHO cells for both understanding CHO cell biology and engineering. However, ER retention machinery, saturation and chaperones' secretion to the medium have not been studied yet.

In this chapter, I investigate the secretion of ER chaperones to the medium in normal conditions, during overexpression of a KDEL chaperone and during ER stress. I overexpress one of the KDEL bearing ER chaperones (PDI A1) and check its secretion and abundance in the medium. I also induce ER stress and detect the secretion of the chaperones to the medium.

Additionally, to detect whether or not chaperones' secretion to the medium is due to saturation of the ER retention machinery (KDEL receptors), I expressed KDELR1 under ER stress sensitive promoter (BiP promoter) and induced ER stress. By studying the trafficking of ER chaperones in CHO cells, I gain better understanding of CHO cell biology and therefore allows us for better engineering of CHO cells for recombinant protein production. The aim of this experiment was to engineer a CHO cell model capable of making the best use of its ER chaperones during stress condition that appear during recombinant protein production. The anticipation of this experiment is to prevent the secretion of chaperones in CHO cell during stress conditions, and therefore they can work intracellularly by regaining cell homeostasis.

One strong advantage of using CHO cell in this context is that CHO cells are easily adapted to serum-free medium. Accordingly, they can grow in large scale suspension cultures. This serum-free condition allowed us to concentrate the medium by ultrafiltration. Serum is highly rich in

albumin and other antibodies that interfere with the concentration by ultrafiltration and mask other proteins in western blotting (H. Wang & Hanash, 2005).

The media concentration protocol was developed stepwise. At the beginning, concentration of media from adherent CHO cells growing in 10% FBS was conducted by salting out with ammonium sulfate. However, this turned to be a major problem because the precipitate contained a lot of proteins (albumins and antibodies) that their origin was not from CHO cells and interfered with the immunoblotting assays. Next, cells were grown in serum-free medium to avoid this obstacle. Ultrafiltration was found to be the most convenient way of media concentration and the chaperones were detected straightforwardly.

Expression of KDELR1 under a stress sensitive promoter is a novel cell engineering approach that has never been conducted in any reported cell model.

3.2 Materials and Methods

Cloning of **KDELR1 and PDI, and generation of a stable cell lines:** I used the previously constructed plasmid to generate stable CHO-K1 cells overexpressing KDELR1. Similarly, PDI was cloned and overexpressed. Briefly, total RNA was extracted from CHO-K1 cells using the FastGene RNA Premium Kit (Nippon Genetics, Tokyo, Japan) followed by first strand cDNA synthesis using the Primescript cDNA synthesis kit (Takara Bio, Shiga, Japan). PDI was PCR amplified the primers in **Table 9** and inserted into the plasmid under the CMV promoter. Transfection was conducted using the Neon Transfection System (Thermo Fisher Scientific, Waltham, MA, USA). The plasmids' maps are shown in **Figure 16**.

Table 9: PDI cloning primers

Forward primer	5'-CCAGCCTCGAGACATGCTGAGCCGTTCTCTGCTG-3'	XhoI site
Reverse primer	5'-GATGCGGCCGCCACCGAGGTCTTGGGTTTGGGT G-3'	NotI site

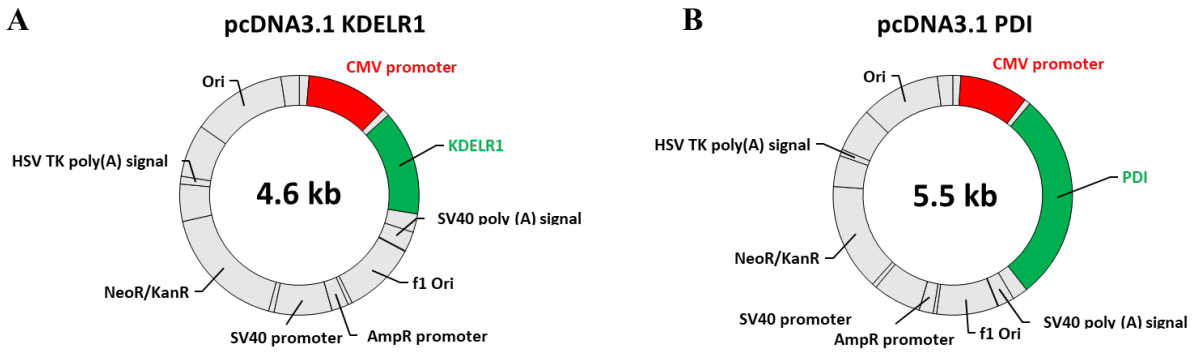

Figure 16: Plasmids expressing KDELR1 or PDI

(A) KDELR1 cloned into pcDNA3.1 backbone, (B) PDI cloned into pcDNA 3.1

Batch culture of KDELR1 and PDI overexpressing cells: CHO-K1, CHO-K1-KDELR1 and CHO-K1-PDI cell suspensions were used as a model to investigate the possibility of ER saturation and secretion of chaperones into the medium. Cells were seeded in 20-mL cultures of serum-free BalanCD CHO growth A medium (Irvine scientific, Santa Ana, CA, USA) containing 6 mM L-glutamine with or without 800 µg/mL G418. The cell concentration was determined using a Vi-CELL XR, Cell Counter (Beckman Coulter, Brea, CA, USA). Samples were taken from harvested cells (RIPA buffer with 1% protease inhibitor) when the cell concentration reached ~50–100 × 10^5 cells/mL.

Media concentration: For concentrating the medium, 12 mL of the culture medium was centrifuged at 10,000 ×*g* for 2 minutes to separate the cell pellet. The supernatant was then collected and filtered using a 0.22-µm syringe filter. Next, 10 mL of this syringe filtered supernatant was concentrated by ultrafiltration using Amicon Ultra-4 Centrifugal Filter Units, MWCO = 30,000 (Merck Millipore, Burlington, MA, USA) at 4,000 ×*g* for 10 minutes each cycle. The supernatant was then buffer-exchanged using 4 mL 1× phosphate buffer saline (PBS).

Western blotting: Samples were loaded onto 12% SDS-PAGE gels unless mentioned otherwise. Electrophoresed proteins were then transferred to PVDF membranes using the semi-dry method. Alternatively, some samples were loaded onto SDS-PAGE and blotting system (Merck, KGaA, Darmstadt, Germany) wherever mentioned. The Immobilon Western Chemiluminescent HRP substrate (WBKLS0500, Merck Millipore) was used for chemiluminescent imaging using a LuminoGraph II, Chemiluminescent Imaging System (ATTO, Tokyo, Japan). Band intensities were measured by using CS Analyzer (ATTO, Tokyo, Japan).

Antibodies: The antibodies that were used for the immunoblotting are summarized in the following table (**Table 10**).

Table 10: Antibodies for immunoblotting

Target	Primary antibody	Secondary antibody
Beta -actin	Mouse mAb [8H10D10, #3700, Cell Signaling Technology, Danvers, MA, USA]	HRP-conjugated rabbit anti-mouse IgG H&L (ab6728, Abcam)
BiP	Rabbit Ab, 3177, Cell Signaling Technology	Goat anti-rabbit IgG H&L (HRP) (ab6721, Abcam).
PDI (P4hb)	Rabbit Ab, ab137110, Abcam, Cambridge, UK	
Calr	Rabbit Ab, 2891, Cell Signaling Technology	
GRP94	Rabbit Ab, 2104S, Cell Signaling Technology	

Cloning of BiP promoter: Genomic DNA was purified from a CHO-K1 suspension culture using the High Pure PCR Template Preparation Kit (Roche Life Science, Penzberg, Germany). The BiP promoter was amplified using primers in **Table 11** using the Q5 High-Fidelity 2× Master Mix (New England Biolabs, Ipswich, MA, USA). The PCR product was then inserted into the pcDNA3.1-Citrine plasmid (Griesbeck et al., 2001) after digestion with HindIII and BamHI. Ligation was conducted by infusion cloning using the In-Fusion HD Cloning Kit (Takara Bio, Shiga, Japan) as per the manufacturers' protocol. The expression was transfected into CHO cells and the expression of Citrine examined (data not shown). Next, the promoter was amplified from the pcDNA3.1-BiP promoter-Citrine constructed plasmid using primers in **Table 11**. The PCR product was inserted into the previously constructed pBudCE4.1-KDELR1 plasmid (see **2.2**) after removing the CMV promoter by restriction digestion with SpeI and HindIII. Then, the mock backbone (pBudCE4.1) and the constructed plasmid were linearized and used to transfect CHO-K1 cells using the Neon Transfection System (Thermo Fisher Scientific). The cells were selected by 200 µg/mL Zeocin for two passages and then maintained at 100 µg/mL Zeocin.

RT-qPCR: RT-qPCR was performed as described previously in Chapter 2 using the same primer pairs.

Table 11: BiP promoter cloning primers

Forward	5′-TCTCGAGCTCAAGCTTCAACCTAACCCAGCCAAAC-3′	HindIII	From: Genome To: pcDNA3.1-Citrine plasmid
Reverse	5′-GGCGACCGGTGGATCCCTTGCCGGCGCTGTGGGC-3′	BamHI	
Forward	5′-CAGACTAGTTCAACCTAACCCAGCCAAACC-3′	SpeI	From: pcDNA3.1-BiP promoter-Citrine To: pBudCE4.1-KDELR1 plasmid
Reverse	5′-AACAAGCTTGATCCCTTGCCGGCGCTGT-3′	HindIII	

ER Stress induction: ER stress was induced using 5 µg/mL working concentration of tunicamycin, as described previously in **Section 2.2**, or 1 µM working concentration of thapsigargin unless mentioned otherwise. An equal volume of the vehicle dimethyl sulfoxide was used as the control. ER stress was induced in a suspension batch culture when the cell concentration was ~20×10^5 cells/mL.

Statistical analysis: Statistical analysis was performed using Tukey's multiple comparisons test. $P < 0.05$ was considered significant.

3.3 Overexpression of PDI or KDELR1 in CHO-K1 cells

CHO-K1 cells overexpressing KDELR1 (KDEL receptor 1) or PDI (family member 1, KDEL chaperone) were engineered to investigate the possibility of saturating the ER retention machinery and the secretion of ER chaperones into the medium. CHO-K1 cells overexpressing either KDELR1 or PDI were grown in batch cultures (**Figure 17A**). Cell samples were taken during the exponential growth phase, and both cell lysates and samples of concentrated medium were analyzed by SDS-PAGE. Media samples were concentrated by ultrafiltration using 30-kDa molecular weight cut-off (MWCO) membranes **(Figure 17B**). Samples were blotted onto PVDF membranes and probed against KDEL chaperones (i.e., GRP94, BiP, Calr and PDI) **(Figure 17C**).

Cells overexpressing KDELR1 did not show any improved retention in cell lysates or secretion into the medium of the KDEL chaperones. Cells overexpressing PDI (CHO-K1-PDI) showed a significant increase in the signal of band intensity of PDI in both the lysate and the sample of concentrated medium when compared with that of the parental CHO-K1 cells and CHO-K1-KDELR1 cells. Calreticulin was not released into the medium or the amount released was below the detection limit (**Figure 18**).

Noteworthy, GRP94 was secreted into the medium as a lower molecular weight species (i.e., 75–86 kDa) when compared with that of full-length GRP94 present in the cell lysate.

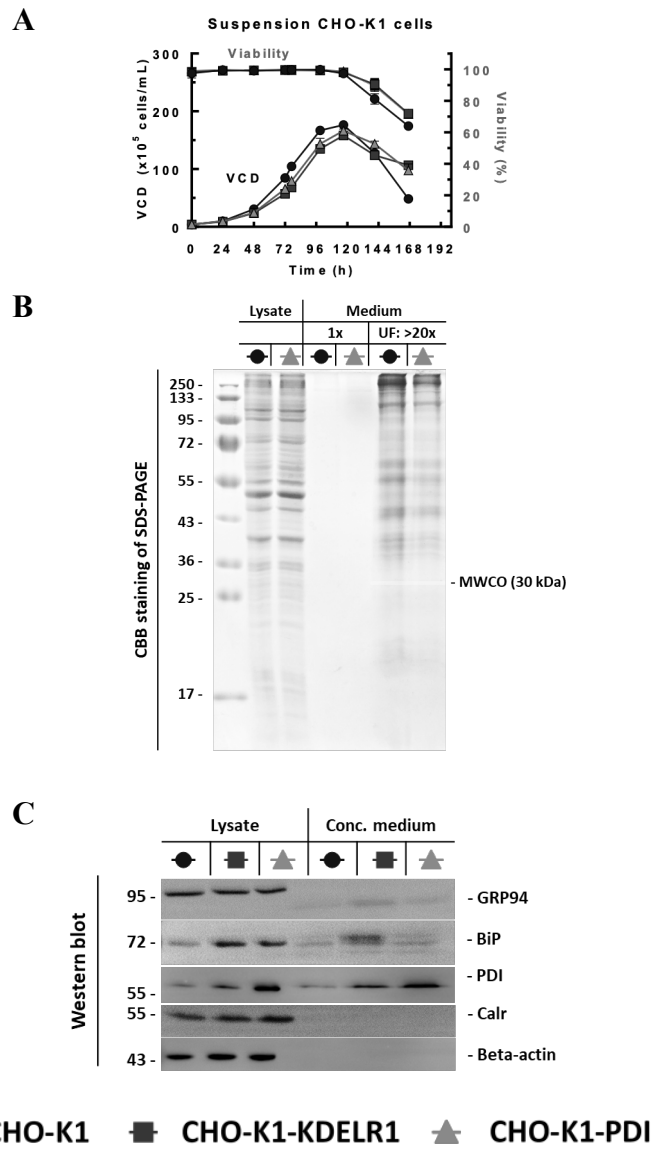

Figure 17: Secretion of PDI to the medium in PDI expressing cell line

(A) CHO-K1 suspension batch cultures showing the viable cell density and viability of the cells. The black arrow indicates the sampling time point during the exponential growth phase of the cultures. (B) CBB stained 12% SDS-PAGE gel showing the results for lysate samples, media samples and samples of concentrated medium prepared by ultracentrifugation using a 30 kDa molecular weight cut-off (MWCO) membrane. (C) Western blot of lysate samples and samples of concentrated medium against ER chaperone proteins BiP, PDI, Calr and GRP94. The experiment was repeated three independent times of the same engineered cell pool.

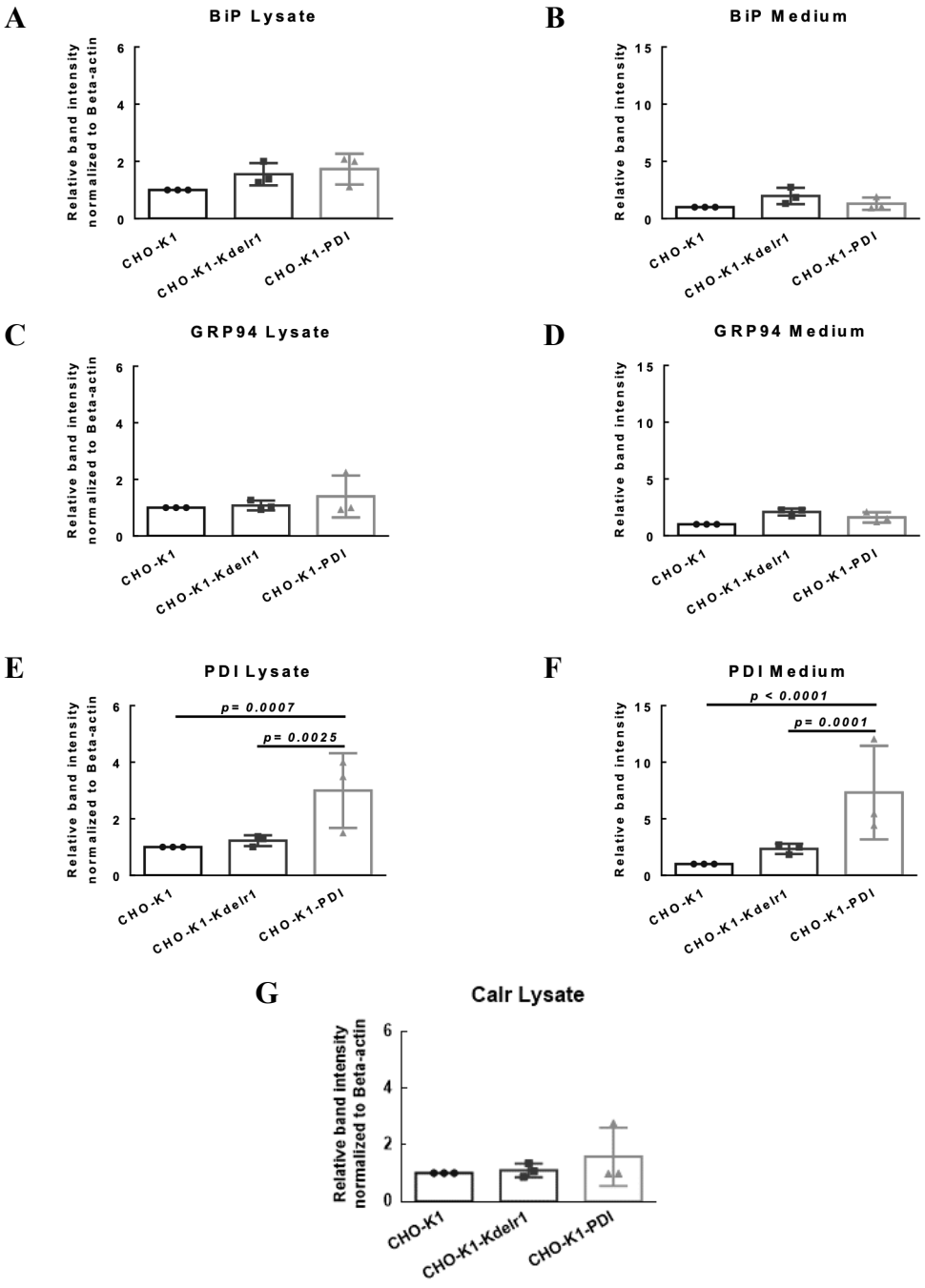

Figure 18: Band intensity analysis of lysates and concentrated medium in CHO-K1-PDI

Relative band intensity analysis normalized to beta-actin and to CHO-K1 cells as a control cell lysate sample. (A) BiP, (C) GRP94, (E) PDI and (G) Calr. (G) Relative band intensity analysis of a sample of concentrated medium normalized to CHO-K1 cells as control samples showing (B) BiP, (D) GRP94 and (F) PDI. Statistical analysis was performed using Tukey's multiple comparisons test. $P < 0.05$ was considered significant.

3.4 Engineering a CHO cell model with improved ER retention machinery

As the overexpression of PDI in the previous experiment (see **3.3**) showed increased abundance of this chaperone in the lysate as well as the medium, I thought to examine the secretion of chaperones to the medium during stress conditions. The previous ER stress induction experiment (see **2.3.2**) showed that KDEL receptors do not respond coordinately with the ER chaperones during stress conditions in CHO cells. This confirms with a previous research done on HeLa cells (Llewellyn et al., 1997). Accordingly, I hypothesized that I could engineer a CHO cell model that is capable of making the best use of ER chaperones during the stress conditions induced by the high protein load on the ER during recombinant protein production. Our approach is to express KDELR1 under a promoter that is responsive to ER stress. I chose BiP (Hspa5 gene) promoter as a highly responsive promoter to different conditions of ER stress. This approach will allow us to better understand the dependency of chaperones' secretion on KDELR1 expression level. KDELR1 under the BiP promoter was expressed and ER stress was then induced.

In order to decide how long of the BiP promoter to clone, the major ER stress elements and transcription factor binding sites were aligned on the BiP promoter upstream of the transcription start site (TSS). The major ER stress elements are shown in **Table 12**. Accordingly, three kilobases (kb) of the BiP promoter upstream of the transcription start site were cloned (**Figure 19A)** after defining the size of this promoter by aligning the known transcription factor binding sites (**Figure 19B**). This 3 kb BiP protomer sequence was cloned into the pcDNA3.1 plasmid and upstream of Citrine (GFP variant) (**Figure 19C**), and then cloned into the previously constructed pBudCE4.1-KDELR1 plasmid to replace the CMV promoter (**Figure 19D**).

Table 12: ER stress elements and motifs in the cloned BiP promoter

Motif name	Sequence	Reference
CHOP amino acid response element (AARE)	ATAGCATCA	(Kober, 2012)
cAMP response elements (CRE)/CREB / ATF4	GTGACGT	(Iozzo et al., 1997)
ER stress element (ERSE) I	CCAAT- cggaggcct*- CCACG	(Kober, 2012; Yoshida et al., 1998)
ER stress element (ERSE) II	ATTGG- t*- CCATG	(Kober, 2012)
ATF6	CCACGA	(Haze et al., 1999)
C/EBP-ATF composite site	TGATGCAAC	(Pan et al., 2007)
UPRE	TGACGTG	(Kober, 2012)

*Small letters represent a spacer sequence between two conserved sequences

A suspension batch culture (**Figure 20A**) was grown and samples taken for RT-qPCR and western blot analysis (**Figure 20B**). The engineered cell model expressing KDELR1 under the BiP promoter showed the expected upregulation of KDELR1 upon ER stress induction (**Figure 20C**). The gene coding for CHOP (C/EBP Homologous Protein) showed significant gene upregulation in both cell lines (**Figure 20D**) indicating the activation of UPR pathway. Quantitative RT-PCR of *Kdelr2* and *Kdelr3* showed minimal upregulation in mock and engineered cell lines (**Figure 20E-F**). Western blots of cell lysates and concentrated culture supernatants were measured to compare BiP and GRP94 specifically. GRP94 showed moderate but insignificant upregulation in cell lysates (**Figure 21C**) and a significant level of secretion (**Figure 21E**) into the medium during ER stress in both cell lines. In contrast, BiP showed significant upregulation in cell lysates and improved retention in engineered model in comparison with the mock cell during ER stress **(Figure 21D**). BiP also showed significant secretion into the medium (**Figure 21F**) in the mock cell line, but insignificant secretion in the BiP promoter-KDELR1 engineered cell model. GRP94 was secreted during ER stress as a low molecular weight species, as shown in **Figure 20B** (black arrows). Interestingly, the low molecular size GRP94 species was also found to be induced intracellularly upon ER stress induction (red arrows). This result suggests that a small molecular

weight species of GRP94 occurred intracellularly during ER stress and this GRP94 species is then secreted into the extracellular medium, and that this secretion is KDELR1 independent. PDI and Calr showed insignificant upregulation in mRNA, lysates or concentrated medium in both cell lines **Figure 22**.

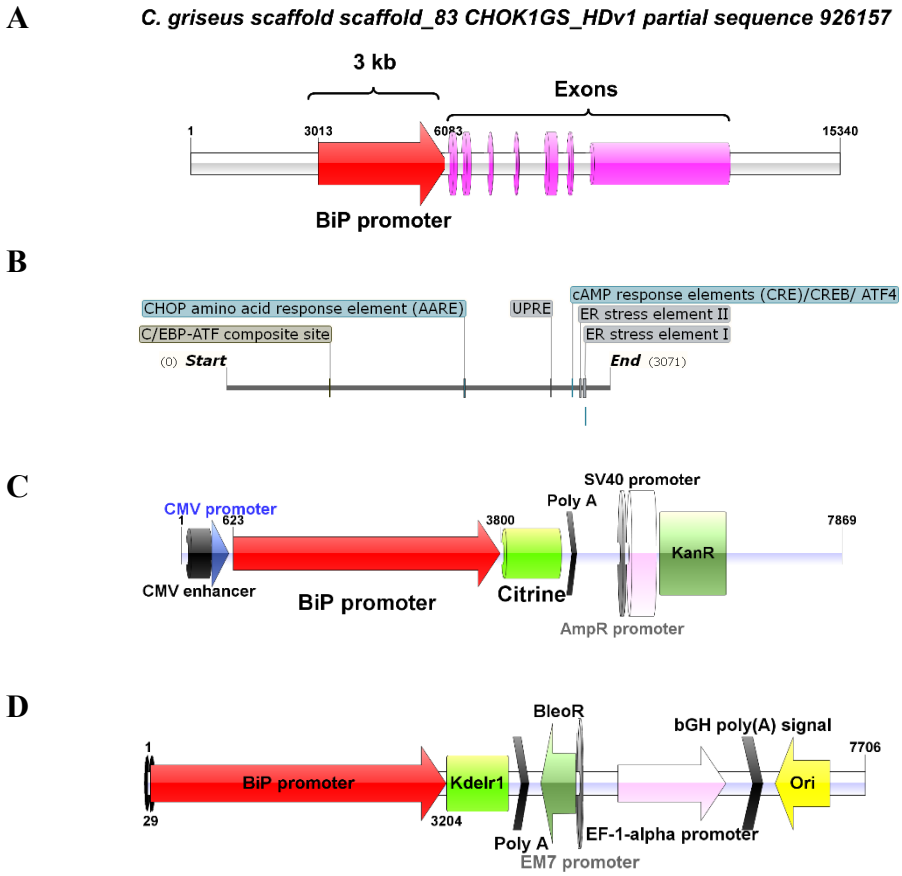

Figure 19: Cloning of KDELR1 under BiP promoter

(A) Scheme showing the Hspa5 gene (expressing BiP) in the CHO-K1 genome with the 3-kb BiP promoter upstream of the transcription start site. (B) Alignment of the ER stress elements on the cloned promoter length. (C) The 3-kb BiP promoter was cloned into the pcDNA3.1 plasmid and upstream of Citrine. (D) The BiP promoter was cloned upstream of KDELR1 in the pBudCE4.1-KDELR1 plasmid.

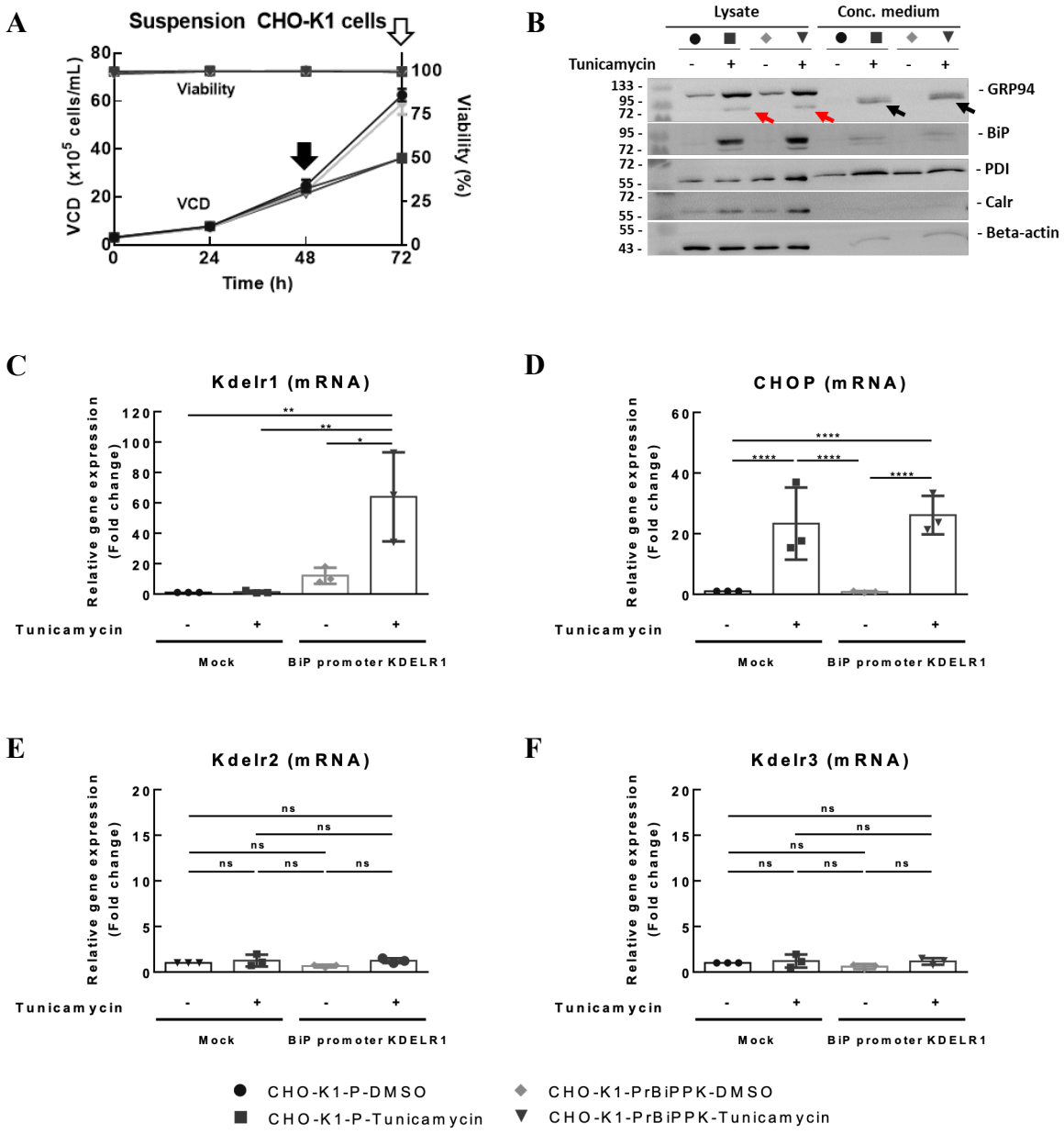

Figure 20: ER stress induction in the engineered CHO cell model (BiP promoter-KDELR1)

(A) ER stress was induced by the addition of 5 µg/mL tunicamycin during the exponential growth phase of the suspension batch culture. Black arrow indicates when ER stress was induced, while white arrow indicates the sampling time point and when medium samples were concentrated. (B) Lysates and samples of concentrated medium were blotted against the four chaperones (GRP94, BiP, PDI, and Calr) and beta-actin. Red arrows represent the truncated form of GRP94 induced by ER stress. Black arrows indicate the truncated form of GRP94 that is secreted into the medium during ER stress. Relative gene expression was measured by RT-qPCR with normalization to the beta-actin gene: (C) Kdelr1, (D) CHOP, (E) Kdelr2, (F) Kdelr3. Error bars represent mean and SD of three independent experiments of the same engineered cell pool. Statistical analysis was performed using Tukey's multiple comparison test. $P < 0.05$ was considered significant (*<0.05, **<0.01, ****< 0.0001). The engineered Kdelr1 mRNA values were calculated separately from the other mRNA results, ns: not significant, VCD: viable cell density.

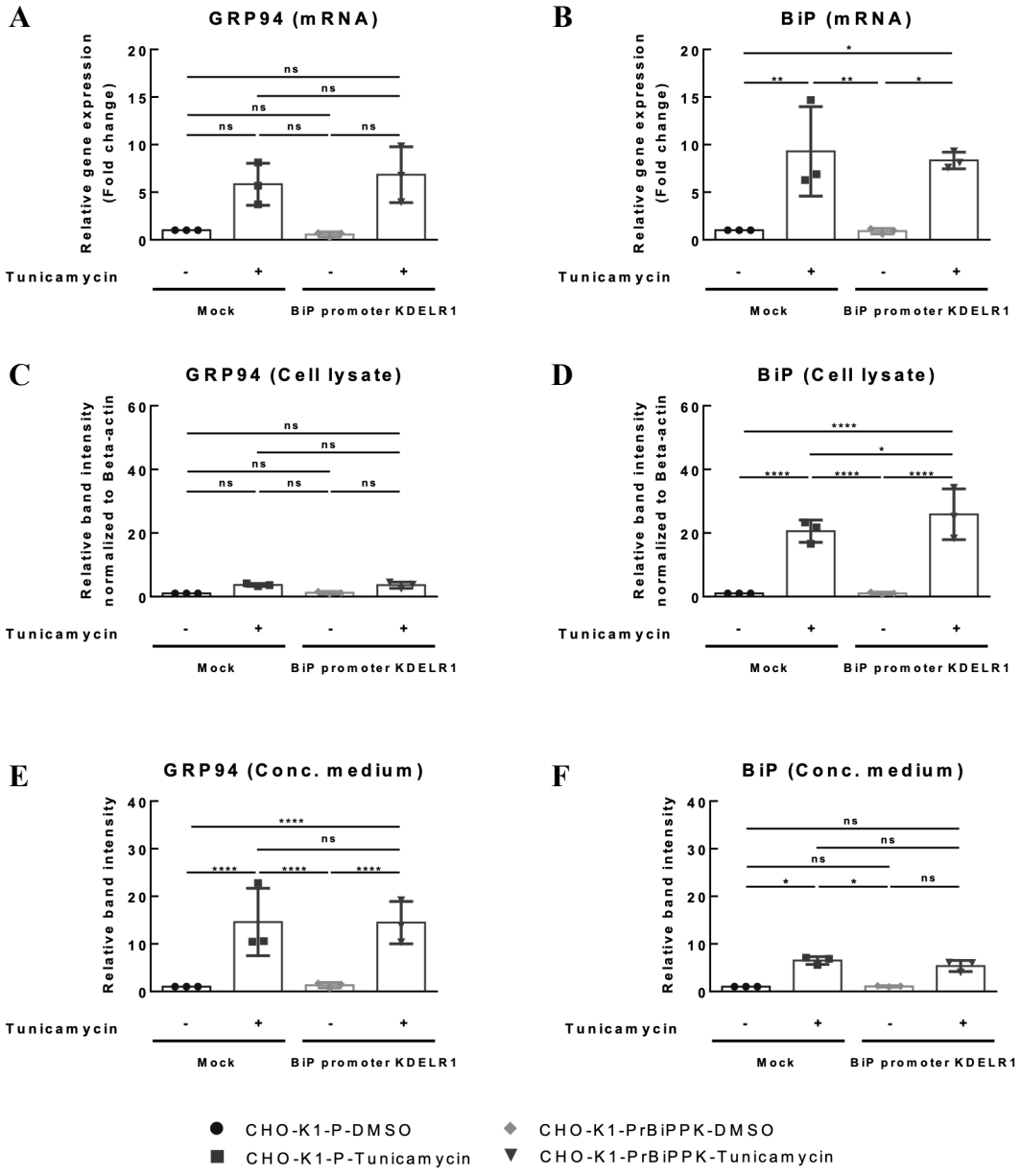

Figure 21: Expression and secretion of BiP and GRP94 in the constructed model

(A, B) mRNA expression, (C, D) lysate analysis and concentrated media analysis of GRP94 and BiP, respectively. Statistical analysis was performed using Tukey's multiple comparison test. $P < 0.05$ was considered significant (*<0.05, **<0.01, ****< 0.0001), ns: not significant.

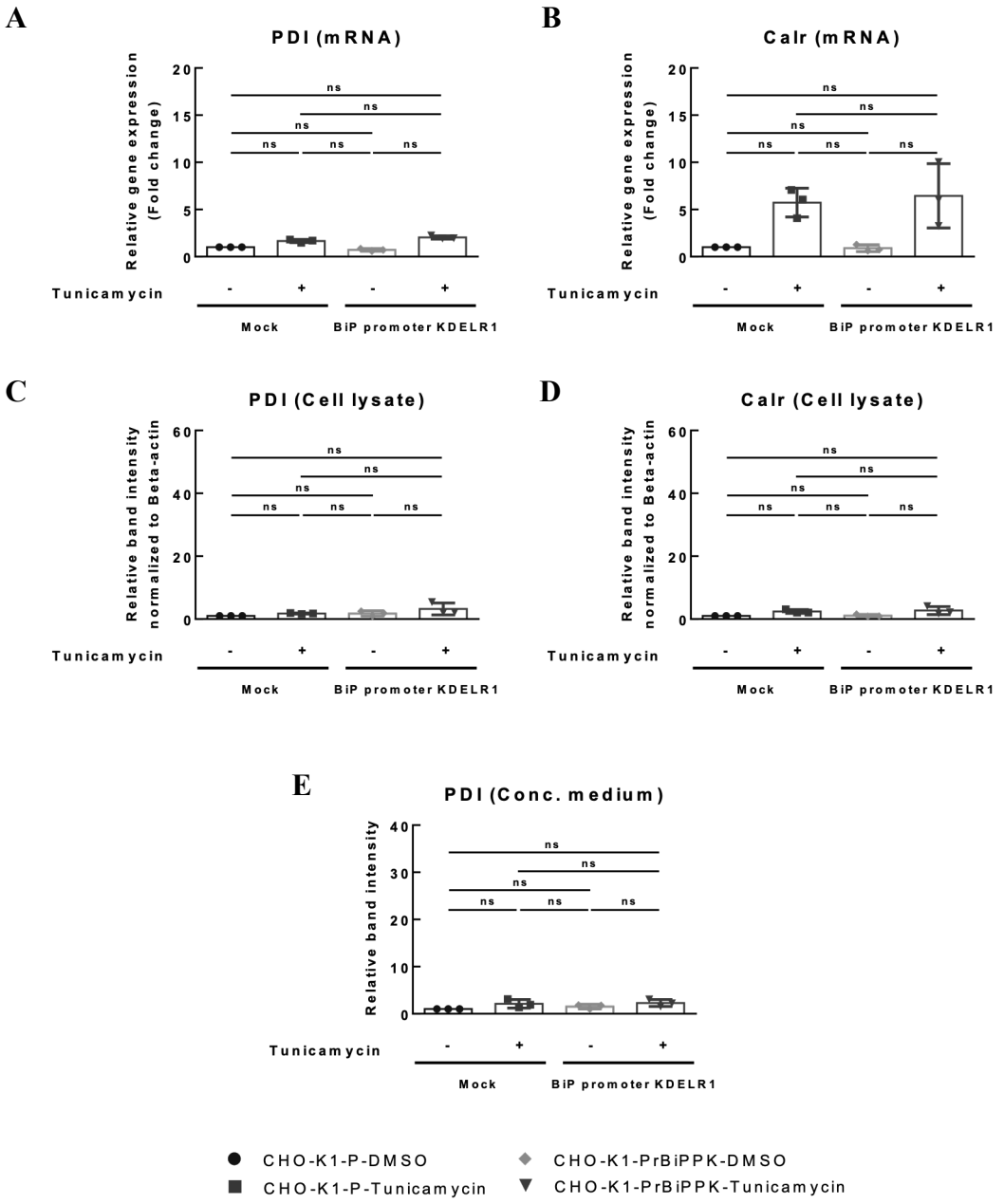

Figure 22: Expression and secretion of PDI and Calr in the constructed model

(A, B) mRNA expression and (C, D) lysate analysis of PDI and Calr, respectively. (E) band intensity analysis of PDI in concentrated media. Error bars represent mean and SD of three independent experiments of the same engineered cell pool. Statistical analysis was performed using Tukey's multiple comparison test. $P < 0.05$ was considered significant (*<0.05, **<0.01, ****< 0.0001), ns: not significant.

3.5 Discussion

The purpose of this chapter is to excavate for new approaches that could allow the best utilization of chaperones in CHO cells during stress conditions. Production of recombinant proteins in high titers imposes stress on the folding machinery of CHO cells (i.e. endoplasmic reticulum). In previous studies, the overexpression of ER chaperones has been examined to improve the productivity of CHO cell (**Table 2**). Accordingly, in this chapter I investigate the capacity of ER in CHO cells by comparing the levels of intracellular and extracellular abundance of chaperones. The ultimate objective is to find - whenever possible - a way to engineer a CHO cell model capable of making the best use of its folding machinery.

For this reason, the saturation of ER retention machinery on the protein level is investigated. As reported earlier in **2.3.2**, the ER retention machinery (i.e. KDEL receptors) are not upregulated during ER stress unlike ER chaperones. In this chapter, I investigated the saturation of ER retention machinery on two stages.

First of all, PDI (a KDEL chaperone) was cloned and overexpressed in CHO-K1 cells. Band intensity analysis of western blot revealed that PDI was detected in the lysate as well as in the concentrated medium (**Figure 17**). This experiment shows that not only the overexpressed chaperones can be retained inside the cells, but they can also be secreted to the extracellular medium during normal conditions. Also, when KDELR1 was overexpressed in this experiment, it did not show improved retention of neither BiP nor PDI.

Secondly, KDELR1 was expressed under BiP promoter in order to investigate whether or not engineering a CHO cell model capable of retaining all ER chaperones without secretion during stress conditions is feasible. It was found that BiP promoter improved BiP retention mildly but

significantly in cell lysates (**Figure 21D**) and decreased its secretion to the medium (**Figure 21F**) compared to mock cells. Interestingly, the whole amount of BiP secreted to the medium was not retained; yet, BiP was still detectable in the concentrated medium during stress condition of the engineered model.

On the other hand, GRP94 showed a KDELR1-independent behavior in both lysates and concentrated medium during ER stress in both cell lines (mock and BiP promoter-KDELR1) as shown in **Figure 21C** and **Figure 21E**. Additionally, GRP94 was released to the medium as a low molecular weight species that is secreted abundantly during stress conditions.

The results combined suggest that the secretion of BiP to the medium is not solely dependent on KDEL receptors. However, the masking of KDEL motif due to conformational changes or post-translational modifications might be a substantial reason for its secretion during stress conditions. And for that reason, it was not an evolutionary requirement for KDEL receptors to encode ER stress elements in their promoters. Accordingly, the engineered CHO cell model expressing KDELR1 under the expression BiP promoter did not prevent the secretion of chaperones to the medium. It only showed mild improvement of BiP retention.

Despite the engineered CHO cell model did not give the anticipated outcome, it shed a light on a special phenomenon which is the secretion of GRP94 as a small molecular weight species independent of KDELR1. This highlights the possibility of the truncation of the acidic C-terminal of GRP94. This will be investigated in the following chapter.

Chapter 4:

ER stress induces GRP94 secretion as low molecular weight species

4.1 Overview

In the previous chapter, while investigating the possibility of saturating the ER retention machinery, GRP94 was found to be secreted into the extracellular medium as a low molecular weight species, unlike the other three KDEL motif-bearing chaperones, BiP, calreticulin (Calr), and protein disulfide isomerase (PDI). Production of this low molecular weight form of GRP94 was induced by ER stress. This led us to deliberate over the importance of GRP94 as a trafficking molecule or as an extracellular antigen-presenting HSP (Murshid et al., 2012; Strbo & Podack, 2008). Accordingly, I studied the truncated form of GRP94 and investigated whether this form retains the ER retention motif.

Heat shock proteins (HSPs) are highly conserved molecular chaperones responsible for folding, intracellular transport, and refolding or degradation of misfolded proteins (Dubey et al., 2015). HSPs localize in different compartments inside the cells; for instance, the nucleus, endoplasmic reticulum (ER), cytosol, and mitochondria (Knowlton & Salfity, 1996; Marzec et al., 2012). HSPs can be classified by either their molecular weight or their dependence on adenosine triphosphate (ATP) (Dubey et al., 2015; Miller & Fort, 2018). According to their size, HSPs are divided into Hsp100, Hsp90, Hsp70, Hsp60, and the small HSPs. Small HSPs are ATP-independent, whereas larger HSPs hydrolyze ATP, which leads to their conformational change and interaction with substrates (Miller & Fort, 2018).

In mammalian cells, HSP90s are a group of four paralogs distributed throughout the cell, with GRP94 (glucose-regulated protein 94) found in the ER, Hsp90α and β in the cytosol (isoforms), and TRAP1 (tumor necrosis factor receptor-associated protein 1) in mitochondria (Huck et al.,

2017; Johnson, 2012). GRP94 is a well-studied HSP chaperone that resides in the ER because of the C-terminal KDEL (lysine, aspartic acid, glutamic acid, and leucine) motif. This member of the HSP90 family (Huck et al., 2017; Luo & Lee, 2013; Marzec et al., 2012) consists of three main domains: an N-terminal domain responsible for ATPase activity, a middle domain responsible for ligand binding, and a C-terminal domain responsible for dimerization. (Marzec et al., 2012). The N-terminal domain is preceded by a pre-N domain, which plays a role in GRP94 client maturation and regulation of the rate of ATP hydrolysis (Huard et al., 2019; Huck et al., 2017). The sequence of the pre-N domain of GRP94 from human and canine is composed predominantly of charged amino acids, making this domain a proteolytically sensitive region (Dollins et al., 2007). GRP94 and Hsp90 are active upon forming a homodimer (Immormino et al., 2004), and although being the most abundant protein in the ER, GRP94 interacts very selectively with specific clients (Argon et al., 2020; Marzec et al., 2012). For example, GRP94 interacts with immunoglobulin heavy and light chains and insulin-like proteins (Argon et al., 2020). It plays important roles in protein folding and ER quality control, specifically in the ER-associated degradation (ERAD) pathway (Christianson et al., 2008; Marzec et al., 2012).

GRP94 has one of the highest mRNA counts in recombinant CHO cells (Maldonado-Agurto & Dickson, 2018). Moreover, similar to binding immunoglobulin protein (BiP), GRP94 is highly upregulated during UPR activation and late-stage batch cultures (Maldonado-Agurto & Dickson, 2018; Prashad & Mehra, 2015) and as illustrated in **2.3.1**.

The mechanism of by which GRP94 is truncated has been studied earlier in human cells and suggested to be due to Calpain (protease) cleavage. It was suggested that Calpain cleaves a

hydrophobic domain in the N-terminal while retaining its C-terminal (Reddy et al., 1999). This assumption was based on Calpain mechanism of action as well as the detection of the low molecular weight GRP94 by western blotting. Although the small molecular weight species of GRP94 could be detected in cell lysates of stressed cells, this does not prove by anyhow that it retains its C-terminal. Also, it was found that GRP94 is decreased in cell lysates upon ER stress induction by 20 μM thapsigargin while appearing as a low molecular weight species (Muruganandan & Cribb, 2006). It was suggested by the authors that this is proteolytic degradation of GRP94. Most of the research done on GRP94 was investigating the effect of GRP94 intracellularly without taking into consideration that this decrease in intracellular GRRP94 upon ER stress/apoptosis might be because of the loss of its C-terminal and thus, its ER localization motif which will eventually lead to its secretion. A summary of previous research on GRP94 cleavage is shown in **Table 13**.

Studying GRP94 in CHO cells is of significant importance. This goes back to the reported function of GRP94 to be a specific chaperone to a limited number of clients including IgG heavy and light chains as reviewed by (Marzec et al., 2012). Understanding GRP94 behavior and localization in CHO cells can open new gates for engineering CHO cells to improve mAbs folding and cell productivity.

In this chapter the low molecular weight of GRP94 that is generated during ER stress in cell lysates and concentrated medium is analyzed in CHO cells. I investigated the effect of ER stress induction by thapsigargin and tunicamycin on GRP94 secretion. Additionally, I investigated whether GRP94 is secreted through the canonical ER-to Golgi pathway by treating the cells by

brefeldin A (BFA). I also tried to check whether this small GRP94 species is a transcript variant i.e. processing on the mRNA level. Finally, I analyzed the truncated GRP94 by peptide mapping and 2D-gel electrophoresis.

Table 13: Reports about proteolytic cleavage of GRP94

Cell type	Treatment	Lysate/media	Comment	Reference
SN Jurkat K12	30 µM etoposide	Lysate	Calpain cleaves GRP94 in-vitro at 3.0 mM $CaCl_2$	(Reddy et al., 1999)
LLC-PK1	20µM thapsigargin	Lysate	20µM Tg treatment showed decrease in intracellular GRP94 as a low molecular size species	(Muruganandan & Cribb, 2006)
SH-SY5Y	200 nM thapsigargin for 8 hours	Media	The truncated form appeared in the media in addition to full length GRP94 in one of the replicates. No band appeared in the lysate sample	(Trychta et al., 2018)

4.2 Materials and Methods

Chemical treatments: ER stress was induced using 5 µg/mL working concentration of tunicamycin, or 1 µM working concentration of thapsigargin unless mentioned otherwise. An equal volume of the vehicle dimethyl sulfoxide was used as a control. ER stress was induced in a suspension batch culture when the cell concentration was ~20 × 10^5 cells/mL. ER to Golgi transport was blocked by 10 µg/ml working concentration of brefeldin A (Nacalai Tesque, Kyoto, Japan).

RT-qPCR: RT-qPCR was performed as described in **2.3** using the same primer pairs. The primers used for Hsp90aa1 were 5′-TCCCAAGACGTGCTCCATTTG-3′ (forward) and 5'-TCCTCAGAATCCACCACTCCTC-3' (reverse).

RT-PCR: To check whether the low-molecular-weight GRP94 is a transcript variant, ER stress was induced by tunicamycin or exposure to DMSO as a control, as mentioned earlier. Total RNA was extracted and cDNA was synthesized as mentioned earlier. Three sets of primers covering the mRNA transcript were used to investigate different PCR products under normal and stress conditions. PCR primers are shown in **Table 14**. The PCR products were subjected to agarose gel electrophoresis.

Table 14: PCR primers for GRP94 transcript

	Forward	Reverse	Amplicon size
Primer set 1	5′-TCCTGCGACCGAAGAGGACTTG-3′	5′AGTGCAGGGGAGAAGGAGGCTG-3′	2565 bp
Primer set 2	5′-GCAGAGAAGGCTCAAGGACAGATG-3′	5′-TTTCCTGCTTGACCCAGCCATGAA-3′	1529 bp
Primer set 3	5′-GCTTGGTGTGATTGAGGACCACTC-3′	5′-TGTCTTCAGGCTCTTCTTCCGGTT-3′	818 bp

Immunoprecipitation: Immunoprecipitation of GRP94 was performed using cell lysates or concentrated media of CHO cells grown in suspension batch cultures. The cultures are grown in serum-free medium. The volume of the sample was adjusted to 500 µL with cell extraction buffer and incubated with 5 µL of the anti-GRP94 polyclonal antibody (rabbit, ab227293; Abcam) for 2 hours on a rotary shaker at room temperature or overnight at 4 °C. The sample was then incubated with 50 µL of Dynabeads magnetic protein G beads (Thermo Fisher Scientific) for 1 h at room temperature. Magnetic protein G beads were pulled down by a magnet, washed three times with 1× PBS, and eluted with 25 µL of 50 mM glycine (pH = 2.8).

Mass spectroscopy: Concentrated culture media of thapsigargin-treated CHO-K1 cells were run on 8% conventional gels and stained by SYPRO Ruby protein gel stain (Thermo Fisher Scientific). Bands corresponding to a molecular weight above 72 kDa were manually cut out and sent for analysis by peptide mapping. Dehydration was performed by 100% MeCN, and then vacuum drying for 60℃ for 5-10 minutes. The gel was reduced by 10 mM DTT/25 mM NH_4HCO_3 and then alkylated by 55 mM (10 mg/mL) IAA/25 mM NH_4HCO_3. In-gel digestion by 10 ng/µl Trypsin/50 mM NH_4CHO_3 was performed overnight. The peptides were extracted and separated on Aurora UHPLC column with CSI Fitting (Ion Opticks, AUR2-25075C18A-CSI, C18, Column Volume 1.1 µL, Pore Size 12 nm) using nanoElute UHPLC (CTC Analytics AG, 1837934 499075, PAL system). The separated peptides were then run on timsTOF Pro (Bruker Daltonik GmbH). A database search was performed using the TrEMBL database against Chinese hamster (*Cricetulus griseus*).

2D gel electrophoresis: Brefeldin A-treated CHO-K1 cell lysate was precipitated with trichloroacetic acid (TCA), washed with acetone, and resuspended in rehydration solution. The sample was run on Auto 2D plus (Merck) on 7.5% gel and a chip of pH range of 3–10. The gel was transferred to a PVDF membrane and blotted against anti-KDEL antibody as previously mentioned. It was then stripped using low-pH stripping solution, washed, re-blocked, incubated with anti-GRP94 antibody, and visualized.

Fluorescence microscopy: Adherent CHO-K1 cells were grown in T25 flasks in IMDM (Iscove's Modified Dulbecco's Medium; Thermo Fisher Scientific) supplemented with 10% fetal bovine serum (Thermo Fisher Scientific). The cells were passaged into 12-well plates on 18 mm lysine-coated coverslips (Neuvitro Corporation, Vancouver, WA, USA). Two days later, the cells were washed three times with 1× PBS, fixed by 4% paraformaldehyde in 1× PBS solution for 15 min, quenched with 100 mM glycine/PBS for 5 min, followed by two washes with 1× PBS for 5 min each. Permeabilization was performed using 0.1% TritonX-100/PBS for 5 min and blocked using 3% bovine serum album in PBS. Fluorescent images of the primary antibodies used were obtained using an All-in-One Fluorescence Microscope, BZ-X710 (Keyence, Osaka, Japan). All chemicals were purchased from Fujifilm Wako (Osaka, Japan), unless mentioned otherwise. Antibodies used for probing BiP, GRP94, calreticulin and PDI are shown in **Table 15**.

Table 15: Antibodies for fluorescence microscopy

Target	Primary antibodies	Secondary antibodies
BiP	Anti-BiP (rabbit Ab, 3177; Cell Signaling Technology)	Goat anti-rabbit IgG H&L Alexa Fluor 488 conjugated (ab150081; Abcam)
PDI (P4hB)	Anti-P4hb (rabbit Ab, ab137110; Abcam, Cambridge, UK)	
GRP94	Anti-GRP94 (rabbit Ab, 2104S; Cell Signaling Technology)	
Calreticulin	Anti-Calr (rabbit Ab, 2891; Cell Signaling Technology)	
GM-130 (*cis*-Golgi)	Anti-GM130 (mouse Ab, 610822; BD Biosciences, Franklin Lakes, NJ, USA)	Goat anti-mouse IgG H&L Alexa Fluor 647-conjugated (ab150119; Abcam)

4.3 Appearance of a small GRP94 species upon ER stress

In order to confirm GRP94 truncation, ER stress was induced in suspension CHO-K1 cells using 5µg/mL tunicamycin. Samples were taken 24 hours after exposure. Media samples were concentrated as mentioned in **3.2**. The result shows an extra -low-molecular weight species of GRP94 in the lysate sample under stress conditions. Also, this low molecular weight species was secreted abundantly to the medium in the stressed samples as shown in **Figure 23**.

It was hypothesized that this small molecular weight species of GRP94 is a truncated form of GRP94 that is induced upon ER stress. Accordingly, this low molecular weight GRP94 happens either on the mRNA level or on the protein level. The cleaved form can be either be cut from the N-terminal, the C-terminal or both. These hypotheses were investigated in this chapter.

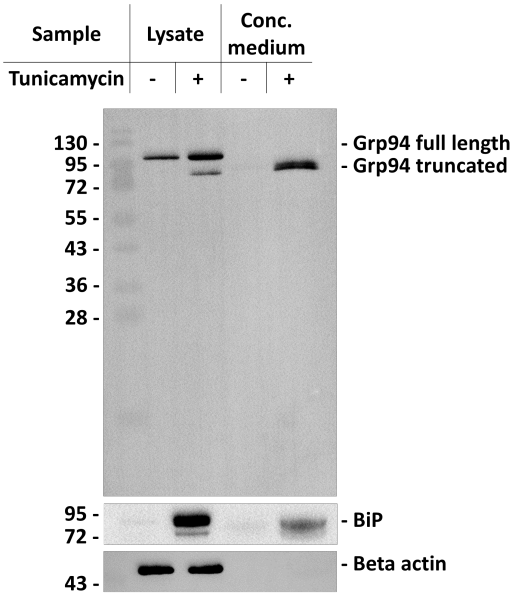

Figure 23: Truncation and secretion of GRP94 upon ER stress induction

ER stress was induced by 5 µg/mL tunicamycin for 24 hours in CHO-K1 suspension cells.

4.4 The extra band is not unspecific binding to the cytosolic paralogue

The small molecular weight band that appears during ER stress induction could be a transcript variant of the same gene, or another gene with high sequence homology. Accordingly, I mined CHO genome for possible genes having significant sequence homology to the coding DNA sequence (CDS) of GRP94. The CHO genome website (https://chogenome.org/index.php) was used to blast the CDS against the genome scaffold "CHO-K_RefSeq2020" (Hilliard et al., 2020). The data used for alignment is shown in **Table 16**. The results of the alignment are shown in **Table 17**. The results shown that the genes having sequence similarities to GRP94 are of much different molecular size of their proteins as shown in the last column of **Table 17**. This is true for all the results except for the cytosolic paralogue Hsp90aa1. Hsp90aa1 is 733 amino acids which could be the band that appears during ER stress.

GRP94 (Hsp90b1) did not show any reported transcript variants. The different isoforms of other heat shock proteins gave a protein with much bigger sizes which were more than 1000 amino acids as shown in **Table 17**.

In the latest report of CHO cell RefSeq annotation (Hilliard et al., 2020), the cytosolic paralogue of GRP94; Hsp90aa1, is reported as only one isoform. GRP94 and Hsp90aa1 have high sequence homology (Marzec et al., 2012). The difference between both of them is mainly the absence of the signal peptide and the acidic C-terminal in the Hsp90 paralogue, in addition to the other sequence similarities as shown in **Figure 24A**. Accordingly, it was hypothesized that the extra-band that appears during ER stress in CHO cells might be a nonspecific binding of the western blotting antibody (rabbit Ab, 2104S, Cell Signaling Technology) with Hsp90aa1, especially that a cytosolic

paralogue is more likely to be secreted to the medium than an ER resident chaperone. Consequently, the response of the Hsp90aa1 gene to ER stress was checked by RT-qPCR as shown in **Figure 24B**. GRP94 and BiP showed the expected upregulation upon ER stress induction. However, Hsp90aa1 showed minimal upregulation that did not exceed two folds. Accordingly, I suggest that the extra band that appears in cell lysate and medium is not a nonspecific binding of the antibody with Hs90aa1.

Table 16: Mining for similarities to GRP94 in CHO genome

Source gene	PREDICTED: Cricetulus griseus heat shock protein 90 beta family member 1 (Hsp90b1), mRNA
Locus	XM_027392542
Length	2797 bp
Accession	XM_027392542
Version	XM_027392542.2
Source	Cricetulus griseus (Chinese hamster)
Operation 1	Alignment of cDNA sequence on CHO-K1 RefSeq 2020
Query length	2409 bp (Coding DNA sequence)

Table 17: Result of alignment of GRP94's cDNA to CHO-K1 genome

Subject	Score	Identities (Query length)	%	Expect	Name of gene/locus	Protein name	Protein size
XM_003505850.5	4334	2409/2412 (2409)	99	0	PREDICTED: Cricetulus griseus heat shock protein 90 beta family member 1 (Hsp90b1), mRNA	endoplasmin [Cricetulus griseus]	803 aa
XM_003497056.2	51.8	41/49 (2409)	84	8.00E-05	PREDICTED: Cricetulus griseus protein phosphatase, Mg2+/Mn2+ dependent 1G (Ppm1g), mRNA	protein phosphatase 1G isoform X1 [Cricetulus griseus]	550 aa
XR_004767901.1	68	57/70 (2409)	81	1.00E-09	PREDICTED: Cricetulus griseus heat shock protein HSP 90-beta-like (LOC100774172), transcript variant X1, misc_RNA	misc_RNA	-
XM_016975220.2	93.3	92/119 (2409)	77	3.00E-17	PREDICTED: Cricetulus griseus heat shock protein HSP 90-beta (LOC100754792), transcript variant X2, mRNA	heat shock protein HSP 90-beta isoform X1 [Cricetulus griseus]	1079 aa
XM_035455355.1	93.3	92/119 (2409)	77	3.00E-17	PREDICTED: Cricetulus griseus heat shock protein HSP 90-beta (LOC100754792), transcript variant X1, mRNA		
XM_016975221.3	93.3	92/119 (2409)	77	3.00E-17	PREDICTED: Cricetulus griseus heat shock protein HSP 90-beta (LOC100754792), transcript variant X3, mRNA	heat shock protein HSP 90-beta isoform X2 [Cricetulus griseus]	1078 aa
XM_016975222.3	93.3	92/119 (2409)	77	3.00E-17	PREDICTED: Cricetulus griseus heat shock protein HSP 90-beta (LOC100754792), transcript variant X4, mRNA		
XM_016975223.3	93.3	92/119 (2409)	77	3.00E-17	PREDICTED: Cricetulus griseus heat shock protein HSP 90-beta (LOC100754792), transcript variant X5, mRNA	heat shock protein HSP 90-beta isoform X3 [Cricetulus griseus]	1077 aa
XR_004838834.2	62.6	86/119 (2409)	72	4.00E-08	PREDICTED: Cricetulus griseus heat shock protein HSP 90-beta-like (LOC100774238), misc_RNA	misc_RNA	-
NM_001246821.1	59	153/231 (2409)	66	5.00E-07	Cricetulus griseus heat shock protein 90 alpha family class A member 1 (Hsp90aa1), mRNA	heat shock protein HSP 90-alpha [Cricetulus griseus]	733 aa

A

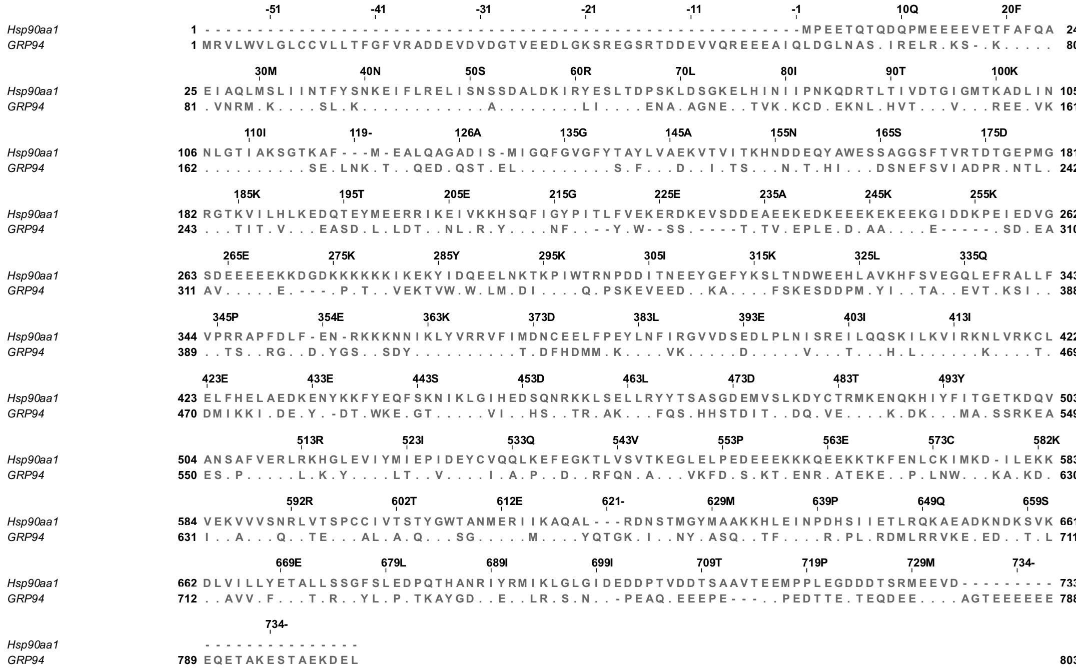

B

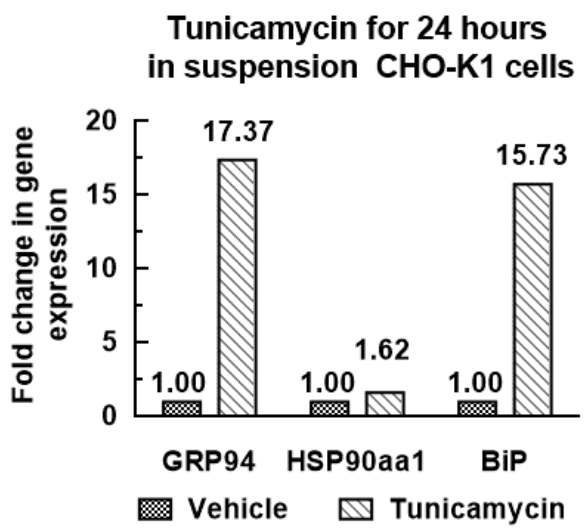

Figure 24: Comparison between GRP94 and Hsp90aa1 and their response to ER stress

(A) Sequence alignment of Hsp90aa1 and GRP94 in CHO cells. (B) Result of RT-qPCR after ER stress induction in CHO-K1 cells and its effect on the expression level of GRP94, BiP and Hsp90aa1

4.5 Canonical secretion of GRP94

To understand the process of secretion of GRP94 during stress conditions in CHO cells, I treated these cells with either tunicamycin (**Figure 25A, B**) or thapsigargin (**Figure 25C, D**). Samples were treated with reducing or non-reducing sample buffers and subjected to SDS-PAGE and then blotted against GRP94 and Beta-actin antibodies. GRP94 was found to be expressed as both a monomer and a dimer intracellularly. GRP94 was found to be secreted abundantly upon tunicamycin or thapsigargin as reported earlier.

Next, CHO cells were treated with thapsigargin, brefeldin A, or both to investigate the pathway of secretion into the medium (**Figure 26**). Brefeldin A was found to induce ER stress in a manner similar to thapsigargin, as demonstrated by the upregulation of BiP, as shown in **Figure 26C**. Treatment with brefeldin A alone induced the intracellular accumulation of low-molecular-weight GRP94 and prevented its secretion into the medium. Additionally, BiP secretion into the medium was inhibited by treatment with brefeldin A. Surprisingly, co-treatment with Tg/BFA induced neither the accumulation of the low-molecular-weight species of GRP94 nor its secretion. Upon co-treatment, the cell diameter was found to increase when measured with a ViCell counter (**Figure 26B**). These results collectively suggest that the low-molecular-weight species of GRP94 originates in the ER and is secreted out of the cell through the canonical ER to Golgi pathway.

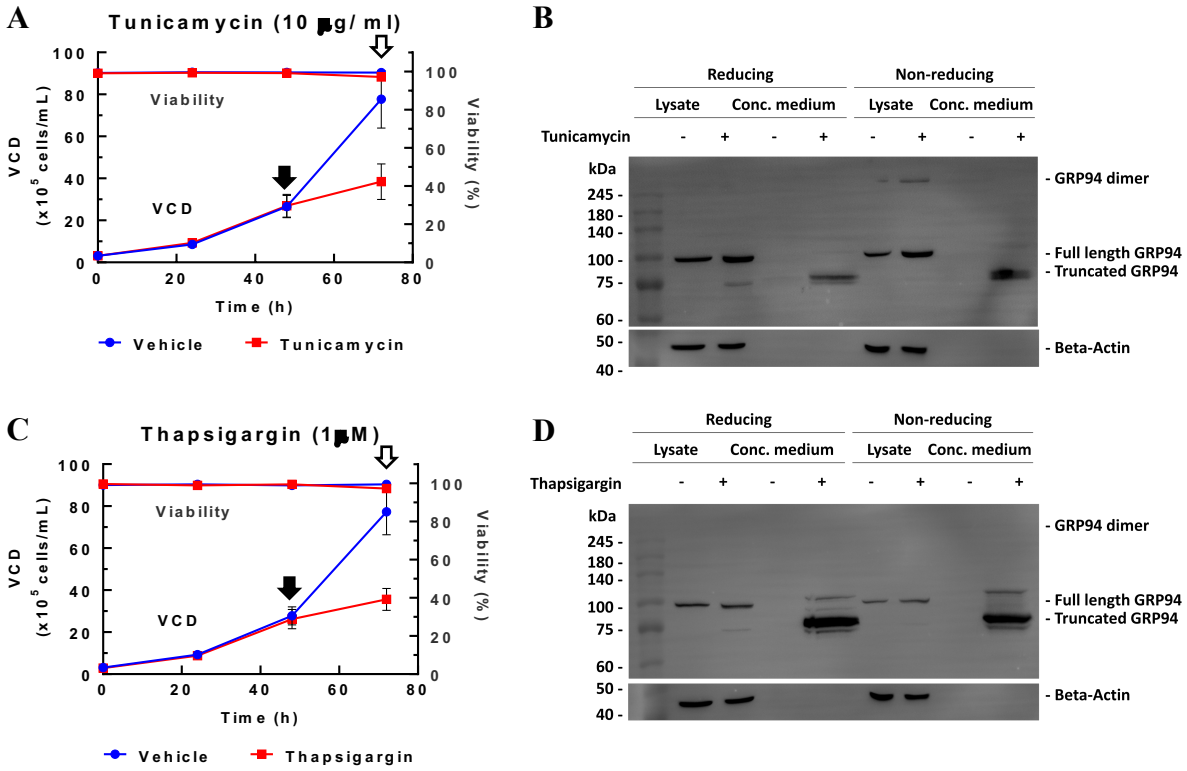

Figure 25: Effect of tunicamycin or thapsigargin treatment on GRP94 secretion

(A and B) ER stress induced by 10 µg/mL tunicamycin for 24 h. (A) Viable cell density and (B) western blot of GRP94 in a cell lysate and concentrated medium under reducing and non-reducing conditions. (C and D) ER stress induced by 1 µM thapsigargin for 24 h. (C) Viable cell density and (D) western blot of GRP94 in a cell lysate and concentrated medium under reducing and non-reducing conditions. Black arrows indicate the time point when ER stress was induced, whereas white arrows indicate the time point when cell and medium samples were taken. Experiments were performed independently two times. VCD: viable cell density

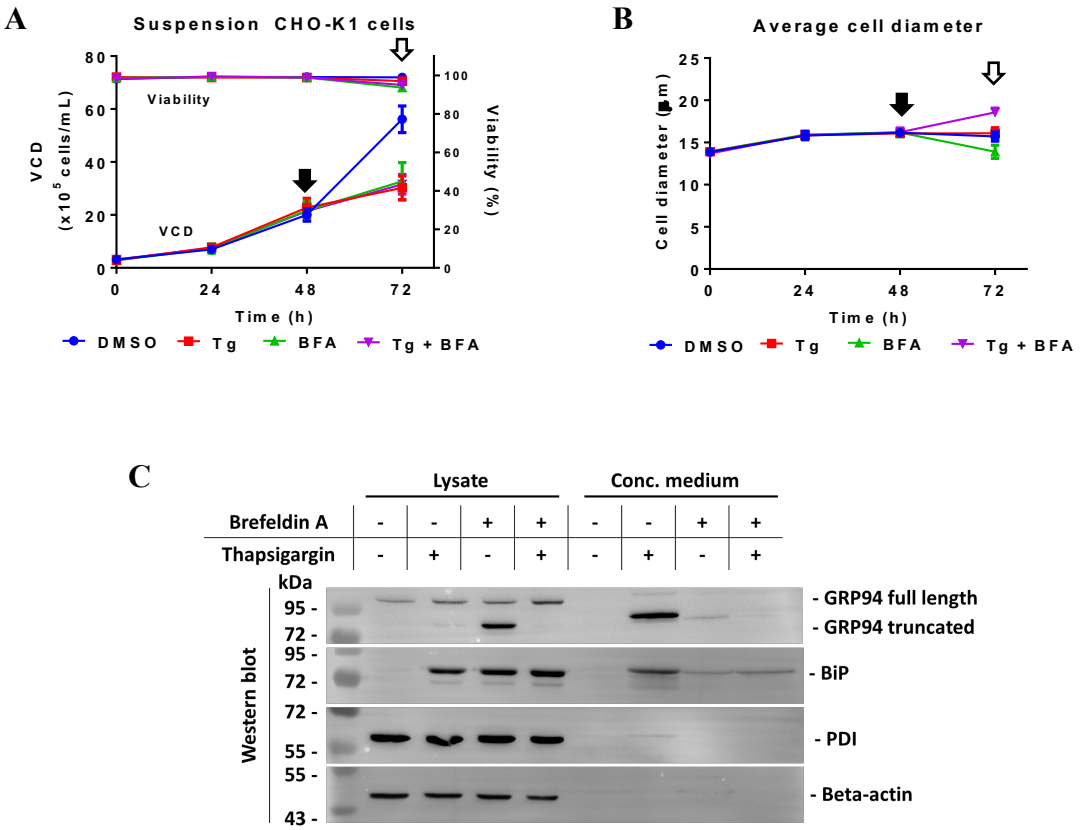

Figure 26: GRP94 is secreted into the medium through the canonical ER to Golgi pathway

Treatment of CHO-K1 with thapsigargin (Tg), brefeldin A (BFA), or both. (A) Viable cell density. (B) Average diameter of cells measured automatically using ViCell counter. (C) Western blot of GRP94, BiP, PDI, and beta-actin in cell lysate and concentrated medium showing that the active secretion of GRP94 and BiP was blocked by BFA treatment and they accumulated inside the cell. Black arrows indicate the time point when ER stress was induced, whereas white arrows indicate the time point when cell and medium samples were taken. Experiments were performed independently two times. VCD: viable cell density.

4.6 The small molecular weight species of GRP94 is not a transcript variant

In the CHO genome database, there are no reported transcript variants of GRP94 (Hilliard et al., 2020) as shown in **Table 17**. To investigate this experimentally, the previously treated sample by tunicamycin at **Figure 23** was used to extract total RNA, synthesize cDNA, and then run RT-PCR. I designed three primer sets that cover the mRNA transcript of Hsp90b1 (gene expressing GRP94) (**Figure 27A**). I then subjected the PCR products to agarose gel electrophoresis, as shown in **Figure 27B**. I did not observe extra bands equivalent to the predicted size of the low-molecular-weight protein upon comparing the vehicle-treated and tunicamycin-treated samples. These results suggest that the low-molecular-weight GRP94 is a result of processing at the protein level and not at the mRNA level.

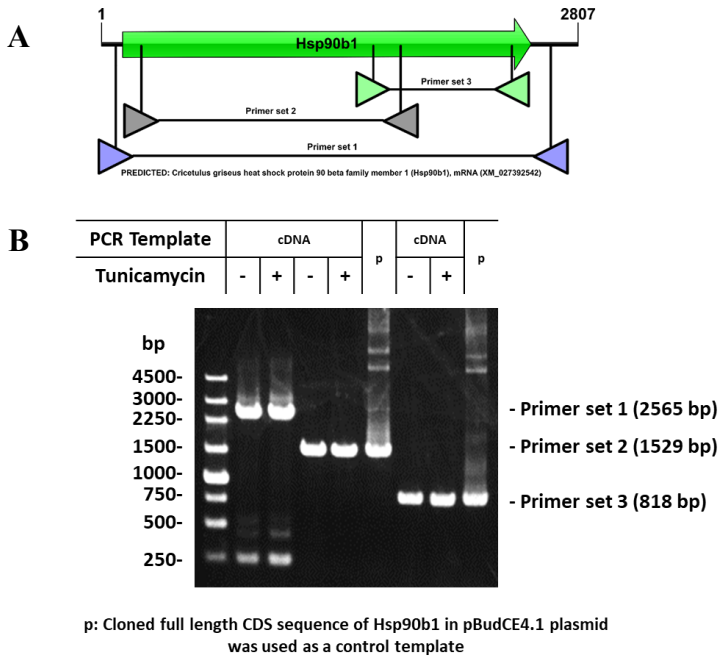

Figure 27: Analysis of GRP94 mRNA transcript during ER stress

ER stress was induced, total mRNA was extracted, cDNA was synthesized, and then PCR was run using three primer sets. The results did not show any smaller size band in tunicamycin-treated samples. (A) mRNA transcript of Hsp90b1 showing the location of the designed primers. (B) Agarose gel electrophoresis of the PCR products.

4.7 The truncated form of GRP94 is devoid of its KDEL motif

To further investigate the truncated form of GRP94, ER stress was induced by thapsigargin (**Figure 28A, B**). I immunoprecipitated GRP94 from concentrated medium samples of thapsigargin-treated cells (**Figure 28A**). The flow-through showed several GRP94 bands: the full-length GRP94 and two truncated forms. The immunoprecipitated GRP94 showed a GRP94 full-length band and two other truncated forms when blotted against GRP94. However, when blotted against anti-KDEL antibody, only full-length GRP94 was detected, while the other truncated forms did not respond to this antibody. The same samples were blotted against anti-BiP antibody and showed a BiP band at the same size as the GRP94 truncated 2 band. GRP94 truncated 2 is the most abundant form of GRP94 that is secreted into the medium. The C-terminal tail of GRP94 is highly acidic and disordered. Accordingly, I hypothesized that the truncated form does not have the KDEL retention motif. Because the level of immunoprecipitated GRP94 was minimal, I subjected the BFA-treated cell lysate to 2D gel electrophoresis, performed blotting against KDEL, and then stripped and re-probed the membrane against GRP94 (**Figure 28C–F**). The low-molecular-weight GRP94 was not detected by anti-KDEL antibody, as shown in **Figure 28F**. The theoretical isoelectric points of GRP94, BiP and truncated GRP94 are shown in **Figure 28G**.

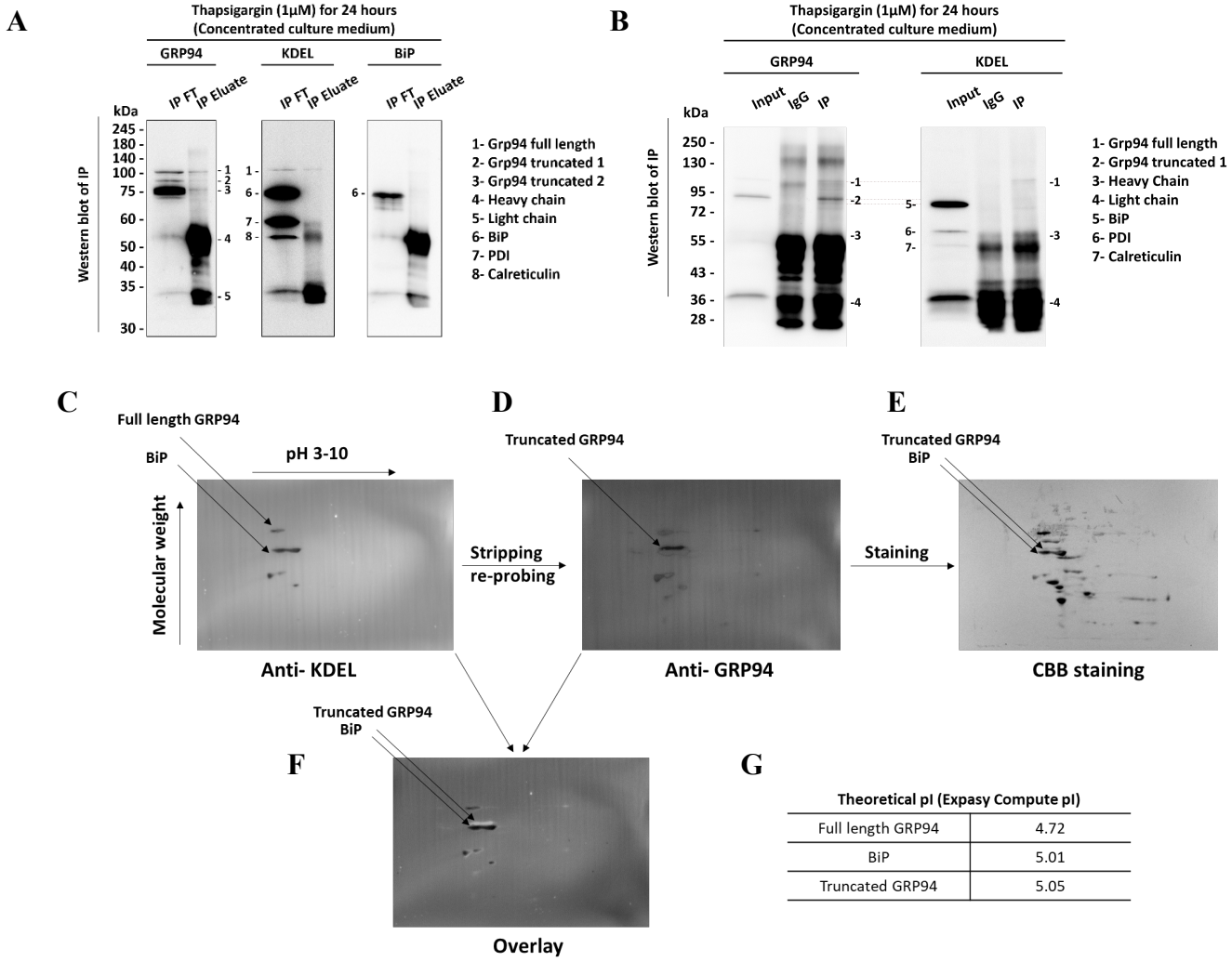

Figure 28: Low-molecular-weight GRP94 is devoid of the KDEL motif

A) Western blot of immunoprecipitation (IP) of concentrated media after inducing ER stress by thapsigargin and probing against GRP94 (left), KDEL (middle), and BiP (right). (B) Western blot of immunoprecipitation (IP) and probing against GRP94 (left) and KDEL (right) with IgG control. (C–F) 2D gel electrophoresis of brefeldin A-treated CHO-K1 cell lysate while probing against KDEL (C), stripping and re-probing against GRP94 (D), and then staining the membrane with CBB (F). Overlay of the 2D membranes showing that the truncated form of GRP94 is not responsive to KDEL antibody. (G) Theoretical isoelectric point (pI) calculation of full-length GRP94, BiP, and GRP94 after losing its acidic C-terminal. IP: immunoprecipitation, FT: Flow through.

4.8 Peptide mapping of secreted GRP94

In the previous section, I analyzed GRP94 by western blotting and 2D gel electrophoresis to examine whether or not it retains its acidic C-terminal, specifically its KDEL motif. In order to do that, the identity of this small molecular weight GRP94 species had to be confirmed. Additionally, the coverage of GRP94 sequence and its peptide abundance will give and idea about the presence of its KDEL motif.

To obtain more concentrated medium, ER stress was induced, as mentioned previously, using 1 µM thapsigargin in a culture volume of 100 mL. The sample of concentrated medium from thapsigargin-treated cells was run on two 8% SDS-PAGE gels, one of which was blotted onto a PVDF membrane and probed for GRP94 (**Figure 29A**), while the other was stained with SYPRO Ruby protein gel stain (**Figure 29B**). The bands corresponding to the molecular weight of GRP94 were cut and sent for peptide mapping (**Figure 29C**).

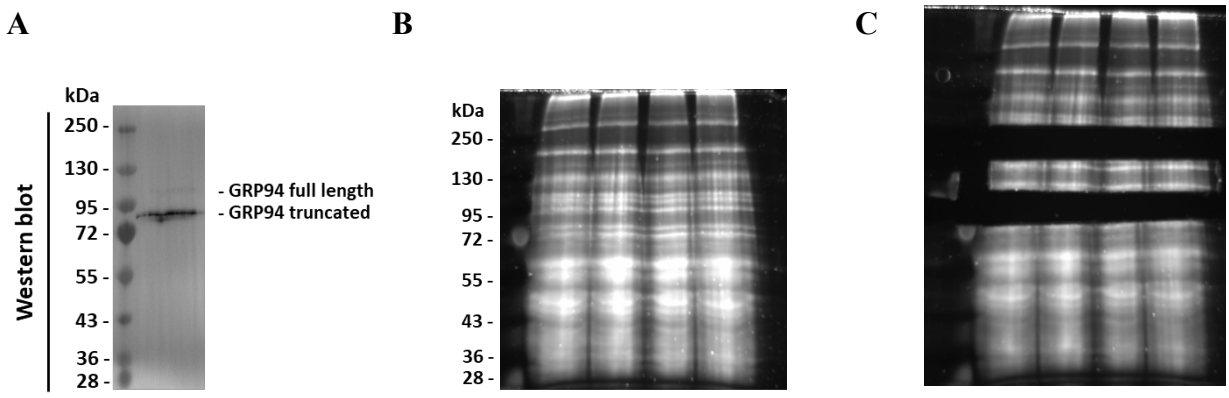

Figure 29: Gel cutting for peptide mapping of secreted GRP94

Concentrated culture media of thapsigargin treated cells were run on two gels. (**A**) Western blot of GRP94 showing the major low molecular weight band and faint band of full length GRP94. The same sample were run on several lanes of SDS-PAGE. (**B**) SYPRO Ruby Protein Gel staining. (**C**) the cut band that was sent for peptide mapping.

The result showed 65% coverage of the GRP94 sequence (**Figure 30**). The signal peptide (M1–A21: MRVLWVLGLC CVLLTFGFVR A) was not detected, that could indicate that this protein is a mature protein that has passed through the ER. The D22–K37 peptide is the N-terminal of the mature protein just after the signal peptide. The whole acidic C-terminal after K733 was not detected, except for the E795–L803 peptide, which was a negligible fraction.

Figure 30: Sequence coverage of GRP94 in concentrated culture media.

Analysis of GRP94 showed 65% sequence coverage. The whole C-terminal from A734 to the end was not detected except for the final E795-L803containig the KDEL sequence.

The peptide map of GRP94 is shown in **Figure 31**. The peptide E795–L803 (RT: 7.05) showed very low abundance compared with the sequences in the N-terminal and middle domains. Its abundance was zero referring to a very low decimal fraction. N-terminal and middle domain peptides showed very high abundance in the sample, while the C-domain peptide S725–K733 showed low abundance. A comparison of the abundance of the peptides is shown in **Figure 31A**.

A

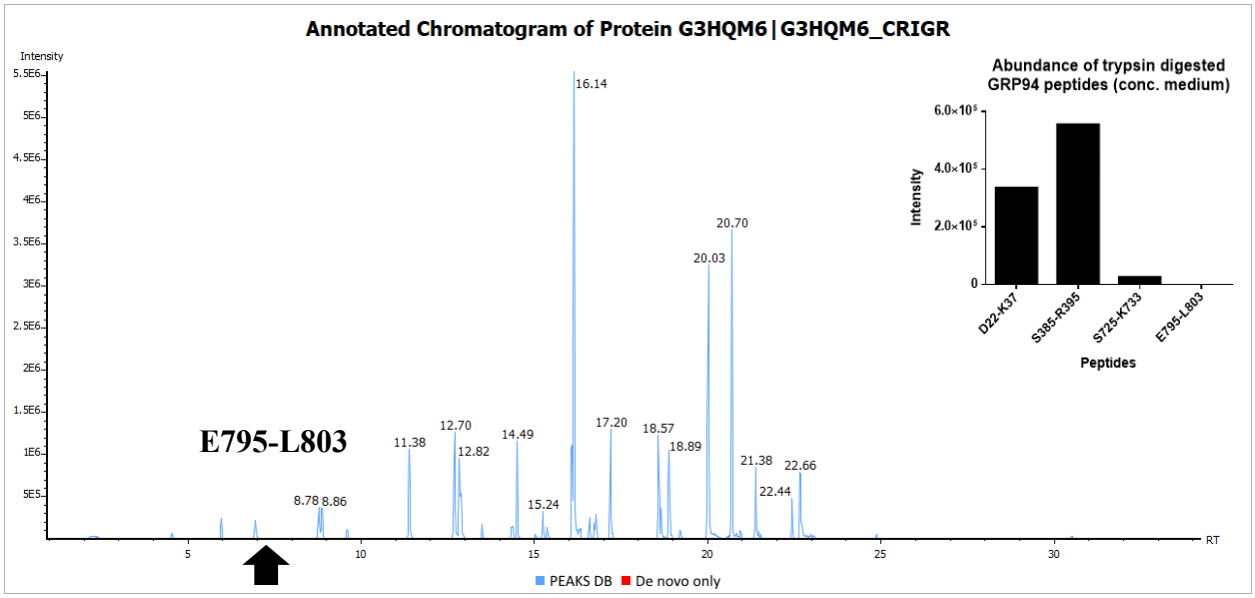

B

Position	Peptide	Uniq	RT	Area Sample	Comment
D22-K37	A.DDEVDVDGTVEEDLGK.S	Y	20.04	334880	Sequence of the N-terminal of the mature protein
S725-K733	R.SGYLLPDTK.A	Y	15.38	25404	Sequence before the acidic C-terminal
E795-L803	K.ESTAEKDEL	Y	7.05	0	9 amino acids at the end of C terminal (containing KDEL)
S385-R395	K.SILFVPTSAPR.G	Y	20.71	554930	Most abundant unique peptide
E103-K114	R.ELISNASDALDK.I	N	16.15	660440	Most abundant non-unique peptide

Figure 31: Annotated chromatogram of GRP94 (G3HQM6)

Black arrow shows the location of the very low abundant E795-L803 peptide containing KDEL motif. The area sample of this peptide was zero indicating a low decimal fraction. The inset shows comparison of the abundance of selected GRP94 peptides: The N-terminal sequence of mature protein after the signal peptide D22-K37, peptide in the middle domain of GRP94 S385-R395, the last relatively abundant detected peptide in the C-terminal S725-K33 and the zero-abundance detected peptide E795-L803 containing the KDEL motif. (**B**) Some of the detected peptides of GRP94.

4.9 Localization of KDEL chaperones in CHO cells

Adherent CHO-K1 cells were fixed on lysine-coated coverslips and immunostained by antibodies against the four KDEL chaperones (GRP94, BiP, Calr, and PDI) to detect their localization with the ER and *cis*-Golgi (**Figure 32**). Four to seven images containing 50 to 60 cells were examined to detect whether the chaperones are located in the *cis*-Golgi. Cells showing overlap between the green (chaperones) and red (*cis*-Golgi) channels indicated colocalization (colored yellow). BiP, PDI, and Calr showed *cis*-Golgi localization. In contrast, all observed cells in GRP94-stained samples showed no *cis*-Golgi localization, as reported previously for human endothelial EAhy926 cells (Paris et al., 2005). The four chaperones localized to the ER in all cells, as expected. Examples of localization and the absence of localization are shown in **Figure 33**. Regions of interest (ROIs) are marked on the image and the intensity profiles of the three channels were measured. Similar patterns between the green (chaperones) and red (*cis*-Golgi) channels indicated localization of the chaperones in the *cis*-Golgi compartment.

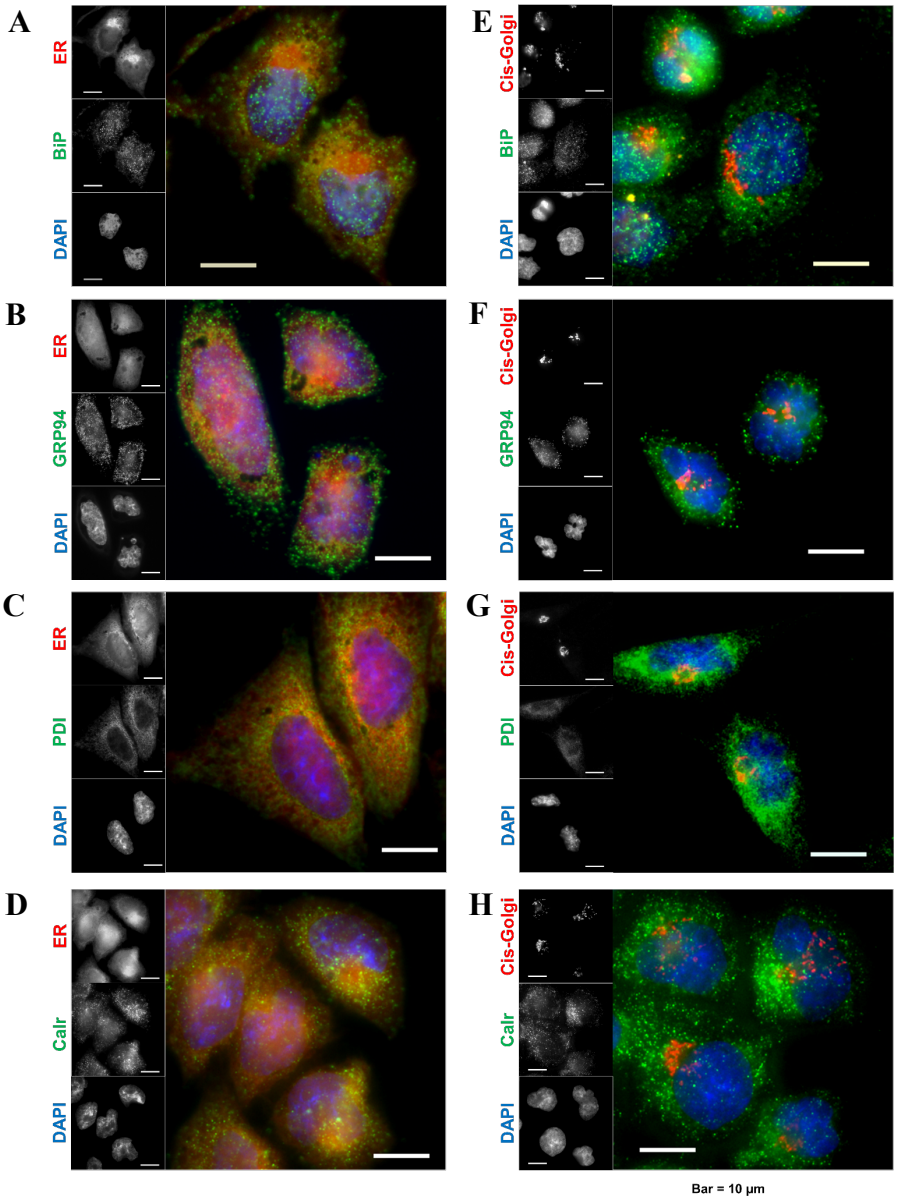

Figure 32: Localization of KDEL chaperones in ER and cis-Golgi

CHO-K1 cells grown on pre-coated coverslips in 12-well plates were fixed and immunostained by antibodies specific for each of the four chaperones against the ER marker (ER-ID dye): (A) BiP, (B) GRP94, (C) PDI, and (D) Calr, or anti-GM130 as a *cis*-Golgi marker: (E) BiP, (F) GRP94, (G) PDI, and (H) Calr. Cells were captured using a 100× oil lens and approximately 50 to 60 cells from four to seven fluorescent images were counted and checked for localization in the *cis*-Golgi and ER. Among the observed cells, GRP94 did not localize in the *cis*-Golgi. The experiment was repeated three times. Each time, GRP94 did not show any localization in *cis*-Golgi. Scale bar is 10 µm.

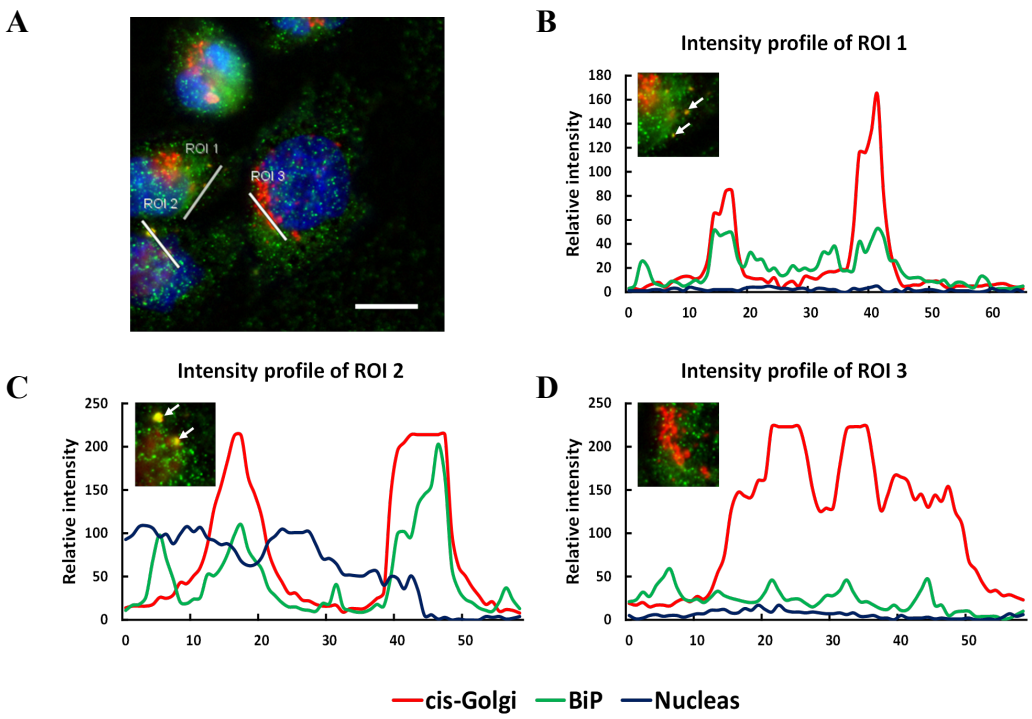

Figure 33: Illustration of chaperones' localizations

An example of *cis*-Golgi localization of (A) BiP with three regions of interest (ROIs) showing localization indicated by white arrows (B and C), or no localization (D) and their intensity profiles. Scale bar is 10 µm.

4.10 Discussion

GRP94 is one of the ER chaperones bearing the KDEL motif in mammalian cells. GRP94 is essentially different than the other KDEL bearing chaperones in that it is selective in choosing its clients. Similar to BiP, it is highly upregulated during ER stress. In the previous chapter, I found that GRP94 shows a small molecular weight species during ER stress that is secreted abundantly to cell exterior. I tried to identify the nature of this low molecular weight species. The results suggest that this low molecular weight species of GRP94 that is generated during ER stress is neither an mRNA variant, nor unspecific binding to its cytosolic paralogue Hsp90aa1. Accordingly, it is suggested to be a result of protein processing rather than mRNA processing. By treating cells with brefeldin A (an ER stress inducer), it was found that the secretion of ER chaperones to the cell exterior is through the canonical ER to Golgi pathway. Brefeldin A inhibited the secretion of the low molecular weight species of GRP94 and accumulated it inside the ER. Interestingly, co-treatment by thapsigargin and BFA induced ER stress (BiP upregulation) but not GRP94 truncation. It was previously reported that GRP94 truncation occurs by Calpain (protease) in a calcium dependent manner (Reddy et al., 1999). It is still unknown why co-treatment did not induce GRP94 truncation; however, I suggest that it could be related to an intramembrane ER protease that utilizes calcium and thus affected by both the blockage of COPII formation and depletion of calcium stores inside the cells.

The small molecular weight species of GRP94 was not responsive to anti-KDEL antibody during immunoprecipitation or 2D-gel electrophoresis. Thus, it is suggested that a part of the acidic C-terminal is truncated upon ER stress.

Next, the band from concentrated culture media was analyzed by peptide mapping for two reasons. Firstly, it was analyzed to confirm the identity of GRP94. Secondly, the peptides' concentration in the sample was used to compare the relative abundance of the N and C termini. The relative abundance of the N-terminal and C-terminal suggested that GRP94 is truncated at its C-terminal and not the N-terminal.

A schematic diagram of GRP94 and the suggested truncated form is presented in **Figure 34**. A three-dimensional model of GRP94 was constructed by i-TASSER (Roy et al., 2010) and the model representation was prepared by UCSF Chimera (Pettersen et al., 2004). It is suggested that the loose C-terminal is cleaved, losing the KDEL motif and thus promoting its secretion into the medium.

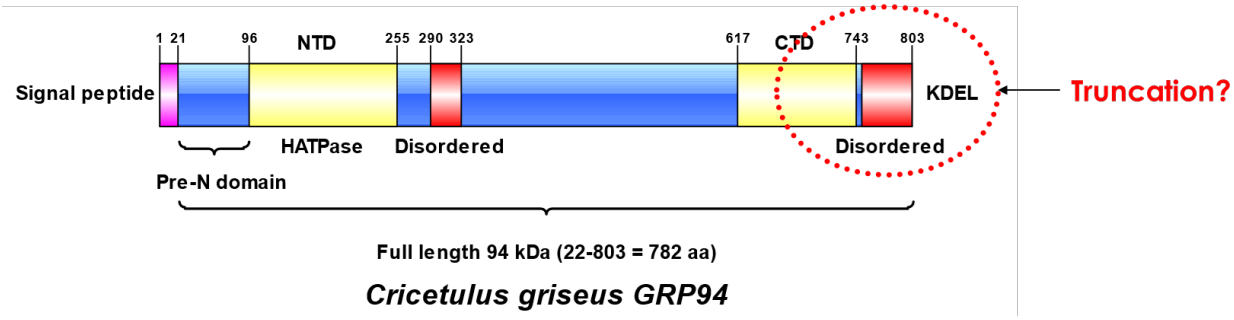

Figure 34: Schematic representation of GRP94 truncation.
Schematic diagram of GRP94 sequence with expected cut site.

Chapter 5:

Concluding remarks and future prospects

Pelham and co-workers discovered the ER retention motif, HDEL (histidine, aspartate, glutamate, leucine) in yeast and KDEL in mammals in several ER resident chaperones, which was hypothesized to be responsible for their retention in the ER (Munro & Pelham, 1987). Later, the same team overexpressed an HDEL-tagged exogenous protein, which led to the secretion of the endogenous HDEL ER chaperone BiP in *Saccharomyces cerevisiae*; thus, suggesting that the retention inside the ER is mediated by a receptor that could be saturated (Dean & Pelham, 1990). This receptor was later defined as the KDEL receptor, which is a seven-transmembrane-domain protein recycling between the ER and *cis*-Golgi and responsible for the retention of missorted ER chaperones from post ER compartments (Capitani & Sallese, 2009). The retention mechanism is based on the pH difference between the ER and *cis*-Golgi, where the pH of the *cis*-Golgi is lower than that of the ER, promoting KDEL receptor and KDEL motif binding (Capitani & Sallese, 2009; Wilson et al., 1993). The KDEL receptor family in *Homo sapiens* consists of three members with a high degree of sequence homology (Capitani & Sallese, 2009; Raykhel et al., 2007). Similarly, the KDEL receptor family in Chinese hamster consists of three members with similar homologies.

In chapter two, the stress induction in CHO-K1 cells, *Kdelr1, Kdelr2 and Kdelr3* showed less than 2-fold upregulation after 20 hours of exposure to tunicamycin in the suspension batch culture compared with the vehicle treated samples. Nevertheless, other KDEL-chaperones like BiP (*Hspa5*) and GRP94 (*Hsp90b1*), showed more than 12-fold upregulation, while Calreticulin (*Calr*) and PDI (*P4hb*) showed more than 2-fold upregulation. This result was confirmed with a reported 1.8-fold upregulation of *Kdelr1* in HeLa cells using tunicamycin or thapsigargin (P. Wang et al., 2011). Noticeably, the expression levels of the three KDEL receptors were mildly affected by the activation of the UPR signaling pathway, although its target proteins were significantly

upregulated. However, Trychta *et al.* recently reported that KDELR2 and KDELR3 were upregulated during ER stress induced by thapsigargin treatment in human cell lines (Trychta et al., 2018).

Recently, it was established that the transgene copy number is no longer the limit of high recombinant protein productivity. Instead, the capability of folding, post-translational processing and secretion of recombinant proteins were shown to hinder recombinant cells from reaching the desired performance (Barnes & Dickson, 2006; Borth et al., 2005; Le Fourn et al., 2014; Peng et al., 2010; Tigges & Fussenegger, 2006; Zhou et al., 2018). Accordingly, this incomparable feedback of cells during ER stress (on the regulation of KDEL receptors from one side and KDEL-bearing ER chaperones from the opposite side) sheds light on a possible natural limitation of the ER folding capacity. In particular, the ER retention machinery was found to be susceptible to saturation in yeast (Dean & Pelham, 1990), HeLa cells (Llewellyn et al., 1997) and plant cells (Crofts et al., 1999). In addition, the escape of soluble ER chaperones from the early secretory pathway, particularly Calr, to the cell surface or the extracellular matrix is a distinctive feature of ER stress in cancerous cells. This was suggested to result from KDEL receptor saturation or the inability of capturing KDEL chaperones owing to the altered pH of the Golgi apparatus (Wiersma et al., 2015). In conclusion, the failure of cells to upregulate KDEL receptors in accordance to ER chaperones upregulation during ER stress or during exogenous overexpression of a KDEL bearing protein leads to the saturation of retention machinery and escape of endogenous ER chaperones to the medium in either case. Conversely, a recently published article reports that KDELR2 and KDELR3, but not KDELR1, are responsive to ER stress induction by thapsigargin where KDELR2 and KDELR3 gene expression showed more than 2-fold increase in human cell lines (Trychta et

al., 2018). However, in CHO cells, I showed that ER stress by tunicamycin induces KDEL receptors upregulation in a similar level, less than two-fold increase.

Although the KDEL receptor is not likely to interact directly with recombinant secretory proteins, the KDEL receptor's target molecules have major roles in the folding and assembly of recombinant secretory molecules as mentioned earlier. However, ER chaperones bearing the KDEL motif are not the only targets of KDEL receptors. In a noteworthy study, Raykhel *et. al* reported that KDEL receptors have affinity to a wide range of motifs, including KEEL (lysine, glutamate, glutamate, leucine), REEL (arginine, glutamate, glutamate, lysine) and others (Raykhel et al., 2007). Most PDI family members in CHO cells have C-terminal motifs that could be recognized by KDEL receptors. For instance, PDI family members 1 and 6 have a KDEL motif, family members 2 and 4 have a KEEL motif, and family member 5 has a REEL motif. Subsequently, this widens the scope of molecules that KDEL receptors recognize and sheds light on their importance as a cell engineering target.

I hypothesized that KDELR1 overexpression in antibody-producing cells will lead to a higher ER chaperone retention rate from post ER compartments; thus, they will increase the rate of IgG1 folding in the ER.

The stable KDELR1 overexpression in the IgG1-producing cell line CHO-K1-IgG1 improved the specific productivity of IgG1 without any significant effect on the specific growth rate. The reason behind this improvement in productivity is not yet clear; however, the mRNA levels of IgG1 heavy and light chains did not show any significant change in stable KDELR1

overexpressing cells suggesting that this improvement is due to functional intracellular role of KDELR1 as previously suggested.

In chapter three, I investigated the secretion of ER chaperones into extracellular medium. I serendipitously found that endogenous GRP94 is secreted into the medium as a low-molecular-weight species devoid of its ER retention motif. I also reported a comparison between GRP94 and BiP, the two most abundant proteins in the ER (Itzhak et al., 2016). Both GRP94 and BiP are highly upregulated at the mRNA level during ER stress. However, BiP shows high upregulation in cell lysates, whereas both proteins are secreted into the medium upon the induction of ER stress.

I expressed KDELR1 under the BiP promoter to investigate whether the secretion of chaperones is dependent on the saturation of ER retention machinery, as reported earlier in CHO (**Section2.3.2**) and HeLa cells (Llewellyn et al., 1997). I report that even though KDELR1 was upregulated in our engineered model in accordance with the upregulation of ER chaperones, this still allowed the secretion of ER chaperones to the medium and improved BiP retention minimally. I suggest that the secretion of chaperones into the medium is due to masking of the KDEL motif and weak upregulation of KDEL receptors.

GRP94 secretion was completely independent of KDELR1. It was secreted as a lower-molecular-weight species. Therefore, I hypothesized that GRP94 is truncated and loses its C-terminal bearing the KDEL motif and thus is secreted abundantly.

In chapter four, I investigated the truncated form of GRP94 during stress conditions. When the cells were treated with brefeldin A, the secretion of ER chaperones BiP and GRP94 was inhibited. Additionally, GRP94 truncation still occurred upon BFA treatment, while co-treatment by Tg/BFA

did not induce truncation. I thus suggest that GRP94 is expressed as a full-length protein; then, upon ER stress, it is truncated inside the ER by ER proteases (probably by intramembrane ER proteases) (Verhelst, 2017; Wolfe, 2009). Subsequently, it loses its acidic C-terminal, preventing its recapture from the *cis*-Golgi.

A novel approach in vaccine engineering is the use of a secreted form of gp96 (GRP94), in which the C-terminal retention KDEL motif is replaced by an IgG Fc-domain in vaccine cells (Podack & Raez, 2007; Strbo & Podack, 2008), leading to a secreted form of the antigen-presenting gp94-IgG complex that generates a very powerful immune response (Strbo et al., 2013). Additionally, engineered GRP94 without the KDEL motif was found to suppress tumor growth (Baker-LePain et al., 2002). In this study, I reported that the KDEL-deprived GRP94 form may occur naturally in mammalian cells by secretion as a truncated form into the medium, or intracellularly by UPR activation.

Finally, further experiments on hamster GRP94 are required to identify proteins responsible for the proteolytic cleavage of GRP94. Studying this phenomenon will pave the road for subsequent engineering of this chaperone, which should lead to improvements in the production of difficult-to-express chimeric antibodies. Additionally, because of the high sequence homology between human and hamster GRP94s, I hypothesize that the reported GRP94 truncations occur at the C-terminal and not the N-terminal as previously reported (Reddy et al., 1999) which subsequently leads to their secretion.

When identified, the C-terminal of GRP94 might also have possible applications as an ER stress sensitive peptide.

This is the end of the thesis

References

Aghdam, A. G., Moradhaseli, S., Jafari, F., Motahari, P., Samavat, S., Mahboudi, R., & Maleknia, S. (2019). Therapeutic Fc fusion protein misfolding: A three-phasic cultivation experimental design. *PLoS ONE*, *14*(1), e0210712. https://doi.org/10.1371/journal.pone.0210712

Alberts, B., Johnson, A., Lewis, J., Raff, M., Roberts, K., & Walter, P. (2008). *Molecular Biology of the Cell* (5th ed.). Garland Science.

Appenzeller-Herzog, C., & Ellgaard, L. (2008). The human PDI family: versatility packed into a single fold. *Biochimica Et Biophysica Acta*, *1783*(4), 535–548. https://doi.org/10.1016/j.bbamcr.2007.11.010

Argon, Y., Bresson, S. E., Marzec, M. T., & Grimberg, A. (2020). Glucose-Regulated Protein 94 (GRP94): A novel regulator of insulin-like growth factor production. *Cells*, *9*(8), 1844. https://doi.org/10.3390/cells9081844

Baker-LePain, J. C., Sarzotti, M., Fields, T. A., Li, C. Y., & Nicchitta, C. V. (2002). GRP94 (gp96) and GRP94 N-terminal geldanamycin binding domain elicit tissue nonrestricted tumor suppression. *Journal of Experimental Medicine*, *196*(11), 1447–1459. https://doi.org/10.1084/jem.20020436

Barnes, L. M., & Dickson, A. J. (2006). Mammalian cell factories for efficient and stable protein expression. *Current Opinion in Biotechnology*, *17*(4), 381–386. https://doi.org/10.1016/J.COPBIO.2006.06.005

Borth, N., Mattanovich, D., Kunert, R., & Katinger, H. (2005). Effect of increased expression of

protein disulfide isomerase and heavy chain binding protein on antibody secretion in a recombinant CHO cell line. *Biotechnology Progress*, *21*(1), 106–111. https://doi.org/10.1021/bp0498241

Cancino, J., Capalbo, A., Di Campli, A., Giannotta, M., Rizzo, R., Jung, J. E., Di Martino, R., Persico, M., Heinklein, P., Sallese, M., & Luini, A. (2014). Control systems of membrane transport at the interface between the endoplasmic reticulum and the Golgi. *Developmental Cell*, *30*(3), 280–294. https://doi.org/10.1016/j.devcel.2014.06.018

Capitani, M., & Sallese, M. (2009). The KDEL receptor: new functions for an old protein. *FEBS Letters*, *583*(23), 3863–3871. https://doi.org/10.1016/j.febslet.2009.10.053

Christianson, J. C., Shaler, T. A., Tyler, R. E., & Kopito, R. R. (2008). OS-9 and GRP94 deliver mutant α1-antitrypsin to the Hrd1-SEL1L ubiquitin ligase complex for ERAD. *Nature Cell Biology*, *10*(3), 272–282. https://doi.org/10.1038/ncb1689

Chung, J. Y., Lim, S. W., Hong, Y. J., Hwang, S. O., & Lee, G. M. (2004). Effect of doxycycline-regulated calnexin and calreticulin expression on specific thrombopoietin productivity of recombinant Chinese hamster ovary cells. *Biotechnology and Bioengineering*, *85*(5), 539–546. https://doi.org/10.1002/bit.10919

Crofts, A. J., Leborgne-Castel, N., Hillmer, S., Robinson, D. G., Phillipson, B., Carlsson, L. E., Ashford, D. A., & Denecke, J. (1999). Saturation of the endoplasmic reticulum retention machinery reveals anterograde bulk flow. *The Plant Cell*, *11*(11), 2233–2248. https://doi.org/10.1105/tpc.11.11.2233

Dean, N., & Pelham, H. R. (1990). Recycling of proteins from the Golgi compartment to the ER in yeast. *The Journal of Cell Biology*, *111*(2), 369–377. https://doi.org/10.1083/jcb.111.2.369

Dollins, D. E., Warren, J. J., Immormino, R. M., & Gewirth, D. T. (2007). Structures of GRP94-nucleotide complexes reveal mechanistic differences between the hsp90 chaperones. *Molecular Cell*, *28*(1), 41–56. https://doi.org/10.1016/j.molcel.2007.08.024

Dubey, A., Prajapati, K. S., Swamy, M., & Pachauri, V. (2015). Heat shock proteins: A therapeutic target worth to consider. *Veterinary World*, *8*(1), 46–51. https://doi.org/10.14202/vetworld.2015.46-51

Ecker, D. M., Jones, S. D., & Levine, H. L. (2015). The therapeutic monoclonal antibody market. *MAbs*, *7*(1), 9–14. https://doi.org/10.4161/19420862.2015.989042

Feige, M. J., & Hendershot, L. M. (2011). Disulfide bonds in ER protein folding and homeostasis. *Current Opinion in Cell Biology*, *23*(2), 167–175. https://doi.org/10.1016/j.ceb.2010.10.012

Fulda, S., Gorman, A. M., Hori, O., & Samali, A. (2010). Cellular stress responses: Cell survival and cell death. *International Journal of Cell Biology*. https://doi.org/10.1155/2010/214074

Gamper, N., Stockand, J. D., & Shapiro, M. S. (2005). The use of Chinese hamster ovary (CHO) cells in the study of ion channels. *Journal of Pharmacological and Toxicological Methods*, *51*(3 SPEC. ISS.), 177–185. https://doi.org/10.1016/j.vascn.2004.08.008

Giannotta, M., Ruggiero, C., Grossi, M., Cancino, J., Capitani, M., Pulvirenti, T., Consoli, G. M. L., Geraci, C., Fanelli, F., Luini, A., & Sallese, M. (2012). The KDEL receptor couples to Gαq/11 to activate Src kinases and regulate transport through the Golgi. *The EMBO Journal*,

31(13), 2869–2881. https://doi.org/10.1038/emboj.2012.134

Griesbeck, O., Baird, G. S., Campbell, R. E., Zacharias, D. A., & Tsien, R. Y. (2001). Reducing the environmental sensitivity of yellow fluorescent protein. *Journal of Biological Chemistry*, *276*(31), 29188–29194. https://doi.org/10.1074/jbc.M102815200

Hammond, C., & Helenius, A. (1994). Quality control in the secretory pathway: retention of a misfolded viral membrane glycoprotein involves cycling between the ER, intermediate compartment, and Golgi apparatus. *The Journal of Cell Biology*, *126*(1), 41–52. https://doi.org/10.1083/jcb.126.1.41

Haze, K., Yoshida, H., Yanagi, H., Yura, T., & Mori, K. (1999). Mammalian transcription factor ATF6 is synthesized as a transmembrane protein and activated by proteolysis in response to endoplasmic reticulum stress. *Molecular Biology of the Cell*, *10*(11), 3787–3799. https://doi.org/10.1091/mbc.10.11.3787

Hebert, D. N., & Molinari, M. (2007). In and out of the ER: protein folding, quality control, degradation, and related human diseases. *Physiological Reviews*, *87*(4), 1377–1408. https://doi.org/10.1152/physrev.00050.2006

Hetz, C., Zhang, K., & Kaufman, R. J. (2020). Mechanisms, regulation and functions of the unfolded protein response. *Nature Reviews Molecular Cell Biology*, *21*(8), 421–438. https://doi.org/10.1038/s41580-020-0250-z

Hilliard, W., MacDonald, M. L., & Lee, K. H. (2020). Chromosome-scale scaffolds for the Chinese hamster reference genome assembly to facilitate the study of the CHO epigenome.

Biotechnology and Bioengineering, *117*(8), 2331–2339. https://doi.org/10.1002/bit.27432

Huang, Y.-M., Hu, W., Rustandi, E., Chang, K., Yusuf-Makagiansar, H., & Ryll, T. (2010). Maximizing productivity of CHO cell-based fed-batch culture using chemically defined media conditions and typical manufacturing equipment. *Biotechnology Progress*, *26*(5), 1400–1410. https://doi.org/10.1002/btpr.436

Huard, D. J. E., Jonke, A. P., Torres, M. P., & Lieberman, R. L. (2019). Different Grp94 components interact transiently with the myocilin olfactomedin domain in vitro to enhance or retard its amyloid aggregation. *Scientific Reports*, *9*(1), 1–12. https://doi.org/10.1038/s41598-019-48751-8

Huck, J. D., Que, N. L., Hong, F., Li, Z., & Gewirth, D. T. (2017). Structural and functional analysis of GRP94 in the closed state reveals an essential role for the Pre-N Domain and a potential client-binding site. *Cell Reports*, *20*(12), 2800–2809. https://doi.org/10.1016/j.celrep.2017.08.079

Hwang, S. O., Chung, J. Y., & Lee, G. M. (2003). Effect of doxycycline-regulated ERp57 expression on specific thrombopoietin productivity of recombinant CHO cells. *Biotechnology Progress*, *19*(1), 179–184. https://doi.org/10.1021/bp025578m

Immormino, R. M., Dollins, D. E., Shaffer, P. L., Soldano, K. L., Walker, M. A., & Gewirth, D. T. (2004). Ligand-induced conformational shift in the N-terminal domain of GRP94, an Hsp90 chaperone. *Journal of Biological Chemistry*, *279*(44), 46162–46171. https://doi.org/10.1074/jbc.M405253200

Iozzo, R. V., Pillarisetti, J., Sharma, B., Murdoch, A. D., Danielson, K. G., Uitto, J., & Mauviel, A. (1997). Structural and functional characterization of the human perlecan gene promoter: Transcriptional activation by transforming growth factor-β via a nuclear factor 1-binding element. *Journal of Biological Chemistry*, *272*(8), 5219–5228. https://doi.org/10.1074/jbc.272.8.5219

Itzhak, D. N., Tyanova, S., Cox, J., & Borner, G. H. H. (2016). Global, quantitative and dynamic mapping of protein subcellular localization. *ELife*, *5*, e16950. https://doi.org/10.7554/eLife.16950

Jayapal, K. P., Wlaschin, K. F., Hu, W. S., & Yap, M. G. S. (2007). Recombinant protein therapeutics from CHO cells-20 years and counting. *Chemical Engineering Progress*, *103*(10), 40–47.

Johnson, J. L. (2012). Evolution and function of diverse Hsp90 homologs and cochaperone proteins. *Biochimica et Biophysica Acta - Molecular Cell Research*, *1823*(3), 607–613. https://doi.org/10.1016/j.bbamcr.2011.09.020

Jossé, L., Smales, C. M., & Tuite, M. F. (2012). Engineering the chaperone network of CHO cells for optimal recombinant protein production and authenticity. *Methods in Molecular Biology*, *824*, 595–608. https://doi.org/10.1007/978-1-61779-433-9_32

Kaneyoshi, K., Uchiyama, K., Onitsuka, M., Yamano, N., Koga, Y., & Omasa, T. (2019). Analysis of intracellular IgG secretion in Chinese hamster ovary cells to improve IgG production. *Journal of Bioscience and Bioengineering*, *127*(1), 107–113.

https://doi.org/10.1016/j.jbiosc.2018.06.018

Kim, J. Y., Kim, Y.-G., & Lee, G. M. (2012). CHO cells in biotechnology for production of recombinant proteins: current state and further potential. *Applied Microbiology and Biotechnology*, *93*(3), 917–930. https://doi.org/10.1007/s00253-011-3758-5

Knowlton, A. A., & Salfity, M. (1996). Nuclear localization and the heat shock proteins. *Journal of Biosciences*, *21*(2), 123–132. https://doi.org/10.1007/BF02703103

Kober, L. (2012). *Generation of high expressing CHO cell lines for the production of recombinant antibodies using optimized signal peptides and a novel ER stress based selection system* [Dr. rer. nat. thesis, Technical University Carolo-Wilhelmina in Braunschweig]. https://doi.org/10.24355/DBBS.084-201206280906-0

Kunert, R., & Reinhart, D. (2016). Advances in recombinant antibody manufacturing. *Applied Microbiology and Biotechnology*, *100*(8), 3451–3461. https://doi.org/10.1007/s00253-016-7388-9

Lalonde, M.-E., & Durocher, Y. (2017). Therapeutic glycoprotein production in mammalian cells. *Journal of Biotechnology*, *251*, 128–140. https://doi.org/10.1016/j.jbiotec.2017.04.028

Le Fourn, V., Girod, P.-A., Buceta, M., Regamey, A., & Mermod, N. (2014). CHO cell engineering to prevent polypeptide aggregation and improve therapeutic protein secretion. *Metabolic Engineering*, *21*, 91–102. https://doi.org/10.1016/J.YMBEN.2012.12.003

Liu, B., Staron, M., Hong, F., Wu, B. X., Sun, S., Morales, C., Crosson, C. E., Tomlinson, S., Kim, I., Wu, D., & Li, Z. (2013). Essential roles of grp94 in gut homeostasis via chaperoning

canonical Wnt pathway. *Proceedings of the National Academy of Sciences of the United States of America*, *110*(17), 6877–6882. https://doi.org/10.1073/pnas.1302933110

Llewellyn, D. H., Roderick, H. L., & Rose, S. (1997). KDEL receptor expression is not coordinatedly up-regulated with ER stress-induced reticuloplasmin expression in HeLa cells. *Biochemical and Biophysical Research Communications*, *240*(1), 36–40. https://doi.org/10.1006/bbrc.1997.7607

Luo, B., & Lee, A. S. (2013). The critical roles of endoplasmic reticulum chaperones and unfolded protein response in tumorigenesis and anticancer therapies. *Oncogene*, *32*(7), 805–818. https://doi.org/10.1038/onc.2012.130

Maldonado-Agurto, R., & Dickson, A. J. (2018). Multiplexed digital mRNA expression analysis profiles system-wide changes in mRNA abundance and responsiveness of UPR-specific gene expression changes during batch culture of recombinant Chinese Hamster Ovary cells. *Biotechnology Journal*, *13*(3), 1700429. https://doi.org/10.1002/biot.201700429

Marzec, M., Eletto, D., & Argon, Y. (2012). GRP94: An HSP90-like protein specialized for protein folding and quality control in the endoplasmic reticulum. *Biochimica et Biophysica Acta*, *1823*(3), 774–787. https://doi.org/10.1016/j.bbamcr.2011.10.013

Miller, D. J., & Fort, P. E. (2018). Heat shock proteins regulatory role in neurodevelopment. *Frontiers in Neuroscience*, *12*, 821. https://doi.org/10.3389/fnins.2018.00821

Mohan, C., Park, S. H., Chung, J. Y., & Lee, G. M. (2007). Effect of doxycycline-regulated protein disulfide isomerase expression on the specific productivity of recombinant CHO cells:

thrombopoietin and antibody. *Biotechnology and Bioengineering*, *98*(3), 611–615. https://doi.org/10.1002/bit.21453

Munro, S., & Pelham, H. R. (1987). A C-terminal signal prevents secretion of luminal ER proteins. *Cell*, *48*(5), 899–907. https://doi.org/10.1016/0092-8674(87)90086-9

Murshid, A., Gong, J., & Calderwood, S. K. (2012). The role of heat shock proteins in antigen cross presentation. *Frontiers in Immunology*, *3*. https://doi.org/10.3389/fimmu.2012.00063

Muruganandan, S., & Cribb, A. E. (2006). Calpain-induced endoplasmic reticulum stress and cell death following cytotoxic damage to renal cells. *Toxicological Sciences*, *94*(1), 118–128. https://doi.org/10.1093/toxsci/kfl084

Nishitoh, H. (2012). CHOP is a multifunctional transcription factor in the ER stress response. *Journal of Biochemistry*, *151*(3), 217–219. https://doi.org/10.1093/jb/mvr143

Ohya, T., Hayashi, T., Kiyama, E., Nishii, H., Miki, H., Kobayashi, K., Honda, K., Omasa, T., & Ohtake, H. (2008). Improved production of recombinant human antithrombin III in Chinese hamster ovary cells by ATF4 overexpression. *Biotechnology and Bioengineering*, *100*(2), 317–324. https://doi.org/10.1002/bit.21758

Omasa, T., Higashiyama, K. -I, Shioya, S., & Suga, K. -i. (1992). Effects of lactate concentration on hybridoma culture in lactate-controlled fed-batch operation. *Biotechnology and Bioengineering*, *39*(5), 556–564. https://doi.org/10.1002/bit.260390511

Omasa, T., Onitsuka, M., & Kim, W.-D. (2010). Cell engineering and cultivation of chinese hamster ovary (CHO) cells. *Current Pharmaceutical Biotechnology*, *11*(3), 233–240.

https://doi.org/10.2174/138920110791111960

Onitsuka, M., Kim, W.-D., Ozaki, H., Kawaguchi, A., Honda, K., Kajiura, H., Fujiyama, K., Asano, R., Kumagai, I., Ohtake, H., & Omasa, T. (2012). Enhancement of sialylation on humanized IgG-like bispecific antibody by overexpression of α2,6-sialyltransferase derived from Chinese hamster ovary cells. *Applied Microbiology and Biotechnology*, *94*(1), 69–80. https://doi.org/10.1007/s00253-011-3814-1

Onitsuka, M., & Omasa, T. (2015). Rapid evaluation of N-glycosylation status of antibodies with chemiluminescent lectin-binding assay. *Journal of Bioscience and Bioengineering*, *120*(1), 107–110. https://doi.org/10.1016/j.jbiosc.2014.11.015

Pan, Y. X., Chen, H., Thiaville, M. M., & Kilberg, M. S. (2007). Activation of the ATF3 gene through a co-ordinated amino acid-sensing response programme that controls transcriptional regulation of responsive genes following amino acid limitation. *Biochemical Journal*, *401*(1), 299–307. https://doi.org/10.1042/BJ20061261

Paris, S., Denis, H., Delaive, E., Dieu, M., Dumont, V., Ninane, N., Raes, M., & Michiels, C. (2005). Up-regulation of 94-kDa glucose-regulated protein by hypoxia-inducible factor-1 in human endothelial cells in response to hypoxia. *FEBS Letters*, *579*(1), 105–114. https://doi.org/10.1016/j.febslet.2004.11.055

Peng, R.-W., Guetg, C., Tigges, M., & Fussenegger, M. (2010). The vesicle-trafficking protein munc18b increases the secretory capacity of mammalian cells. *Metabolic Engineering*, *12*(1), 18–25. https://doi.org/10.1016/J.YMBEN.2009.08.007

Pettersen, E. F., Goddard, T. D., Huang, C. C., Couch, G. S., Greenblatt, D. M., Meng, E. C., & Ferrin, T. E. (2004). UCSF Chimera - A visualization system for exploratory research and analysis. *Journal of Computational Chemistry*, *25*(13), 1605–1612. https://doi.org/10.1002/jcc.20084

Podack, E. R., & Raez, L. E. (2007). Allogeneic tumor-cell-based vaccines secreting endoplasmic reticulum chaperone gp96. *Expert Opinion on Biological Therapy*, *7*(11), 1679–1688. https://doi.org/10.1517/14712598.7.11.1679

Prashad, K., & Mehra, S. (2015). Dynamics of unfolded protein response in recombinant CHO cells. *Cytotechnology*, *67*(2), 237–254. https://doi.org/10.1007/s10616-013-9678-8

Puck, T. T., Cieciura, S. J., & Robinson, A. (1958). Genetics of somatic mammalian cells. III. Long-term cultivation of euploid cells from human and animal subjects. *The Journal of Experimental Medicine*, *108*(6), 945–956. https://doi.org/10.1084/jem.108.6.945

Raykhel, I., Alanen, H., Salo, K., Jurvansuu, J., Nguyen, V. D., Latva-Ranta, M., & Ruddock, L. (2007). A molecular specificity code for the three mammalian KDEL receptors. *The Journal of Cell Biology*, *179*(6), 1193–1204. https://doi.org/10.1083/jcb.200705180

Reddy, R. K., Lu, J., & Lee, A. S. (1999). The endoplasmic reticulum chaperone glycoprotein GRP94 with Ca2+- binding and antiapoptotic properties is a novel proteolytic target of calpain during etoposide-induced apoptosis. *Journal of Biological Chemistry*, *274*(40), 28476–28483. https://doi.org/10.1074/jbc.274.40.28476

Roy, A., Kucukural, A., & Zhang, Y. (2010). I-TASSER: A unified platform for automated protein

structure and function prediction. *Nature Protocols*, *5*(4), 725–738. https://doi.org/10.1038/nprot.2010.5

Segar, K., Chandrawanshi, V., & Mehra, S. (2013). Systems biology of unfolded protein response in recombinant CHO cells. *BMC Proceedings*, *7*(Suppl 6), P67. https://doi.org/10.1186/1753-6561-7-s6-p67

Strbo, N., Garcia-Soto, A., Schreiber, T. H., & Podack, E. R. (2013). Secreted heat shock protein gp96-Ig: Next-generation vaccines for cancer and infectious diseases. *Immunologic Research*, *57*(1–3), 311–325. https://doi.org/10.1007/s12026-013-8468-x

Strbo, N., & Podack, E. R. (2008). Secreted heat shock protein gp96-Ig: An innovative vaccine approach. *American Journal of Reproductive Immunology*, *59*(5), 407–416. https://doi.org/10.1111/j.1600-0897.2008.00594.x

Tigges, M., & Fussenegger, M. (2006). Xbp1-based engineering of secretory capacity enhances the productivity of Chinese hamster ovary cells. *Metabolic Engineering*, *8*(3), 264–272. https://doi.org/10.1016/J.YMBEN.2006.01.006

Torres, M., Akhtar, S., McKenzie, E. A., & Dickson, A. J. (2020). Temperature down-shift modifies expression of UPR-/ERAD-related genes and enhances production of a chimeric fusion protein in CHO cells. *Biotechnology Journal*, *16*(2), 2000081. https://doi.org/10.1002/biot.202000081

Tripathi, N. K., & Shrivastava, A. (2019). Recent Developments in Bioprocessing of Recombinant Proteins: Expression Hosts and Process Development. *Frontiers in Bioengineering and*

Biotechnology, *7*, 420. https://doi.org/10.3389/fbioe.2019.00420

Trychta, K. A., Bä, S., Henderson, M. J., & Brandon, K. H. (2018). KDEL Receptors Are Differentially Regulated to Maintain the ER Proteome under Calcium Deficiency. *Cell Reports*, *25*, 1829–1840. https://doi.org/10.1016/j.celrep.2018.10.055

Verhelst, S. H. L. (2017). Intramembrane proteases as drug targets. *FEBS Journal*, *284*(10), 1489–1502. https://doi.org/10.1111/febs.13979

Walsh, G. (2018). Biopharmaceutical benchmarks 2018. *Nature Biotechnology*, *36*(12), 1136–1145. https://doi.org/10.1038/nbt.4305

Wang, H., & Hanash, S. (2005). Intact-protein based sample preparation strategies for proteome analysis in combination with mass spectrometry. *Mass Spectrometry Reviews*, *24*(3), 413–426. https://doi.org/10.1002/mas.20018

Wang, P., Li, B., Zhou, L., Fei, E., & Wang, G. (2011). The KDEL receptor induces autophagy to promote the clearance of neurodegenerative disease-related proteins. *Neuroscience*, *190*, 43–55. https://doi.org/10.1016/j.neuroscience.2011.06.008

Weiner, G. J. (2015). Building better monoclonal antibody-based therapeutics. *Nature Reviews. Cancer*, *15*(6), 361–370. https://doi.org/10.1038/nrc3930

Wiersma, V. R., Michalak, M., Abdullah, T. M., Bremer, E., & Eggleton, P. (2015). Mechanisms of translocation of ER chaperones to the cell surface and immunomodulatory roles in cancer and autoimmunity. *Frontiers in Oncology*, *5*, 7. https://doi.org/10.3389/fonc.2015.00007

Wilson, D. W., Lewis, M. J., & Pelham, H. R. (1993). pH-dependent binding of KDEL to its

receptor in vitro. *The Journal of Biological Chemistry*, *268*(10), 7465–7468. https://doi.org/10.1016/S0021-9258(18)53197-5

Wolfe, M. S. (2009). Intramembrane-cleaving proteases. *Journal of Biological Chemistry*, *284*(21), 13969–13973. https://doi.org/10.1074/jbc.R800039200

Yamamoto, K., Fujii, R., Toyofuku, Y., Saito, T., Koseki, H., Hsu, V. W., & Aoe, T. (2001). The KDEL receptor mediates a retrieval mechanism that contributes to quality control at the endoplasmic reticulum. *The EMBO Journal*, *20*(12), 3082–3091. https://doi.org/10.1093/emboj/20.12.3082

Yoshida, H., Haze, K., Yanagi, H., Yura, T., & Mori, K. (1998). Identification of the cis-acting endoplasmic reticulum stress response element responsible for transcriptional induction of mammalian glucose- regulated proteins: Involvement of basic leucine zipper transcription factors. *Journal of Biological Chemistry*, *273*(50), 33741–33749. https://doi.org/10.1074/jbc.273.50.33741

Zhou, Y., Raju, R., Alves, C., & Gilbert, A. (2018). Debottlenecking protein secretion and reducing protein aggregation in the cellular host. *Current Opinion in Biotechnology*, *53*, 151–157. https://doi.org/10.1016/J.COPBIO.2018.01.007

Zhu, G., & Lee, A. S. (2015). Role of the unfolded protein response, GRP78 and GRP94 in organ homeostasis. *Journal of Cellular Physiology*, *230*(7), 1413–1420. https://doi.org/10.1002/jcp.24923

Publication list

Samy, A., Kaneyoshi, K., & Omasa, T. (2020). Improvement of Intracellular Traffic System by Overexpression of KDEL Receptor 1 in Antibody-Producing CHO Cells. Biotechnology Journal, 15(6), 1900352 (Chapter 2, PhD thesis).

Samy, A., Yamano-Adachi, N., Koga, Y. & Omasa, T. (2021). Secretion of a low-molecular-weight species of endogenous GRP94 devoid of the KDEL motif during endoplasmic reticulum stress in Chinese hamster ovary cells. *Submitted to Traffic* (Chapter 3 and 4, PhD thesis).

Acknowledgement

I would like to deeply thank Professor Takeshi Omasa for supervising this PhD study and being my advisor in both my Master and PhD at Osaka University. He gave me the opportunity to propose my idea and work independently on it. Despite the laboratory focus is primarily Biochemical engineering and Molecular biotechnology, he warmheartedly accepted my idea to work on the unfolded protein response in CHO cells from a cell biology perspective, specifically the interesting ER retention machinery. My sincere thanks and gratitude to him.

I would also thank the Department of Biotechnology at Osaka University for making this double degree MSc and PhD program. It is a nicely organized program made with the Japanese style of education. I would like to also thank the Japanese government for funding this program.

I would like to thank Associate Professor Yuichi Koga for advising me during the last year of PhD while working on GRP94. He has been supportive and friendly, Thank you!

I would like to show in every possible way my gratitude to my mother for her constant support and mentoring. Without her, nothing would have been possible. My brother has been my backbone and support. The most important conclusion of this PhD for me is that family comes first.

Also, I would like to thank all the other lab members for being there.

My dear friend, Laura, who broke through my iron skull, Thank you!

Finally, no matter how much we study and learn, there is a lot that we do not know and we will never reach the ultimate knowledge. But that should never stop us from trying. And that is the philosophy.

" The Sea

Will be the Sea

Whatever the drop's philosophy."

- Attar of Nishapur